TANDEM MASS SPECTROMETRY FOR THE IDENTIFICATION AND QUANTITATION OF TRYPTOLINES (TETRAHYDRO-BETA-CARBOLINES) IN RAT BRAIN EXTRACTS

BY

JODIE VINCENT JOHNSON

A DISSERTATION PRESENTED TO THE GRADUATE SCHOOL
OF THE UNIVERSITY OF FLORIDA IN
PARTIAL FULFILLMENT OF THE REQUIREMENTS
FOR THE DEGREE OF DOCTOR OF PHILOSOPHY

UNIVERSITY OF FLORIDA

1984

To my loving wife, Karen,
and our son, Joshua

ACKNOWLEDGEMENTS

I would like to express my sincere gratitude to Dr. Kym F. Faull at the Stanford University Medical Center for his initiation of this project and provision of samples and for his advice, patience, and valued friendship during this collaborative research. I would like to thank Dr. Olof Beck, at Stanford University also, who helped plan and prepare samples for the experiments in Chapter 5, and Jack D. Barchas, M.D., for securing funding for the work performed at Stanford.

I would like to express my gratitude to Dr. Richard A. Yost for his acceptance and guidance during this research. His editorial assistance during the preparation of this dissertation and various papers is very much appreciated. I will always value his friendship. I thank him also for offering me a postdoctoral appointment.

I acknowledge the members of my research committee, including Drs. John G. Dorsey, Gerhard M. Schmid, Martin T. Vala, and Clyde M. Williams for their suggestions and guidance. I especially thank Dr. Dorsey for reviving my interest in pursuing a Ph.D. degree.

This research would not have been possible or as much fun without the support of and discussions with my colleagues and friends in the MS/MS research group. I would like to give special thanks to Neil Brotherton and Dean Fetterolf for many helpful discussions. In addition, I thank Linda Hirschy, Barbara Kirsch, Jonell Kerkhoff, and Joe Foley for their friendship, help, and lunch-time talks, which helped to maintain our sanity while taking classes and doing research.

I gratefully acknowledge the Chemistry Department for the first year scholarship and Proctor and Gamble for sponsoring my fellowship during this past year. I also thank Dr. Roy King for accepting me as his graduate assistant and teaching me the varied aspects of high resolution mass spectrometry. I also acknowledge research funding in part by grants from the National Science Foundation (CHE-8106533) at the University of Florida and from the National Institute on Alcohol Abuse and Alcoholism (AA 0592) and the National Institute of Mental Health (Program Project grant MH 23861) at Stanford.

I would like to acknowledge the support of my family during all the years of my education, whether in or out of the classroom. Most of all, I thank my wife, Karen, for her love, understanding, and patience during these years in graduate school. She has made it all possible and worthwhile.

TABLE OF CONTENTS

Abstract of Dissertation Presented to the Graduate School
of the University of Florida in Partial Fulfillment of the
Requirements for the Degree of Doctor of Philosophy

TANDEM MASS SPECTROMETRY FOR THE IDENTIFICATION AND QUANTITATION OF TRYPTOLINES (TETRAHYDRO-BETA-CARBOLINES) IN RAT BRAIN EXTRACTS

By

Jodie Vincent Johnson

December, 1984

Chairman: Richard A. Yost
Major Department: Chemistry

The natural occurrence of tryptolines in mammalian tissue is the subject of controversy. This is due to the lack of sensitivity and/or selectivity in the methods used for identification and the possibility of artefactual formation of tryptolines during sample preparation. Due to its excellent sensitivity and inherent selectivity, tandem mass spectrometry (MS/MS) has been used successfully for the direct analysis of complex mixtures for trace components with minimal, if any, sample clean-up.

The triple quadrupole tandem mass spectrometer consists of, in series, a dual chemical ionization/electron impact ionization source, a quadrupole mass filter (Q1), a radio-frequency-only quadrupole (Q2), a second quadrupole mass filter (Q3), and an electron multiplier. In the analysis of an extract, methane positive or electron capture negative chemical ionization (PCI or NCI, respectively) of the extract produced ions characteristic of the components of the extract. The MS/MS quantitation in these studies was performed by selected reaction monitoring

(SRM) whereby the ion characteristic of a tryptoline is mass selected by Q1 for fragmentation in Q2 through collisions with neutral gas molecules, and only the most abundant and characteristic daughter ion is selected by Q3 for monitoring. The MS/MS quantitation was compared to selected ion monitoring (SIM), whereby Q1 and Q2 pass all ions and only the characteristic ion of a tryptoline is selected by Q3 for monitoring. With sample introduction via a capillary column, the limits of detection of the heptafluorobutyryl (HFB) derivative of tryptoline were determined to be 0.50, 0.45, 19, and 60 pg of standard injected onto the column for NCI-SIM, NCI-SRM, PCI-SIM and PCI-SRM, respectively. The greater selectivity of the NCI-SRM technique made it the preferred technique for the analysis of crude extracts of rat brain.

With GC/NCI-SRM analysis of HFB-derivatized crude extracts of rat brains, it was demonstrated that artefactual formation of tryptoline during the sample preparation used in these studies was negligible. Tryptoline (19.2 ± 3.6 ng/g wet tissue, n=7), methtryptoline, 5-hydroxytryptoline, and 5-hydroxymethtryptoline, and their presumed precursor indoleamines, tryptamine and 5-hydroxytryptamine, were identified in rat brain extracts.

CHAPTER 1
INTRODUCTION

This dissertation describes the use of tandem mass spectrometry for the qualitative and quantitative characterization of tryptolines (tetrahydro-β-carbolines) in crude extracts of rat brains. The *in vivo* presence of tryptolines in mammalian systems has been an area of much controversy since the first report describing their presence in 1961 (1). This has largely been due to the inability of the analytical methods used to consistently identify and quantitate these compounds at the trace (sub-parts-per-billion) levels reported. This dissertation demonstrates that, due to its inherent selectivity and sensitivity, tandem mass spectrometry is able to detect reliably and consistently sub-parts-per-billion levels of derivatized tryptoline in standards. Furthermore, it describes the use of tandem mass spectrometry to identify four tryptolines (two of which have not been previously reported) and to quantitate one of these tryptolines in heptafluorobutyryl-derivatized crude extracts of rat brain.

Organization of Dissertation

This dissertation is divided into six chapters. This introductory chapter provides background information necessary for understanding the significance of the research presented in later chapters. An overview of the tryptolines is presented with regard to their physiological significance and their *in vivo* presence in mammalian systems. A brief historical review of tandem mass spectrometry is followed by a descrip-

tion of the operational modes and applications of the triple quadrupole tandem mass spectrometer used in these studies.

Chapter 2 describes the use of tandem mass spectrometry for trace organic analysis. This chapter, in combination with some of the findings of chapters 4 and 5, has been prepared for publication in Analytical Chemistry and Applied Spectroscopy Reviews. A brief review of the fundamental analytical requirements and inherent difficulties of trace analysis in general is presented. A review of the fundamental aspects of tandem mass spectrometry is followed by descriptions of several applications of this technique to trace mixture analysis. The successful determinations of trace organics in complex matrices in these applications serve as the basis for the research presented in chapter 3.

In chapter 3, the use of tandem mass spectrometry to structurally characterize and quantitate underivatized tryptoline standards is discussed. The fragmentation pathways of the ions resulting from electron impact and positive and negative chemical ionization are elucidated. Following optimization of the experimental conditions, quantitation of underivatized tryptoline standards is performed. The significance of the limits of detection thus obtained is discussed with regard to determining the tryptolines in mammalian tissues.

The characterization and determination of the heptafluorobutyryl derivatives are described in chapter 4. Many of the findings reported in this chapter have been published recently in Analytical Chemistry (2). Following a description of the mass spectral characterization of the standards, the effect of experimental conditions on sensitivity is discussed and optimized. Quantitation of the heptafluorobutyryl-derivative of the tryptoline standard is performed by normal and tandem mass

spectrometry with positive and negative chemical ionization and with sample introduction via packed and capillary gas chromatographic columns. The sensitivity, limit of detection, and speed of analysis of each of the techniques are discussed. An application of each technique to the determination of an amount of tryptoline added to a derivatized crude extract of rat brain is demonstrated and discussed.

The use of tandem mass spectrometry for the identification and quantitation of tryptolines in heptafluorobutyryl-derivatized extracts of rat brains is described in chapter 5. Much of this work has been submitted for publication as a chapter in "Aldehyde Adducts in Alcoholism" (3). The tandem mass spectrometric methods developed in chapter 4 are used to investigate the possibility of artefactual tryptoline formation occurring during the sample work-up procedure, to quantitate tryptoline, and to tentatively identify three other, two previously unreported, tryptolines in derivatized crude extracts of rat brains.

The final chapter summarizes the results of this work and presents some ideas for continued research in the area of tryptolines as well as in the area of tandem mass spectrometry.

Tryptolines (Tetrahydro-β-Carbolines)

The tryptolines (1,2,3,4-tetrahydro-β-carbolines) are a class of compounds resulting from the Pictet-Spengler condensation of indoleamines and aldehydes (Figure 1-1) (4). The laboratory synthesis of tryptolines by this reaction occurs readily under physiological conditions (1,5). This property has been used in the past as the basis for the histochemical detection of indoleamines by fluorometry, whereby the indoleamines are converted to tetrahydro-β-carbolines via condensation

with formaldehyde gas and then oxidized to the highly fluorescent β-carbolines (6). In vitro formation of tryptolines also results from the incubation of methyl tetrahydrofolate and indoleamines with various tissue extracts having certain enzymatic activities (7-9). This reaction involves the enzymatic formation of formaldehyde from methyl tetrahydrofolate followed by non-enzymatic condensation of formaldehyde with indoleamines (10-12). These results, in conjunction with the fact that indoleamines (13-16) and formaldehyde (17) are common constituents in mammalian tissues, have led to the speculation that the tryptolines could occur naturally in mammalian tissues.

Interest in the physiological significance of the tryptolines stems largely from three sources. Firstly, they are known to elevate the levels of serotonin (5-hydroxytryptamine) in the brain. Administration of tryptolines inhibits the action of monamine oxidase A (18-20), inhibits the re-uptake of serotonin by the synaptosomal cells (20-24), and facilitates the release of serotonin (25). Serotonin has been postulated to be a putative neurotransmitter (26), and imbalance in the brain serotonin levels has been associated with various mental illnesses (27). Thus, the in vivo presence of tryptolines may have important influences upon neurotransmission and mental illness (28,29).

Secondly, tryptolines have been associated with the alcohol abuse syndrome (30). The level of acetaldehyde, the major metabolite of ethanol in mammalian systems, increases in the plasma and brain following intake of ethanol (31,32), thus increasing the likelihood of acetaldehyde-indoleamine condensation reactions. This hypothesis has been supported by the determination of such tryptolines in the urine of normal subjects after, but not before, intake of ethanol (33,34), and by

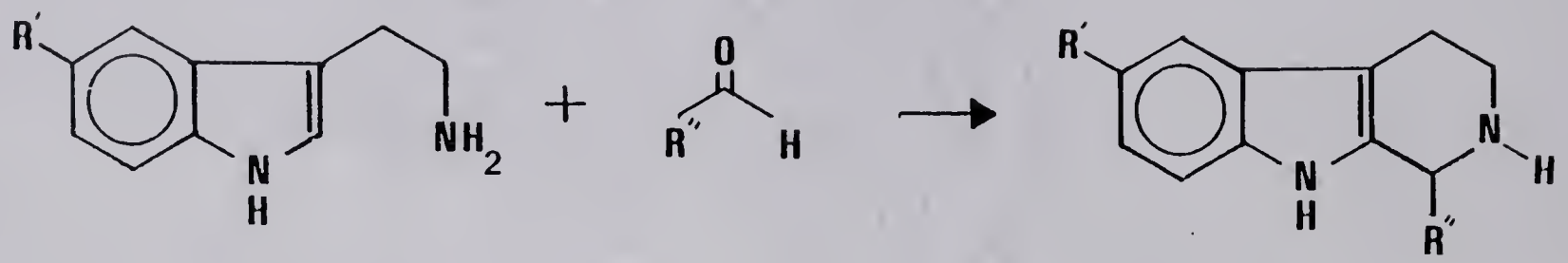

INDOLEAMINE ALDEHYDE TRYPTOLINE

Figure 1-1. Pictet-Spengler condensation of an indoleamine and an aldehyde to produce the corresponding tryptoline.

the increased excretion of such tryptolines in the urine of alcoholics (35,36). In addition, after administration of tryptolines, rats preferred drinking alcohol over water (37,38). Thus, the *in vivo* production of tryptolines may have important implications with respect to alcoholism.

Thirdly, the identification of receptor sites in mammalian brain specific for the benzodiazepines, a class of mild tranquilizers, led to the search for possible endogeneous ligands (39-42). A β-carboline derivative was isolated from human urine which showed a very high affinity for the benzodiazepine receptors (43). Although this compound had been chemically altered during the extraction procedure, it did lead to the speculation that a member of the β-carbolines or tetrahydro-β-carbolines could be an endogeneous ligand for the benzodiazepine receptor. This speculation was strengthened when it was shown that several tryptolines and β-carbolines which have been found in mammalian systems were powerful displacers of tritiated flunitrazepam from brain tissue homogenates (44). Related to this aspect, certain tryptolines have recently been shown to exert LSD-like effects and to be associated with the opiate receptors in the brain (45-48).

On the basis of combined thin-layer chromatography (TLC) and fluorometry (49,50), liquid chromatography with electrochemical detection (51), TLC with scintillation counting (52), and gas chromatography/mass spectrometry (GC/MS) (33,53-57), the *in vivo* presence of tryptolines has been described in various extracts of mammalian tissues and fluids. Despite these numerous reports, widespead support for the natural occurrence of these compounds in mammalian tissues has not been forthcoming. This has been largely due to the lack of the sensitivity

and/or the selectivity of the above methods necessary for the consistent detection of the tryptolines at the trace levels reported. In addition, the possibility of artefactual formation of tryptolines during the sample work-up procedure has further confused this issue (58,59).

Tandem Mass Spectrometry (MS/MS)

The demand for more sensitive, selective, rapid, and cost-effective techniques for mixture analysis has been the spur for the continuing improvements in mass spectrometry over the years. The need to quantitatively analyze petroleum fractions was the impetus for the commercial development of single-focusing magnetic mass spectrometers in the 1940s. The desire for higher selectivity and more information resulted in the advent of double-focusing instruments which combined the momentum analyzing property of a magnetic sector and the kinetic energy analyzing property of an electric sector in order to obtain higher mass spectral resolution. However, these instruments were fairly expensive to purchase, operate and maintain. This led to the commercial development of quadrupole mass spectrometers in the 1960s. It was quite apparent early on that in order to obtain qualitative information about the components of a mixture, the individual components had to be introduced into the mass spectrometer in a relatively "pure" form. This was the incentive for the development of gas chromatography/mass spectrometry (GC/MS) in the late 1950s (60). The ability to separate and identify hundreds of components in a mixture at trace levels has made GC/MS one of the most powerful and widely-used techniques for organic mixture analysis (61). The need to analyze thermally labile and/or nonvolatile compounds not amenable to GC prompted the coupling of liquid chromatography to mass

spectrometry (LC/MS) in the late 1970s (62). Both of these chromatographic systems provide, it is hoped, not only the introduction of relatively pure substances into the mass spectrometer, but also the additional information contained in the elution time of a component after its injection onto the column, referred to as its retention time. The combination of having a characteristic retention time and having a characteristic mass spectrum of a component in a mixture is now the accepted criterion used for confirming the identity of a compound. One of the major drawbacks with the use of chromatography/MS for mixture analysis is the relatively long analysis time. This is not only due to the time required for the separation and elution of the component of interest, but also due to the extensive sample clean-up and derivatization procedures often necessary prior to the chromatographic step (62).

The mass separation of ions for subsequent fragmentation and mass analysis, tandem mass spectrometry (MS/MS), has long been used in the study of ion-molecule reactions (63) and, more recently, in the study of ion photodissociation (64,65). With the development of mass-analyzed ion kinetic energy spectrometry (MIKES) (66) and an instrument specifically designed for MIKES (67), the ability to separate and study ions mass spectrometrically was dramatically extended. A MIKES instrument is a double-focusing mass spectrometer having the magnetic sector prior to the electric sector (reversed geometry). In MIKES, an ion is mass-selected by the magnetic sector and allowed to undergo metastable (unimolecular) or collisionally activated dissociation in the following field-free region to produce various daughter ions and neutral fragments. The kinetic energy of the daughter ions is then analyzed with the electric sector. The resulting MIKE spectrum provides information

about both the daughter ions' mass-to-charge ratios (m/z) and the kinetic energy released upon fragmentation (68). Such information enables the elucidation of many of the fragmentation pathways, and thus the structure, of a molecule following its ionization and fragmentation under electron impact.

As MIKES can involve the separation of ions resulting from the ionization and fragmentation of a single compound, the next logical progression was the exploitation of this MS/MS capability of MIKES for mixture analysis. Subsequent research in the labs of Cooks (69,70) and McLafferty (71) demonstrated that the inherent selectivity and sensitivity of MIKES-type tandem mass spectrometry (MS/MS) permitted the rapid analysis of complex mixtures for trace components with minimal, if any, sample clean-up and preparation. The development in the late 1970s by Yost and Enke (72) of a triple quadrupole tandem mass spectrometer, with an RF-only quadrupole serving as an efficient collision cell and powerful focusing device, led to the commercial development of practical MS/MS instruments. Since then, many types of tandem mass spectrometers have been built utilizing magnetic sectors, electric sectors, quadrupoles, time-of-flight, ion cyclotron resonance cells and various combinations of these, each with their own specific characteristics (73). As in the early days of mass spectrometry, it was soon realized that more than just tandem mass spectrometry may often be required for complex mixture analysis. Thus, the combination of various chromatographic systems with MS/MS has further increased the selectivity of the technique (2,3,74,75).

Instrument Description, Operation, and Application

The triple quadrupole tandem mass spectrometer used in these studies consists of, in series, a dual chemical ionization/electron impact (CI/EI) ionization source, a quadrupole mass filter (Q1), a radio-frequency-only quadrupole (Q2), a second quadrupole mass filter (Q3), and an electron multiplier. While Q1 and Q3 are operated as mass filters in the MS/MS modes, Q2 acts as a collision chamber and focusing device, allowing all ions to be efficiently transmitted. In mixture analysis, "soft" ionization, e.g. chemical ionization, of a mixture is utilized in the ion source to produce ions characteristic of the components of the mixture. The separation and analysis of the component of interest is performed by the mass selection of its characteristic ion by Q1 for fragmentation in Q2 through collisions with neutral gas molecules, and the mass analysis of the resulting daughter ions by Q3.

The four most common MS/MS scan or operating modes of the triple quadrupole instrument are daughter scan, parent scan, neutral loss scan, and selected reaction monitoring (Figure 1-2). The specific MS/MS operational mode chosen for a particular analysis will depend upon the information desired. A daughter scan (Figure 1-2a) consists of selecting a single parent ion characteristic of the analyte by Q1, fragmenting it by collisionally activated dissociation (CAD) in Q2, and then scanning Q3 to obtain a daughter mass spectrum. Analogous to a normal mass spectrum, the daughter mass spectrum can be used for identification of an analyte by standard mass spectral interpretation or by matching the spectrum to that of an authentic sample. In the parent scan mode (Figure 1-2b), Q1 is scanned over a specific mass range, allowing parent ions of different m/z to sequentially enter and undergo fragmentation in

Q2 to produce various daughter ions. Then Q3, instead of scanning, selects only an ion of a particular m/z to be transmitted to the detector. The resulting parent mass spectrum contains all the ions which fragment to yield a specific daughter ion, and can be used to screen for a class of compounds which fragment to yield a common substructure. Fragmentation of the positive CI $(M+H)^+$ ions of most of the phthalates yields the characteristic daughter ion 149^+. Therefore, a parent scan of 149^+ would be a method for screening mixtures for phthalates. In a neutral loss scan (Figure 1-2c), both Q1 and Q3 are scanned with a specific mass difference between them. The resulting neutral loss spectrum contains the daughter ions which result from the loss of a specific neutral fragment from the parent ions, and is useful for screening for a class of compounds characterized by the loss of a specific fragment. The molecular ions of chlorinated organics often lose Cl or HCl during CAD, and thus a neutral loss scan of 35 or 36 (and/or 37 and 38) would provide a rapid screening procedure for chlorinated organics in a mixture. Although the three operational modes just described are very selective, as in full scan normal mass spectrometry, they may not have the sensitivity necessary for the determination of trace components. Thus, for trace analysis, selected reaction monitoring (SRM) (Figure 1-2d) is normally employed, wherein only one characteristic daughter ion, typically the most abundant, resulting from the fragmentation of the analyte's characteristic parent ion, is selected by Q3. Thus, an enhancement in the sensitivity is obtained, albeit at the expense of some selectivity. In addition to these MS/MS modes, the tandem mass spectrometer can also be operated as a normal mass spectrometer by allowing all ions to pass through Q1 and Q2, in the

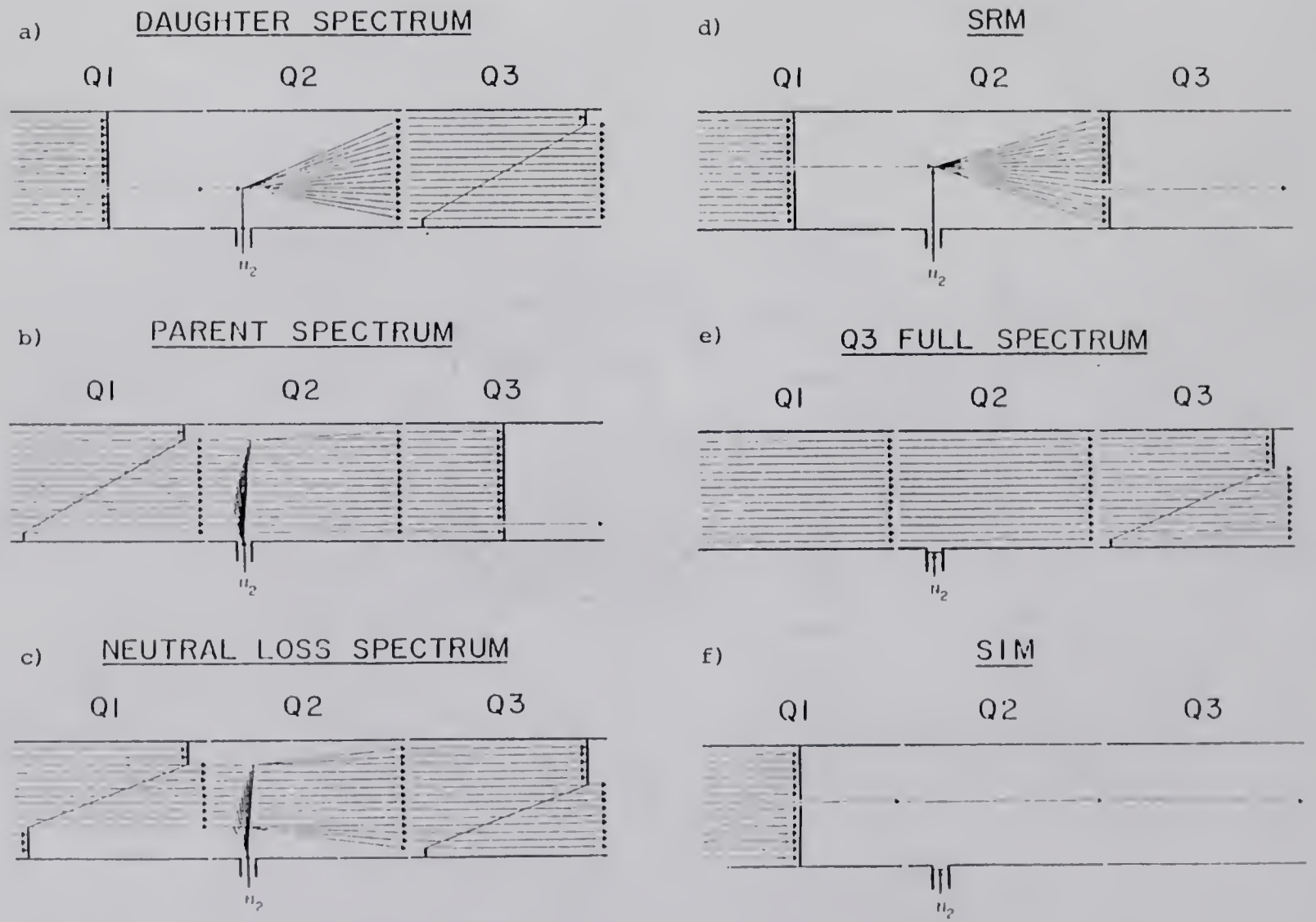

Figure 1-2. MS/MS operational modes.

absence of a collision gas. The second mass analyzer, Q3, can then be scanned to produce a normal mass spectrum (Figure 1-2e) or it can select only ions of a specific m/z for selected ion monitoring (SIM) (Figure 1-2f). This allows direct comparisons to be made betweem MS and MS/MS techniques on the same MS/MS instrument.

In light of the difficulties associated with the determination of tryptolines in tissue extracts, a study was initiated to assess the applicability of triple quadrupole tandem mass spectrometry for determining the trace levels of tryptolines reported in rat brain extracts. With its inherent selectivity and excellent sensitivity, MS/MS should be able to more reliably determine these compounds than the more conventional techniques presently in use.

CHAPTER 2
TANDEM MASS SPECTROMETRY FOR TRACE ANALYSIS

Introduction

Tandem mass spectrometry (MS/MS) has gained rapid acceptance with the analytical community since its development in the 1970's. Although it has been applied successfully for structure elucidation of unknowns (76), its rapid acceptance has largely been due to its ability to rapidly provide sensitive and selective analysis of complex mixtures, often with minimal, if any, sample clean-up (69-72,77,78). A recent book (79) and several recent reviews (73,80,81) contain extended explanations of the theory, instrumentation, and applications of tandem mass spectrometry. Here, we will deal with the application of tandem mass spectrometric techniques to the determination of trace organic components in complex matrices. The fundamentals and difficulties associated with trace organic analyses and the basic MS/MS operating modes will be reviewed. Various examples taken from research in our labs, as well as from the general literature, will be used to illustrate how tandem mass spectrometry meets the needs and overcomes some of these difficulties associated with trace analyses.

Requirements for Trace Analysis

In order to perform trace analyses successfully, it is necessary to think in terms of what McLafferty has referred to as the 4 S's of analysis (82): sensitivity, selectivity, speed, and $. The figure of merit

often used to describe an analytical technique is the first "S", sensitivity, defined by the slope of a calibration curve as the change in the signal obtained from a change in amount of analyte (Equation 2-1). Sensitivity may be a useful figure of merit for "pure" analytes, but may become meaningless for the determination of the analyte in a complex, or even a simple, matrix. This is due to the possibility that

$$\text{(2-1)} \qquad \text{Sensitivity} = \text{slope of the calibration curve} = \frac{\text{d Signal}}{\text{d Amount}}$$

other chemical constituents of the matrix or background may give a response at or interfere with the signal of the analyte. These types of effects can be referred to as chemical noise. The factor which then determines the smallest amount of analyte which can be determined by a technique may not be its sensitivity but rather its ability to discern the signal of the analyte from the chemical noise. This is the second "S", selectivity. Thus, a more descriptive figure of merit for an analytical technique is the limit of detection, defined as the amount of signal which results in a signal to noise ratio adequate to provide the desired confidence (typically S/N = 3). With the rearrangement of equation 2-1, and substitution of the resulting definition of the signal into the definition of the limit of detection, equation 2-2 is obtained.. This equation shows that the limit of detection takes into account both the sensitivity and the selectivity (measured by the level of chemical noise) of an analytical technique.

$$\text{(2-2)} \qquad \text{Limit of detection} = (\text{amount for S/N} = 3) = 3\ \frac{\text{noise}}{\text{sensitivity}}$$

In order to achieve the limits of detection necessary for trace analyses, the selectivity is normally improved through the use of extensive clean-up, separation, and often derivatization procedures in order to physically separate or enhance, respectively, the analyte's signal with respect to the chemical noise. In trace analyses, such sample manipulations can increase the possibilities for sample contamination and sample loss through adsorption onto glassware, oxidation, etc. In addition, if the methods necessary to increase the selectivity become too time-consuming and/or expensive, then the analytical method may become too impractical for routine work. Thus, the final two "S's", speed of analysis and cost effectiveness, are also important figures of merits.

Instrumental Methods to Improve the Limit of Detection

An alternative method to increase the selectivity is through the use of two or more types of analytical techniques in conjunction. Cooks and Busch have shown that, as the number of analytical techniques used simultaneously for the analysis of a sample increases, the absolute levels of the signal and noise decrease (83). However, because of the selectivity that each of the techniques has for the signal over the noise, the noise level decreases much more rapidly than does the signal, and an overall improvement in the S/N ratios is obtained. Since the limit of detection is determined by the S/N ratio, as long as there is a detectable signal, an increase in the number of analytical techniques used simultaneously for an analysis will result in improved limits of detection. Two commonly used analytical methods which utilize this principle are fluorometry (84) and gas chromatography/mass spectrometry (GC/MS) (61).

Fluorometry

Fluorometry can be considered to be a combination of absorption and emission spectroscopy. In the absorption experiment, a specific wavelength of light is selected by the first monochromator for irradiation of the sample. Absorption of this radiation by the sample results in its excitation and possible emission of light. The second monochromator then selects a specific wavelength of the emitted light for detection as the analytical signal. As the quantum efficiency for the conversion of the absorbed energy into emitted light is not one, and only a specific wavelength is selected for detection, there is a loss in the absolute signal detected, and therefore, in the sensitivity. However, in order for a compound to be detected, it must not only absorb energy at a specific excitation wavelength, but it must also emit radiation at a specific wavelength. This increase in selectivity reduces the spectral interference or chemical noise relative to the signal, so that often lower limits of detection are possible.

Gas Chromatography/Mass Spectrometry (GC/MS)

In GC/MS the selectivity is improved by the actual physical separation of the components of a mixture by chromatography prior to their mass analysis. In order to be detected an analyte must elute from the chromatographic column at a specific retention time and be ionized to produce ions of specific m/z. The sensitivity is reduced due largely to the dilution of the analyte during the chromatographic separation. In addition to reduced sensitivity, another major trade-off for the increased selectivity is an increased analysis time.

Tandem Mass Spectrometry

Instead of using two different methods of analysis, tandem mass spectrometry, as its name implies, uses one technique, mass spectrometry, twice in tandem. A tandem mass spectrometer consists of an ion source, two mass analyzers separated by a fragmentation region, and an ion detection device. The mass analyzers which have been used in these instruments include quadrupoles, magnetic sectors, electric sectors, time of flight, ion cyclotron resonance cells, and combinations of these (73 and references therein). Although each of these has its own specific characteristics, they are based upon the same MS/MS principles.

Principles of MS/MS

The principles of MS/MS are straightforward, and can be compared to conventional GC/MS as described above. A mixture is introduced into the ion source of the tandem mass spectrometer, where "soft" ionization methods can be used to produce ions characteristic of the mixture components. The separation of the analyte from the other mixture components (the chromatographic step of GC/MS) is then achieved by the mass selection of the characteristic ion of the analyte by the first mass analyzer. The parent ion, thus selected, undergoes collisionally activated dissociation (CAD) through collisions with neutral gas molecules in the fragmentation region to yield various fragment or daughter ions, analogous to the fragmentation occuring during the ionization step of GC/MS. As in GC/MS, subsequent mass analysis of the daughter ions by the second mass analyzer results in the analytical signal. When the second mass analyzer is scanned, a daughter spectrum is obtained. As with a normal mass spectrum, the daughter mass spectrum can be used for

identification of the parent ion (and thus, the analyte) through conventional mass spectral interpretation or by comparison with an authentic sample. In order to increase the sensitivity for trace analysis, only a single characteristic daughter ion, usually the most abundant, may be selected by the second mass analyzer for monitoring. This selected reaction monitoring (SRM) is analogous to the selected ion monitoring (SIM) used for maximal sensitivity in conventional GC/MS. Thus, in order for an analyte to be detected, it must be ionized to a characteristic ion and this parent ion must produce a daughter ion of specific m/z. This again results in decreased sensitivity with respect to normal MS due to the inefficiencies of the conversions of parent ions to daughter ions and the subsequent mass analysis of these daughter ions. However, the significant reduction in chemical noise often results in increased S/N ratios and improved limits of detection.

Applications of MS/MS for Trace Analysis

MS/MS trace analysis with MIKES instruments. The increase in selectivity which results from the use of two mass analyzers in tandem, in conjunction with the excellent sensitivity of the electron multiplier for ion detection, has enabled the direct analysis of complex mixtures for trace components with little or no sample preparation. From a historical viewpoint, the early MS/MS applications were conducted with MIKES instruments (see Chapter 1) modified to allow pressurization of the second field-free region (between the magnetic and electric sectors). One of the first applications of MS/MS for trace analysis of mixtures was the determination of cocaine in coca leaf samples and urine (80,86). Solids probe isobutane PCI-SRM analysis of cocaine standards

resulted in a calibration curve extending over 2 or 3 orders of magnitude with a limit of detection of approximately 1 ng where the error was estimated as 30%. This technique permitted the determination of 4 ng of cocaine in a 1 μg sample of coca leaf diluted in 1 mg of chalk dust, and of 1.7 ng of cocaine in a 1 μL urine sample. This work was extended with multiple reaction monitoring (MRM) to the simultaneous mapping of cocaine and cinnamonylcocaine in 1 mg samples of coca plant tissue. The only sample preparation used in these samples was grinding of the coca leaf samples in liquid nitrogen.

The speed of analysis with MS/MS techniques can be increased by minimizing the sample preparation, as above, and by eliminating any chromatographic separation of the mixture components prior to mass spectrometric analysis. Instead, mixtures can be introduced directly into the ion source by heatable solids probe. The component separation then occurs by mass selection of ions characteristic of individual components for fragmentation and subsequent mass analysis of the daughter ions. The rapidity of sample analysis possible with a solids probe is illustrated by the PCI-SRM determination of 20 ng of urea in 1 μL samples of diluted blood serum at a rate of 15 samples per hour (77). Due to the increased speed of analysis, a more reliable determination of the amount of analyte and an estimation of the precision of the analysis can be obtained by performing replicate analyses of the sample. Thus, the precision of the peak heights in the solids probe PCI-SRM of urea in blood serum was ±15 % relative standard deviation.

MS/MS trace analysis with triple quadrupole instruments. The research with MIKES instruments demonstrated that several trace components could be rapidly determined in complex mixtures with little or no

sample preparation. However, MIKES instruments have several disadvantages. Besides having less than unit mass resolution in the daughter spectra, the scan laws for the parent and neutral loss scans are complicated and the magnetic sector can not be quickly and accurately "jumped" between parent ions. With the development of a triple quadrupole instrument, these disadvantages were overcome (72). The quadrupoles, having a linear scan function and lacking the hysteresis effects of a magnet, can be quickly and accurately jumped between many different parent ions. These same characteristics allows all the various MS/MS scan modes to be placed under computer control. With a center quadrupole as a collision cell and focusing device, very efficient CAD of parent ions and collection of daughter ions for mass analysis by the third quadrupole are realized.

The application of triple quadrupole MS/MS to trace mixture analysis is illustrated by the direct determination of illicit drugs in the urine and blood serum of racing animals by solids probe PCI-MS/MS techniques (78). Presently, screening for illicit drugs is performed by thin layer chromatography, with confirmation performed on any positives by GC/MS. These methods entail extensive sample workup prior to their analysis and therefore only the top three to four animals of each race typically are tested. With the introduction of 1 μL of blood serum via a heated solids probe, the MS/MS detection limits for most of the illicit drugs studied were in the low parts-per-million (ppm) (ng/μL) range with PCI-SRM. With a simple solvent extraction of the blood serum, the detection limits were reduced to the low part-per-billion (pg/μL) range. The selectivity of MS/MS is more dramatically illustrated by the fact that three isobaric (same nominal mass) drugs could

be independently quantitated due to their unique daughter ions. Confirmation of the drugs at the parts-per-million (ng/μL) level in the blood serum was possible by comparison of the complete daughter spectra from the simple extract to those of authentic standards. With this procedure, it was possible to screen for as many as 50 drugs and metabolites in a single sample in less than 5 minutes. The advantages gained by the simplicity and time-saving of the MS/MS procedure over that currently in use are quite apparent.

The selectivity, sensitivity, and speed of analysis possible with MS/MS is dramatically illustrated in the determination of hexachlorobenzene (HCB) and 2,4,5-trichlorophenol (TCP) in human blood serum and urine by GC/triple quadrupole MS/MS (85). Rapid sample introduction was possible using a 50 cm long, 0.75 mm i.d., packed GC column operated isothermally to give retention times of 10 and 20 s for HCB and TCP, respectively. With this rapid means of sample introduction and a simple 1:1 solvent:sample extraction, it was possible to perform triplicate determinations of TCP (spiked levels ranging from 0.25 to 100 ppb, 1 μL sample size) in six serum samples, six urine samples, six standards, and associated blanks in approximately 36 minutes, which corresponds to ca. 100 injections/hr. This speed of analysis did not compromise the sensitivity and selectivity, as the absolute limits of detection for HCB and TCP were 50 and 250 femtograms, respectively, injected onto the column. The rapid analysis also made it possible to perform replicate analyses of each sample, which permitted an estimation of the precision of quantitation (consistently ±10 percent relative standard deviation). Often with normal GC/MS, the length of time required for the chromatographic step makes such replicate analyses impractical. A

comparison with the analyses performed with capillary column GC/MS showed the limits of detection for HCB and TCP with the short packed column GC/MS/MS to be 4 and 80 times lower, respectively, than those with GC/MS. In addition, GC/MS/MS was able to perform the same set of analyses in approximately 1/6 the time of that of the capillary GC/MS method. This was largely attributed to the time of the actual sample analyses, although significant savings were also apparent in the sample and instrument preparation.

Conclusion

The MS/MS examples above demonstrate that MS/MS meets the requirements necessary for trace analysis: sensitivity, selectivity, speed, and low cost per sample. Due to the high sensitivity and increased selectivity of MS/MS, rapid determinations of picogram and femtogram quantities of analytes have been demonstrated in small (mg and μL) quantities of complex mixtures with only minimal, if any, sample clean-up. The reduced sample clean-up not only increases the speed of analysis but also reduces the possibility of contamination of the sample or loss of the analyte. In addition, the ability to analyze small quantities becomes a major advantage in biological investigations where the amount of sample is often limited. Although the initial cost of MS/MS instruments is in the $\$10^5$ range, because of the rapidity of sample analysis, MS/MS becomes a very cost-effective technique for performing trace analyses.

CHAPTER 3
TANDEM MASS SPECTROMETRY FOR THE IDENTIFICATION AND QUANTITATION OF UNDERIVATIZED TRYPTOLINES

Introduction

In Chapter 2, the ability of MS/MS to successfully analyze complex mixtures directly, with minimal or no sample preparation, was illustrated. With a reduction in the sample clean-up prior to analysis, the possibilities of both loss of the trace analytes and contamination of the sample can be reduced. In particular, the chances of contamination of the brain extracts with aldehydes, which may lead to artefactual formation of tryptolines, can be reduced. Thus, this chapter investigates the use of tandem mass spectrometry for the identification and quantitation of underivatized tryptolines in crude extracts of rat brains.

Artefactual Tryptoline Formation

The Pictet-Spengler condensation reaction of indoleamines and aldehydes to produce the corresponding tryptolines occurs readily in the laboratory under conditions of physiological pH and temperature (1,5). This fact has led to the possibility of artefactual formation of tryptolines occurring during the extensive sample clean-up procedures necessary prior to determination of tryptolines by TLC-fluorescence and/or GC/MS. It was demonstrated that a major portion of the tryptolines determined in several instances has largely been due to artefactual

formation, with the source of the problem being traced to the presence of formaldehyde in the solvents used in the sample clean-up procedures (8,58). This has necessitated the use of aldehyde-trapping reagents in the solvents and redistillation of solvents just prior to sample clean-up. These steps have helped to reduce the level of the problem. In addition, deuterium-labelled indoleamines are now routinely added in the first step of sample clean-up as internal checks upon the level of artefactual formation. The formation of deuterium-labelled tryptolines would be a measure of the amount of artefactually-formed tryptolines relative to endogeneous levels. Faull and others were able to demonstrate that, by reducing the length and complexity of the clean-up procedure, the possibility of artefactual tryptoline formation during the sample clean-up could be minimized, if not eliminated (59). However, in order to obtain high selectivity and sensitivity, it was still necessary to derivatize the sample and perform gas chromatographic separation prior to mass spectral analysis.

MS/MS for Mixture Analysis

The use of two mass analyzers in tandem gives MS/MS a high degree of selectivity. Because of this, it has been possible to successfully determine targeted compounds or classes of compounds in very complex matrices by MS/MS techniques with minimal, if any, sample clean-up. Examples include the mapping of cocaine and cinnamonoylcocaine in coca leaves (86), the determination of urea in human blood serum (77), and the determination of illicit drugs in racing animals' serum (78). Not only is there a time-saving by having minimal sample clean-up, but further time-saving results from the ability to do mass separation of

components (in a few ms) instead of chromatographic separation (in tens of min) prior to further mass analysis.

The use of highly selective MS/MS techniques should enable further reduction in the sample clean-up of brain homogenates. This in turn should reduce the possibility of contamination with, loss of, and artefactual formation of tryptolines during the sample clean-up. In light of this, tandem mass spectrometry was assessed with regard to its ability to directly determine trace levels of underivatized tryptolines without prior chromatographic separation.

MS/MS for Structure Elucidation

In addition to mixture analysis, MS/MS has been used for structure elucidation studies of organic molecules and ions (72,76,87,88). In normal EI mass spectrometry, many fragment ions are often produced following the ionization of a compound. Without tandem mass spectrometry, the fragmentation pathways (and thus, the structure of the compound) resulting in these fragment ions can be elucidated with the use of high resolution mass spectrometry for determination of the elemental compositions of the ions, isotopic labelling studies, and/or with reference to compilations of logical fragmentation mechanisms which have been elucidated by similar methods (89,90). With the use of tandem mass spectrometric techniques, however, the fragmentation pathways of an ionized compound can be directly determined by systematically fragmenting and obtaining daughter spectra of all of the ions in the EI mass spectrum of the compound (72). This results in obtaining a "genetic tree" of an ionized molecule, indicating all the interrelationships and fragmentation pathways between various daughter ions. Interpretation of

the mass spectral information in order to elucidate the structure of a compound can then be performed more quickly and reliably.

An additional advantage with MS/MS is realized with the "soft" ionization techniques generally used in the trace analysis by mass spectrometry. These "soft" ionization techniques (e.g. chemical ionization) increase the selectivity and often the sensitivity of mass spectrometric analyses by reducing the fragmentation of the characteristic ions of the mixture components. However, with normal mass spectrometry, this results in a loss of structural information about the ions produced. MS/MS analysis of the ions produced by CI of a mixture is often able to provide the structural information necessary to identify a component without the sample separation necessary in conventional mass spectrometry. Therefore, a second objective of the work presented in this chapter is to investigate the ability of MS/MS to structurally characterize the tryptolines in relatively "pure" forms with EI-CAD, and in mixtures with CI-CAD techniques.

Experimental

Materials and Reagents

All chemicals and reagents were of the highest purity available. The tryptoline standards were kindly supplied as their HCl salts by Kym Faull, Ph.D., and Jack Barchas, M.D. (Department of Psychiatry and Behavioral Sciences, Stanford Medical Center, Stanford, CA). Ultrahigh purity methane (Matheson, Morrow, GA) and zero grade nitrogen (Airco Industrial Gases, Researach Triangle Park, NC) were used as a CI reagent/GC carrier and collision gas, respectively.

Instrumentation

All data were collected with a Finnigan MAT (San Jose, CA) triple stage quadrupole GC/MS/MS (91) equipped with a 4500 series ion source, pulsed positive and negative chemical ionization and INCOS data system. The Finnigan 9610 gas chromatograph was equipped with packed and Grob-type capillary injectors. A packed GC column and a heated direct insertion solids probe were utilized for sample introduction in these studies.

A short packed glass column was used to introduce samples into the ion source during the optimization studies. The column was constructed of a 38 cm length of 6 mm o.d. and 0.75 mm i.d. U-shaped glass tubing. A 6.4 cm piece of 0.64 cm o.d. and 4 mm i.d. glass tubing was joined to each end of the 38 cm length to allow room for the injection needle and for connection to the GC/MS interface. The tubing was rinsed three times each with the following solvents, in order: distilled water, acetone, methanol, and methylene chloride. Upon drying, the tubing was filled with a 10% solution of dimethylchlorosilane in toluene for ca. 1.5 hours, after which it was rinsed three times with toluene and dried in a GC oven. The tubing was hand-packed with 3% OV-101 on 80/100 mesh Chromosorb 750. The resulting column was conditioned overnight at 250 °C with 20 ml/min He flow prior to use (note: during conditioning the column was not connected to the mass spectrometer). The GC/MS interface consisted of a glass-lined stainless steel tube direct inlet fitted with a micro-needle valve. During the optimization studies, the GC column was kept isothermal at 225 °C with a carrier gas flow rate of ca. 18 ml/min CH_4. The injection port and the GC/MS interface temperatures were 220 °C and 250 °C, respectively. These conditions resulted in a retention time for tryptoline-HCl of ca. 10 s.

Procedures

Mass spectra of standards. Standards were introduced into the ion source by vaporization from a solids probe heated from ca. 50 °C to 400 °C at varying rates under data system control. Electron impact (EI, 70 eV electron energy) and positive and negative chemical ionization (PCI and NCI, respectively, 100 eV electron energy, 1.0 torr CH_4 source pressure) mass spectra were obtained with a source temperature of 100 °C in the Q3 normal MS mode. Daughter spectra were acquired for the characteristic ions in the EI and CI mass spectra of each of the tryptolines at collision gas pressures of 2.0 and 2.9 mtorr N_2, respectively, and at a collision energy of 24 eV. The NCI-CAD daughter spectra of the $(MHCl-H)^-$ (M denotes the tryptoline, while MHCl denotes the tryptoline-HCl salt) ions were obtained at a collision gas pressure of 2.0 mtorr N_2 and a collision energy of 26 eV. The EI-CAD daughter spectra used to generate the "genetic tree" of each tryptoline were obtained at a source temperature of 130 °C with a collision gas pressure of 1.3 mtorr N_2 and a collsion energy of 20 eV. The mass spectra acquired during the highest level of the analyte's ion current were averaged and background-subtracted, if necessary, to yield a representative mass spectrum of each standard.

Selection of positive or negative chemical ionization. Samples of tryptoline-HCl were introduced via the heated solids probe while performing Q3 selected ion monitoring (SIM) of the $(M+H)^+$ ion, m/z 173, and the $(M-H)^-$ ion, m/z 171, with the pulsed positive and negative chemical ionization feature of the tandem mass spectrometer. The integrated ion currents of the two ions were compared.

PCI-CAD collision energy and collision gas pressure studies. For each CAD parameter, studies were conducted with two different techniques at an ion source temperature of 120 °C. In the first study, tryptoline-HCl was introduced via the heated solids probe and PCI-CAD daughter spectra from m/z 140 to m/z 176 were acquired of the $(M+H)^+$ ion, m/z 173, at a collision gas pressure of 1.2 mtorr N_2 and at varying collision energies. This procedure was repeated for a second sample. The ion intensity ratios of m/z 144 to m/z 173 obtained at each collision energy were averaged and plotted versus the collision energy (Q2 offset). A similar procedure was utilized for the collison gas pressure study with the exception of having the collision energy set at 26 eV and analyzing a single sample for each collision gas pressure.

In a second study, for each combination of collision energy and collision gas pressure, duplicate or triplicate 1.0 µL injections of a standard solution of tryptoline-HCl were made onto the packed GC column (225 °C isothermal). PCI-selected reaction monitoring (SRM) of m/z 173 to m/z 144 was performed, and the areas of the resulting GC peaks were plotted against the desired parameter. The collision energy study was conducted at 1.2 mtorr N_2. The collision gas pressure study was conducted at 24 eV.

Quantitative studies. Serial dilutions were prepared of tryptoline-HCl and methtryptoline-HCl to give a series of solutions ranging in concentration from the parts-per-trillion (pptr) to the parts-per-million (ppm) level. Triplicate 1.0 µL samples of each solution were placed in separate 5 µL glass vials, with care to ensure that no large air bubbles were present. These were allowed to air dry for ca. 1 hr. The samples were then introduced into the ion source via a solids probe,

whereupon vaporization of the sample ocurred by ballistically heating from 50 °C to 400 °C in ca. 1 min. PCI-SRM (100 eV, 0.3 mA, 1.0 torr CH_4 source pressure, 140 °C ion source-26 eV, 2.0 mtorr N_2, 1 nominal mass unit, u, wide scan at 10 Hz) of the 173^+ to 144^+ and 187^+ to 144^+ CAD reactions was performed for tryptoline-HCl and methtryptoline-HCl, respectively, at an electron multiplier voltage of 2200 V and a preamp sensitivity of 10^{-8} A/V. Quantitation was obtained by integrating the ion current over the scans during which tryptoline-HCl and methtryptoline-HCl were vaporized from the solids probe. Peak areas are reported in data system counts. It was estimated that 1 count corresponds to the detection of one ion.

Results and Discussion

Nomenclature and Structure

The compounds of interest in these studies are tryptoline (TLN), methtryptoline (MTLN), 5-methoxytryptoline (CH_3O-TLN), 5-hydroxytryptoline (HTLN), and 5-hydroxymethtryptoline (HMTLN) (Table 3-1). These compounds are substituted 1,2,3,4-tetrahydro-β-carbolines. Holman et. al. (30) have suggested a change in the numbering system from that of the β-carbolines (parenthesized numbers) to one reflecting the numbering system of the presumed precursor indoleamines (unparenthesized numbers). They have also suggested the class of compounds be referred to as tryptolines, which again reflects the presumed indoleamine precursor tryptamine. Thus, 5-hydroxytryptoline would be the reaction product resulting from the condensation of 5-hydroxytryptamine with formaldehye. The tryptoline numbering system and nomenclature will be

used thoughout the remainder of the text. When referring to specific tryptolines, the abbreviations will be used while the term tryptolines will be applied to the entire class of compounds.

EI and EI-CAD Mass Spectra of Standards

The normal EI mass spectra of the tryptolines, M, (as their HCl salts, MHCl) are characterized by relatively intense molecular ions and numerous fragment ions (Table 3-2). The $(M-29)^+$ fragment ions, presumably arising from the loss of CH_2=NH from the piperidine ring, are the most abundant ions in the mass spectra of the tryptolines which lack a substituent at the 9-position (R"=H). For the tryptolines having a 9-methyl substituent (R"=CH_3), i.e. MTLN and 5-HMTLN, cleavage of the methyl radical from the molecular ion results in the $(M-15)^+$ fragment ions being the most abundant, with the $(M-29)^+$ fragment ions being the next most abundant ions. The loss of the methyl radical, presumably from the methoxy group of the $(M-29)^+$ fragment ion of 5-CH_3O-TLN, results in the second most abundant fragment ion in its mass spectrum.

The fragmentation of the molecular ions of the tryptolines under CAD conditions resulted in good yields of several abundant daughter ions, with the intensities of the parent molecular ions ranging from 5 to 16% of the most abundant daughter ion (Table 3-3). The most abundant daughter ions resulted from the same processes as seen in the normal EI mass spectra, and serve to support the presumed fragmentation pathways, i.e. the $(M-15)^+$ and $(M-29)^+$ daughter ions from the tryptolines with and without the 9-methyl substituent, respectively. The $(M-29)^+$ daughter ions were also relatively abundant in the daughter spectra of MTLN and 5-HMTLN. A relatively abundant daughter ion at m/z 158, presumably due

Table 3-1. Characteristics of the tryptolines of interest.

				Molecular Weight	
Tryptoline	Abbr.	R'	R"	M	MHCl
tryptoline	TLN	H	H	172	208
methtryptoline	MTLN	H	CH_3	186	222
5-methoxytryptoline	CH_3O-TLN	CH_3O	H	202	238
5-hydroxytryptoline	HTLN	HO	H	188	224
5-hydroxymethtryptoline	HMTLN	HO	CH_3	202	238

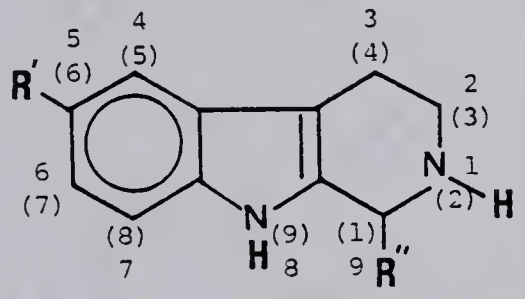

Table 3-2. EI mass spectral characteristics of the tryptoline-HCl salts.

Ions[a]	TLN	MTLN	CH_3O-TLN	HTLN	HMTLN
M^+	172(42[b])	186(60)	202(70)	188(32)	202(62)
$(M-CH_3)^+$	nd	171(100)	nd	nd	187(100)
$(M-R"NH)^+$	156(<2)	156(35)	186(4)	172(<2)	172(39)
$(M-H_2O)^+$	-	-	-	170(2)	184(3)
$(M-R"NH-H_2)^+$	154(3)	154(20)	184(3)	170(2)	170(16)
$(M-CH_2=NH)^+$	143(100)	157(35)	173(100)	159(100)	173(46)
$[M-(CH_2=NH)-CH_3]^+$	-	-	158(78)	-	-
$[M-(CH_2=NH)-HCN]^+$	-	-	-	-	146(15)

[a]The mechanisms shown for the formation of the ions is supported by the work of Coutts et. al. (92) and the EI-CAD studies here. R" is the substituent at the 9-position, as defined in Table 3-1.

[b]Percent abundance relative to the most abundant ion.

Table 3-3. EI-CAD (24 eV, 2.0 mtorr N_2) daughter mass spectral characteristics of the M^+ ions of the tryptoline-HCl salts.

Ions[a]	TLN	MTLN	CH_3O-TLN	HTLN	HMTLN
P^+	172(5[b])	186(16)	202(10)	188(6)	202(15)
$(P-H)^+$	171(2)	185(24)	201(2)	187(2)	201(25)
$(P-CH_3)^+$	nd	171(100)	187(1)	nd	187(100)
$(P-CH_2=NH)^+$	143(100)	157(37)	173(100)	159(100)	173(44)
$(P-CH_3-HCN)^+$	-	144(1)	-	-	160(6)
$[P-(CH_2=NH)-CH_3]^+$	-	-	158(16)	-	-

[a]The mechanisms for daughter ion formations is supported by the work of Coutts et. al. (92). P is the parent ion, i.e. M^+.

[b]Percent abundance relative to the most abundant ion.

to $[(M-CH_2{=}NH)-CH_3]^+$ also resulted from the CAD of the M^+ ion of 5-CH_3O-TLN.

The characteristic loss of $CH_2{=}NH$ from the EI molecular ions of the tryptolines under CAD conditions could be used in the neutral loss MS/MS mode to screen for other possible compounds having a piperidine ring. Complete characterization of such an unknown, once isolated, could be accomplished by systematically obtaining daughter spectra of all the ions in its normal EI mass spectrum. The information thus obtained would give all the genetic relationships between all the substructures of the molecule, i.e. from what ions a substructure is produced and to what ions a substructure fragments, and would allow for easier and more reliable interpretation of the mass spectral fragmentation pathways. Such information is illustrated for MTLN in Figure 3-1. Coutts et al. (92) have previously determined some of the fragmentation pathways of the 9-alkyl substituted tryptolines using metastable ions and high resolution mass spectrometry. However, as relatively few metastable transitions are observed for these compounds, only a few of the fragmentation pathways could be directly confirmed (indicated by asterisks in Figure 3-1). However, with an EI-CAD generated "genetic tree" of a molecule, direct confirmation and analysis were possible of all the fragmentation pathways. The completeness of this information should lend itself well to computerized structural analysis. Research is proceeding towards this goal (93).

The numerousness of fragment ions generated under EI conditions makes this the preferred technique for structure elucidation of unknown compounds by MS/MS. However, this characteristic becomes a liability in quantitative analyses. In the direct determination of trace components

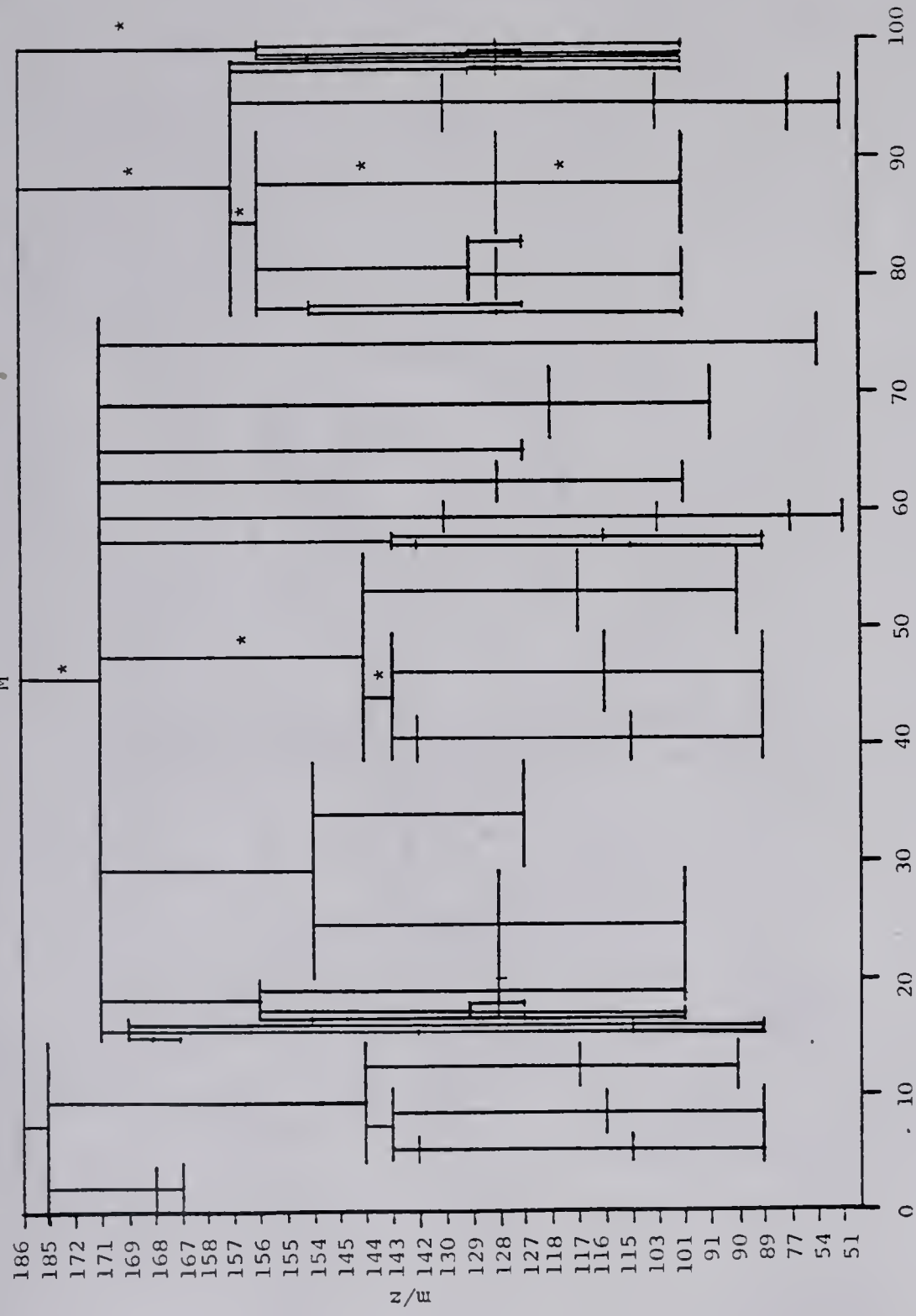

Figure 3-1. "Genetic tree" of MTLN-HCl. Horizontal bars are proportional to percent relative abundance. * denotes pathways confirmed by MIKES.

in complex matrices without prior separation, ideally each component should be ionized to yield a single characteristic ion. This is advantageous for two reasons. Firstly, by reducing the fragmentation of a molecule after ionization, one can achieve an increase in sensitivity when monitoring just the characteristic molecular ion. Secondly, by reducing the number of fragment ions from other compounds in the matrix having higher molecular weights than the compound of interest, the possibility of spectral interference at the m/z of interest is reduced, with a subsequent increase in the selectivity of the technique.

PCI and PCI-CAD Mass Spectra of Standards

Chemical ionization has been shown to be one method of achieving the above goals (94,95). With methane as a reagent gas, gas-phase chemical reactions occur in the ion source which result in the ionization of the sample with little transfer of energy to the sample molecules. This results in ions of low internal energy, and therefore little fragmentation of the original ions occurs.

The positive chemical ionization (PCI) mass spectra of the tryptoline-HCl salts are dominated by the protonated parent tryptoline molecules, $(M+H)^+$, and major fragment ions presumably due to loss of $CH_2{=}NH$ from the $(M+H)^+$ ions to yield $(M+H-29)^+$ (Table 3-4). The 5-substituted tryptolines have several additional fragment ions, which are explained below. In addition to the fragment ions, all the tryptolines yield the adduct ions $(M+29)^+$ and $(M+41)^+$ characteristic of methane PCI. The presence of these adduct ions serves to confirm the molecular weight of the compounds.

Table 3-4. Methane PCI mass spectral characteristics of the tryptoline-HCl salts.

Ions	TLN	MTLN	CH_3O-TLN	HTLN	HMTLN
$(M+41)^+$	213(2[a])	227(2)	243(2)	229(2)	243(2)
$(M+29)^+$	201(6)	215(7)	231(10)	217(8)	231(9)
$(M+H)^+$	173(100)	187(100)	203(100)	189(100)	203(100)
$(M+H-15)^+$	158(1)	172(4)	188(3)	174(1)	188(3)
$(M+H-18)^+$	nd	nd	nd	171(5)	185(5)
$(M+H-29)^+$	144(50)	158(11)	174(19)	160(20)	174(16)
$(M+H-43)^+$	nd	144(9)	nd	nd	160(3)

[a]Percent abundance relative to the most abundant peak.

The $(M+H)^+$ ions of the tryptolines fragment efficiently under the CAD conditions used (2.0 mtorr N_2, 26 eV) to yield several abundant daughter ions (Table 3-5). For the non-methylated tryptolines, the most abundant daughter ion, $(M+H-29)^+$, is presumably due to the loss of CH_2=NH from the $(M+H)^+$ ions. This serves to confirm the fragmentation pathway of the $(M+H)^+$ ions in the PCI spectra. Although the corresponding daughter ions are seen in the daughter spectra of the $(M+H)^+$ ions of the 9-methylated tryptolines, the most abundant daughter ions correspond to $(M+H-43)^+$ ions, presumably from the loss of CH_3CH=NH from the piperidine ring. The $(M+H-43)^+$ ions could also be explained by a rearrangement involving migration of the methyl group from the 9-position to the piperidine nitrogen, and the subsequent loss of CH_2=NCH_3. Coutts et. al. have shown some evidence for such a rearrangement occurring under EI conditions (92). The $(M+H-15)^+$ ions do fragment to yield some $(M+H-43)^+$ ions (ca. 40-50 % of the most abundant $(M+H-29)^+$ daughter ions) by loss of 28 u. Thus, a third possible explanation of the formation of the $(M+H-43)^+$ ion may be loss of the methyl group followed by loss of H and HCN.

In addition to the formation of the $(M+H-43)^+$ ions, the $(M+H)^+$ ions of the methylated tryptolines also yield relatively intense $(M+H-17)^+$ daughter ions. These could result from the loss of the CH_3 group, followed by loss of H_2. However, the daughter spectra of the $(M+H-15)^+$ fragment ion has little if any ion corresponding to a loss of H_2. Perhaps a more reasonable explanation is a migration of a hydrogen from the methyl group to the presumably protonated piperidine NH and subsequent loss of NH_3. High resolution mass spectrometry and isotopic-labelling would help to confirm the two possible mechanisms.

Table 3-5. Methane PCI-CAD (24 eV, 2.9 mtorr N_2) daughter mass spectral characteristics of the $(M+H)^+$ ions of the tryptoline-HCl salts.

Ions[a]	TLN	MTLN	CH_3O-TLN	HTLN	HMTLN
P^+	173(2[b])	187(1)	203(2)	189(2)	203(2)
$(P-15)^+$	158(<0.6)	172(1)	188(5)	nd	188(2)
$(P-17)^+$	156(<0.3)	170(7)	186(0.4)	172(0.3)	186(16)
$(P-18)^+$	nd	nd	nd	171(7)	185(7)
$(P-29)^+$	144(100)	158(11)	174(100)	160(100)	174(24)
$(P-43)^+$	nd	144(100)	nd	nd	160(100)
$(P-47)^+$	nd	nd	nd	142(57)	156(13)
$(P-32)^+$	nd	nd	171(2)	nd	nd
$(P-33)^+$	nd	nd	nd	nd	170(37)
$(P-44)^+$	nd	nd	159(79)	nd	nd
$(P-61)^+$	nd	nd	142(9)	nd	nd
$(P-29-R"CN)^+$	117(1)	117(2)	nd	nd	nd
$(P-29-R"CN-R'OH)^+$	nd	nd	nd	115(2)	nd
$(R"CH=N=CH_2)^+$	42(1)	56(0.5)	42(1)	42(1)	56(0.5)

[a]P is the parent ion, i.e. $(M+H)^+$.

[b]Percent abundance relative to the most abundant ion.

The $(M+H)^+$ ions of the 5-hydroxytryptolines yield characteristic daughter ions $(M+H-18)^+$ and $(M+H-47)^+$. The former daughter ions are presumably due to the protonation of the 5-hydroxy group and subsequent loss of H_2O. The latter are presumably due to the combined losses of H_2O and CH_2=NH from the $(M+H)^+$ ions. This is confirmed by the formation of the daughter ion corresponding to $(M+H-47)^+$ from the CAD of the $(M+H-18)^+$ and $(M+H-29)^+$ PCI fragment ions. In addition, the CAD of the $(M+H)^+$ ion of 5-HMTLN yields a daughter ion characteristic of both of its substituents, i.e. $(M+H-33)^+$. This could presumably occur by the combined losses of H_2O and CH_3 from the $(M+H)^+$ ion. This is confirmed by the appropriate losses occurring from the $(M+H-15)^+$ and $(M+H-18)^+$ PCI fragment ions under CAD to yield the daughter ion corresponding to $(M+H-33)^+$.

The CAD of the $(M+H)^+$ of the 5-CH_3O-TLN also produces unique daughter ions corresponding to (M+H-32) and $(M+H-61)^+$. These ions could possibly result from mechanisms analogous to the formation of $(M+H-47)^+$ ions from the 5-hydroxytryptolines' $(M+H)^+$ ions. Presumably, protonation of the CH_3O group occurs, and its loss as methanol results in the $(M+H-32)^+$ ion. The subsequent loss of CH_2=NH from this ion would result in the $(M+H-61)^+$ daughter ion. Little or no evidence was apparent for loss of methanol from the $(M+H-29)^+$ fragment ion, and the CAD spectrum was not obtained of the $(M+H-32)^+$ fragment ion. However, examination of the analogous pathways in the 5-hydroxytryptolines reveals that the major portion of the $(M+H-47)^+$ ions comes from the loss of CH_2=NH from the $(M+H-18)^+$ fragment ions as opposed to loss of H_2O from the $(M+H-29)^+$ fragment ions. This supports the above proposed mechanism.

Thus, PCI of the tryptolines results in the residing of most of the ion current in the $(M+H)^+$ ions and several fragment ions. The PCI-CAD of the $(M+H)^+$ ion of each tryptoline yields a unique daughter spectrum, reflecting the substituents at the 5- and 9-positions of the parent tryptoline structure. The daughter ions observed can be readily explained by the loss of CH_2=NH, R", CH_2=N-R', and R'H, and combinations of these losses from the $(M+H)^+$ ions.

NCI and NCI-CAD Mass Spectra of Standards

The electron-capture NCI mass spectra of the tryptoline-HCl salts are dominated by the ions resulting from loss of H from both the HCl salt (MHCl) to yield $(MHCl-H)^-$ and the parent tryptoline molecule (M) to yield $(M-H)^-$ ions (Table 3-6). The $(M-H)^-$ ions may also arise from the loss of HCl from the $(MHCl-H)^-$ ions. This is supported by the NCI-CAD of the $(MHCl-H)^-$ ions which fragment to yield the $(M-H)^-$ as daughter ions (Table 3-7). Also possible is the attachment of Cl^- to the neutral tryptoline molecules in the gas phase to produce the ion at $(M+35)^-$, equivalent to $(MHCl-H)^-$. Each of the tryptolines shows a major fragment ion corresponding to $(M-29)^-$, which is again presumably due to loss of CH_2=NH from the molecular ion and supported by the NCI-CAD of the M^- ions (Table 3-8). The 9-methyl tryptolines have a cluster of three fragment ions, $(M-15)^-$, $(M-16)^-$, and $(M-17)^-$, presumably corresponding to loss of CH_3 from the M^-, $(M-H)^-$, and $(M-H_2)^-$, respectively. The 5-hydroxytryptolines have a major fragment ion $(M-17)^-$ apparently due to loss of OH from the M^-. Such a loss is substantiated by the daughter ions corresponding to a loss of OH from the $(M-29)^-$ fragment ions and a loss of CH_2=NH from the $(M-17)^-$ fragment ions. The 5-methoxytryptoline,

in addition, shows a fragment ion at m/z 159 which could correspond to the loss of CH_2=NH from the m/z 188 fragment ion or by loss of CH_3 from the M^- followed by loss of CO.

All the tryptolines have ions in their NCI mass spectra at higher m/z than those of their M^- and $(MHCl)^-$ ions. The prominent $(M+12)^-$ and $(MHCl+12)^-$ ions have been explained in the CH_4 NCI of organic nitriles by the attachment of C_2H_5, present in the methane CI plasma, to the neutral molecule followed by loss of NH_3 prior to ionization (96). An alternative, but less likely, explanation could be the formation of the reactant ion C^-, which could then attach to and ionize the molecule (97). The mass analyzer was not scanned to low enough mass to see if this ion was indeed present. The $(M+28)^-$ and $(MHCl+28)^-$ ions are very prominent in the spectra of the HCl salts of HTLN and HMTLN, but of only low relative abundance in the other tryptolines' spectra. These ions may also be adduct ions due to the addition either of CO to the molecule prior to ionization or of CO^- to cause ionization. The CO could possibly be formed from the reaction of CH_4 with O_2 (from air leaks) at the hot filament surface. Another possible source of CO could be the sample itself, as phenols have been shown to lose CO under EI conditions (89). Subsequent loss of oxygen from the CO-adducts could also be an explanation of the $(M+12)^-$ and $(MHCl+12)^-$ ions. In addition to these possible adduct ions, the mass spectra of the tryptolines contain ions corresponding to $(M+46)^-$ and 46^-. These ions are of relatively low abundance for all of the tryptolines, with the exception of TLN-HCl, for which they represent the two most abundant ions in the NCI mass spectrum. The $(M+46)^-$ ions could be due to attachment of NO_2 to the neutral molecule prior to ionization, or, due to the attachment of NO_2^- to the

Table 3-6. Methane electron-capture NCI mass spectral characteristics of the tryptoline-HCl salts.

Ions	TLN	MTLN	CH_3O-TLN	HTLN	HMTLN
$(MHCl+28)^-$	236(<2[a])	250(<0.5)	266(<0.5)	252(1)	266(2)
$(MHCl+12)^-$	220(4)	234(11)	250(7)	236(4)	250(5)
$(MHCl-H)^-$	207(100)	221(100)	237(100)	223(56)	237(100)
$(M+46)^-$	218(148)	232(6)	248(2)	234(1)	248(5)
$(M+28)^-$	200(<2)	214(1)	230(1)	216(8)	230(7)
$(M+12)^-$	184(20)	198(27)	214(15)	200(15)	215(14)
M^-	172(14)	186(16)	202(12)	188(54)	202(56)
$(M-H)^-$	171(60)	185(46)	201(46)	187(100)	201(93)
$(M-H_2)^-$	170(25)	184(25)	200(18)	186(49)	200(44)
$(M-17)^-$	nd	169(9)	nd	171(18)	185(25)
$(M-29)^-$	143(23)	157(5)	173(14)	159(53)	173(18)
$(M-43)^-$	nd	nd	159(12)	nd	nd
m/z 46	(381)	(6)	(<0.5)	(<0.5)	(3)
m/z 35	(47)	(17)	(18)	(18)	(18)

[a]Percent abundance relative to the most abundant ion in the mass spectrum, with the exception of TLN's spectrum, where ions were normalized to the $(MHCl-H)^-$ ion.

Table 3-7. Methane electron-capture NCI-CAD (26 eV, 2.0 mtorr N_2) daughter mass spectral characteristics of the $(MHCl-H)^-$ ions of the tryptoline-HCl salts.

Ions[a]	TLN	MTLN	CH_3O-TLN	HTLN	HMTLN
P^-	207(20[b])	221(21)	237(12)	223(14)	237(21)
$(P-36)^-$	171(5)	185(32)	201(6)	187(58)	201(77)
$(P-38)^-$	nd	nd	199(7)	185(13)	199(40)
$(P-65)^-$	nd	nd	nd	158(5)	172(5)
m/z 35	(100)	(100)	(100)	(100)	(100)

[a]P is the parent ion, i.e. $(MHCl-H)^-$.

[b]Percent abundance relative to the most abundant ion.

Table 3-8. Methane electron-capture NCI-CAD (24 eV, 2.9 mtorr N_2) daughter mass spectral characteristics of the M^- ions of the tryptoline-HCl salts.

Ions[a]	TLN	MTLN	CH_3O-TLN	HTLN	HMTLN
P^-	172(100[b])	186(100)	202(7)	188(100)	202(100)
$(P-H)^-$	171(5)	185(43)	201(1)	187(21)	201(25)
$(P-15)^-$	157(1)	nd	187(100)	173(5)	187(5)
$(P-16)^-$	nd	170(2)	186(3)	172(2)	186(3)
$(P-29)^-$	143(76)	157(85)	171(1)	159(68)	173(58)
$(P-30)^-$	142(7)	156(17)	nd	158(57)	172(22)
$(P-43)^-$	nd	nd	nd	145(16)	nd
$(P-44)^-$	nd	nd	158(14)	144(37)	158(19)
$(P-45)^-$	nd	nd	157(2)	nd	157(4)
$(P-58)^-$	nd	nd	nd	nd	144(7)

[a]P is the parent ion, i.e. M^-.

[b]Percent abundance relative to the most abundant ion.

Table 3-9. Methane electron-capture NCI-CAD (24 eV, 2.9 mtorr N_2) daughter mass spectral characteristics of the $(M-H)^-$ ions of the tryptoline-HCl salts.

Ions[a]	TLN	MTLN	CH_3O-TLN	HTLN	HMTLN
P^-	171(95[b])	185(99)	201(13)	187(100)	201(100)
$(P-H_2)^-$	169(1)	183(2)	199(0.4)	185(2)	199(1)
$(P-15)^-$	nd	170(<0.3)	186(100)	172(7)	186(1)
$(P-16)^-$	nd	169(2)	nd	171(0.4)	185(2)
$(P-29)^-$	142(100)	156(100)	nd	158(81)	172(70)
$(P-44)^-$	nd	nd	157(18)	nd	157(9)
				145(3)	145(2)

[a]P is the parent ion, i.e. $(M-H)^-$.

[b]Percent abundance relative to the most abundant ion.

neutral molecule. The latter is supported by the presence of 46^- ions in the background. That NO_2 may have added to the molecule is further supported by the NCI-CAD daughter spectrum of the m/z 218 ion in the TLN-HCl spectrum. Fragmentation of this $(M+46)^-$ ion results in daughter ions at m/z 171 (loss of 47) and m/z 142 (loss of 76), both of relatively low abundance, and at m/z 46, the most abundant ion. The first two daughter ions are indicative of the TLN molecule. The 46^- ion could be NO_2^- as its CAD spectrum contains only a single daughter ion at m/z 16, O^-, presumably due to loss of NO. The NO_2^- ion could result from the reaction of N_2 and O_2 (from an air leak) in the CH_4 plasma. NO_2 may also originate from the decomposition of the sample in the reagent plasma as the m/z 46 ion is seen to increase with sample pressure. $(M+NO_2)$ adduct ions have been reported in the PCI and NCI spectra of other nitrogen-compounds, but with no explanation of their formation (98). However, as the compounds studied in this case contained nitro groups, they could serve as the source of the NO_2. The possibility that all of the adduct ions described above are not adduct ions, but are instead due to impurities, seems less likely, as the corresponding ions are not present for such components in the EI and PCI spectra.

The source of the air in the ion source and CI plasma is most likely due to the steady leak of air at the O-ring fittings of the solids probe. The reproducibility of the NCI mass spectra obtained on different days was much lower than that for the PCI mass spectra. This is probably directly attributable to the varying amount of air which can enter through the direct inlet during operation of the solids probe, depending upon the condition and tightness of the O-ring seals and the operator's technique. This susceptibility of CH_4 electron-capture NCI

spectra to air as an impurity has been previously noted (97,99,100). The formation and nonreproducibility of these adduct ions would result in an unpredictable decrease in the sensitivity when monitoring only a single ion, and could introduce large errors into the technique. However, these adduct ions could also serve to help identify the molecular weight of an unknown compound, just as the $(M+29)^+$ and $(M+41)^+$ adduct ions do in the PCI spectra. A more thorough study of the NCI conditions and CAD spectra of all the NCI ions would be helpful in order to obtain more conclusive evidence concerning the above. Due to the consistently higher sensitivity and reproducibility obtained with PCI of these compounds, this area was not pursued.

The abundant NCI $(M-H)^-$ fragment ions do not fragment as efficiently as the $(M+H)^+$ ions under the same set of CAD conditions (Tables 3-5 and 3-9). However, the $(M-H)^-$ ions do fragment characteristically, forming largely daughter ions resulting from the loss of 29 u, CH_2=NH, from the parent ion. The $(M-H)^-$ ion of 5-methoxytryptoline is an exception in that two major daughter ions are formed. The most abundant, 186^-, is presumably due to loss of the methyl group from the 5-methoxy group and then subsequent loss of CH_2=NH from this ion to produce the next most abundant daughter ion, 157^-.

Thus, electron-capture NCI of the tryptolines results in the formation of abundant $(M-H)^-$ and $(MHCl-H)^-$ ions, as well as several fragment and adduct ions. The NCI mass spectra varied considerably when obtained on different days, largely with respect to the relative abundance of the adduct ions and also the relative yields of the $(M-H)^-$ and $(MHCl-H)^-$ ions. The NCI-CAD of the abundant $(M-H)^-$ ions of each of the tryptolines yields a simple but unique daughter mass spectrum, dominated by

the daughter ion due to loss of CH_2=NH. The NCI-CAD of the $(M-H)^-$ ion of CH_3O-TLN was an exception to this, in that its most abundant daughter ion was due to loss of CH_3 followed by loss of CH_2=NH to yield the next most abundant daughter ion.

Optimization Studies

Mode of ionization. To determine a mixture component reliably at trace levels, the highest possible sensitivity and selectivity is desired. Therefore, the optimum mode of ionization and optimum conditions must be obtained. A comparison was made between positive and negative CI-SIM of the m/z 173, $(M+H)^+$, and m/z 171, $(M-H)^-$, ions, respectively, of TLN-HCl. The tandem mass spectrometer is able to sample alternately positive and negative ions from the ion source very rapidly. Therefore, it was possible to do this comparison on individual samples, without taking into account the actual sample amount, but ensuring the signals for both modes were not near their limits of detection. In doing this comparison, it was determined that the integrated area ratios, $(M+H)^+/(M-H)^-$, were very dependent upon the tuning of the ion optics, varying from 0.4 to 1000 for seven different tunings and measurements. In general, when the optics were tuned for the "best" sensitivity of each of the ionization modes for the ions of perfluoro-tri-N-butylamine, a mass calibration compound, PCI was more sensitive than NCI for TLN-HCl, with $(M+H)^+/(M-H)^-$ ratios averaging approximately 60. In addition, in order to have good sensitivity with SRM, it is necessary to have a good yield of the characteristic daughter ion from the characteristic parent ion. From Tables 3-5 and 3-9, it can be seen that the $(M+H)^+$ ions of all the tryptoline-HCl salts fragment to give higher yields of

their characteristic daughter ions than do the corresponding $(M-H)^-$ ions under the same, relatively harsh, CAD conditions. Therefore, PCI was chosen as the preferred ionization technique due to its greater sensitivity. However, NCI could offer an advantage with regard to selectivity. In analyzing complex mixtures directly, many components which lack electrophilic atoms are transparent to NCI, and thus chemical interference at the m/z of interest may be reduced. With methane's nearly universal protonating ability, however, almost all mixtures components are ionized. Due to the quantitative results below, however, NCI was not further investigated.

PCI-CAD collision energy. It has already been mentioned, that in order to obtain high sensitivity with SRM, it is necessary to have a good yield of a characteristic daughter ion from the characteristic parent ion of the analyte. The yield of daughter ions is very much dependent upon the collision energy and the collision gas pressure. The former parameter determines the energy which will be transferred to the parent ion during a collision, and thus the internal energy available for bond cleavage and daughter ion formation. The latter parameter is a measure of the number of collisions that a parent ion (and/or its daughter ions) will undergo in the transit of the collision region. Thus, it is important to optimize these parameters for the compounds of interest. The optimization of the CAD conditions was performed in two different manners. In the first study, the collision energy was varied during the vaporization and ionization of TLN-HCl from the solids probe, while obtaining daughter spectra over a limited mass range (m/z 140 to m/z 176). The variation with collision energy in the ratio of the intensities of the major daughter ion at m/z 144 and the parent ion at

m/z 173 revealed an optimum collision energy of 28 eV for the $(M+H)^+$ to $(M+H-29)^+$ reaction (Figure 3-2). However, the variation in the ion intensity ratios does not reveal any scattering losses of the parent and daughter ions. The presence of such losses would result in loss of sensitivity. In order to evaluate this aspect, a second collision energy study was performed with gas chromatographic introduction of TLN-HCl. The variation with collision energy of the GC peak areas of TLN-HCl resulting from the SRM of $(M+H)^+$ to $(M+H-29)^+$ was then obtained (also in Figure 3-2). From this study, a collision energy of ca. 22.5 eV was determined to be optimal for this reaction. The decrease in peak area following the maximum in both graphs may be due to focusing, scatter, or an increase in the yield of other daughter ions at the expense of the daughter ion of interest. As a compromise between the two methods, 26 eV was chosen as the collision energy to be used in the PCI-SRM studies.

PCI-CAD collision gas pressure. Similar studies were performed for the optimization of collision gas pressure for maximum CAD sensitivity. With the use of the solids probe for sample introduction, a large increase is seen in the $144^+/173^+$ ratio in going from 0.7 to 2.1 mtorr N_2 (Figure 3-3). With the chromatographic sample introduction, the peak area increases to a maximum as the collision gas pressure is increased, and then begins declining (Figure 3-3). This decline in peak area is most likely due to scattering losses of the parent ions. Although 4.0 mtorr N_2 was apparently the optimum pressure for the highest sensitivity, it was felt that operating the instrument at such high collision gas pressures for long periods of time might be detrimental to the vacuum system. Therefore, a collision gas pressure of 2.0 mtorr N_2 was selected for PCI-SRM assays for the tryptolines.

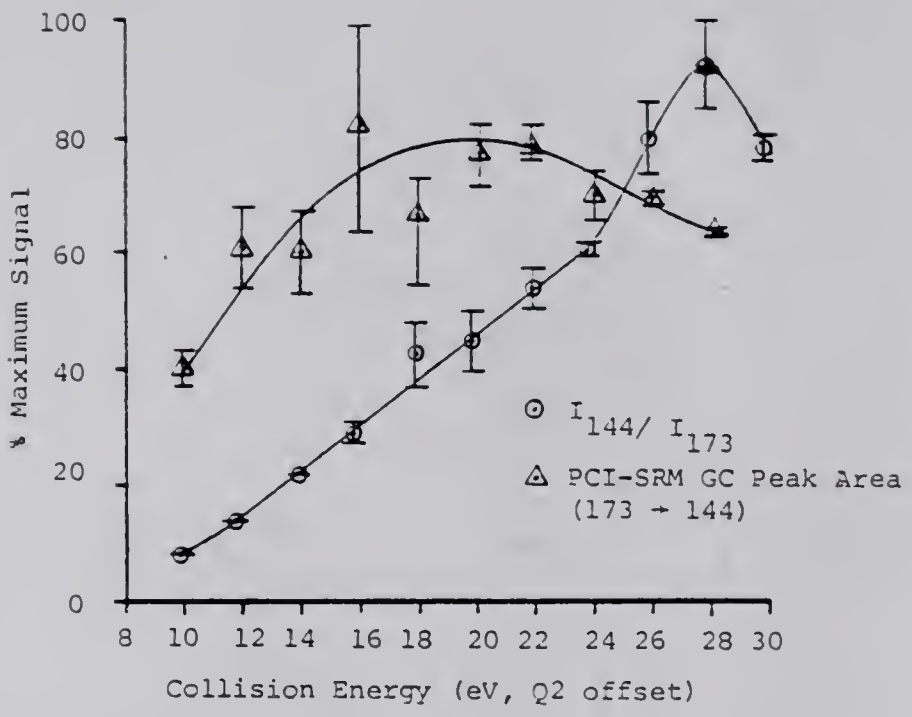

Figure 3-2. Optimization of the PCI-CAD collision energy for TLN-HCl.

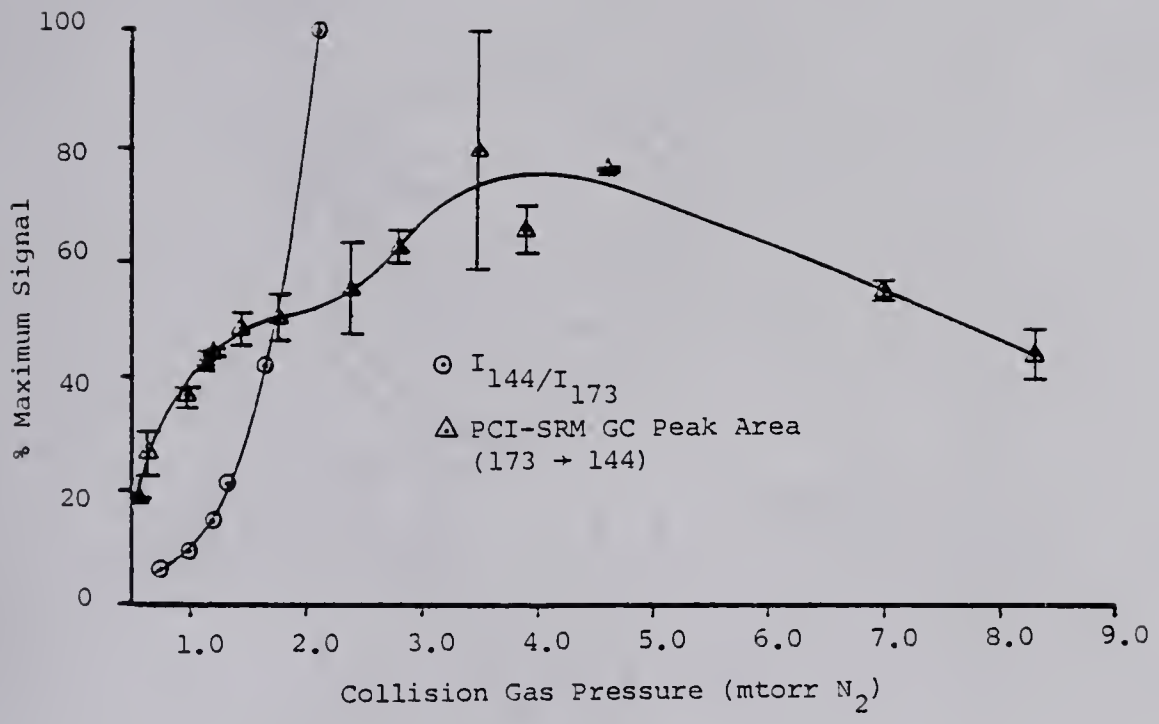

Figure 3-3. Optimization of the PCI-CAD collision gas pressure for TLN-HCl.

Quantitative Studies

With the short, packed GC column operated at the conditions used in the optimization studies, it was possible to get retention times for TLN- and MTLN-HCl of ca. 10 s. This allowed very rapid analyses of many samples much more conveniently than could be done by the solids probe (ca. 5 min per sample, typically). However, the GC peaks of the tryptolines exhibited extreme tailing, most probably due to solute interactions with the stationary phase and, especially, with the active sites on exposed hot metal in the GC/MS interface. This extreme tailing was not a large factor in the studies above, as the large levels of tryptoline used gave very high signal-to-noise ratios (S/N). However, the adsorption problem might become the limiting factor for trace analysis. Therefore, quantitative studies were performed by vaporization of the samples from a glass vial inserted in a heated solids probe.

In the PCI-SRM analyses, the most abundant and characteristic PCI ion of an analyte is selected as a parent ion by Q1, fragmented in Q2, and only the most abundant daughter ion is monitored by Q3. Thus, for PCI-SRM quantitation of TLN-HCl and MTLN-HCl, the reaction of their $(M+H)^+$ ions, m/z 173 and m/z 187, respectively, yielding the m/z 144 daughter ions, was monitored. The quantitation signal was obtained by integrating the ion current over the time during the vaporization of the analyte. The limit of detection (LOD) was defined as the amount of sample necessary to give a (S/N) of 3. The responses obtained from three solvent blanks were averaged and used as the chemical noise level.

The results of the assay of a series of standard TLN-HCl and MTLN-HCl solutions (Figures 3-4 and 3-5, and Tables 3-10 and 3-11) were used

to construct calibration curves (Figure 3-6). These calibration curves of the two tryptolines are very similar to each other, as would be expected from their chemical similarity. From all three figures, it can be observed that no discernable signal representative of the tryptolines occurs until the nanogram region is reached, whereupon the signal rises rapidly with increasing amounts of tryptolines. As more concentrated solutions were not analyzed, it was not possible to assess the linear dynamic range of the technique. The lack of reproducibility of the solids probe quantitation is reflected by the relative standard deviations of the integrated signals varying from ±20 to ±52 % for the triplicate analyses having S/N ratios greater than 3. Most of the lack of precision is probably due to the process of injecting and drying the 1.0 μL samples in the 5 μL sample vials. During this process, it was important to ensure that no air bubbles were enclosed in the sample solution, so that uniform drying would occur. In order to do this, it was necessary to "jiggle" the syringe needle in the sample solution until the air bubbles were excluded. However, this could have resulted in the drying of some of the analyte on the needle and its subsequent removal. With this amount of variability, the need for incorporating an internal standard for reliable quantitation is apparent.

In Figures 3-4 and 3-5, some of the analyte peaks are split or have shoulders on their leading edges. Based upon mass spectrometric evidence, this is not due to a separate component in the sample. Rather, it is most likely due to the uneven drying of the sample on different portions of the sample vials. As the vial is not heated evenly, this may lead to differential vaporization of the sample. An additional source of this peak splitting may be the interaction of the sample with

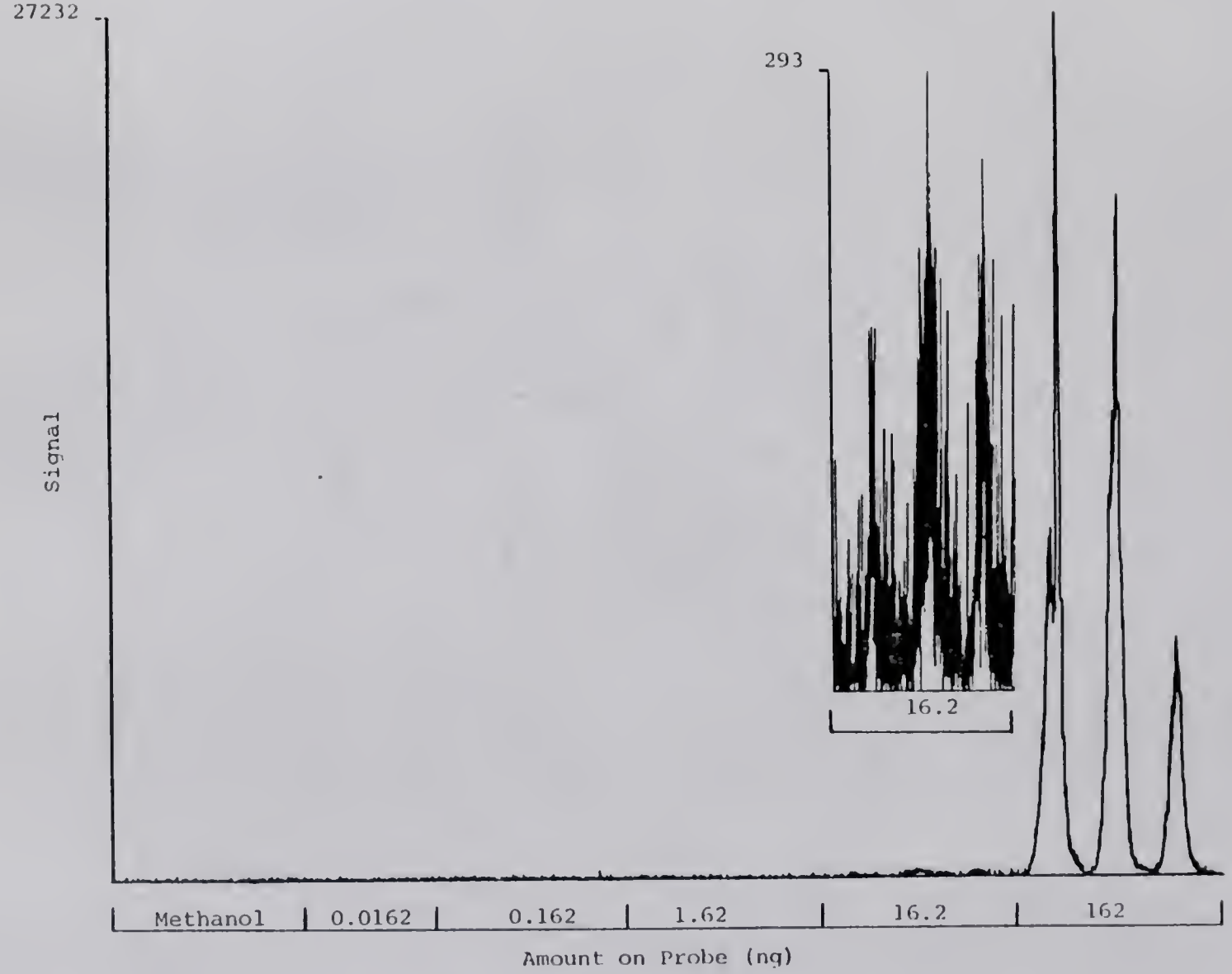

Figure 3-4. Solids probe PCI-SRM (173 → 144) quantitation of TLN-HCl.

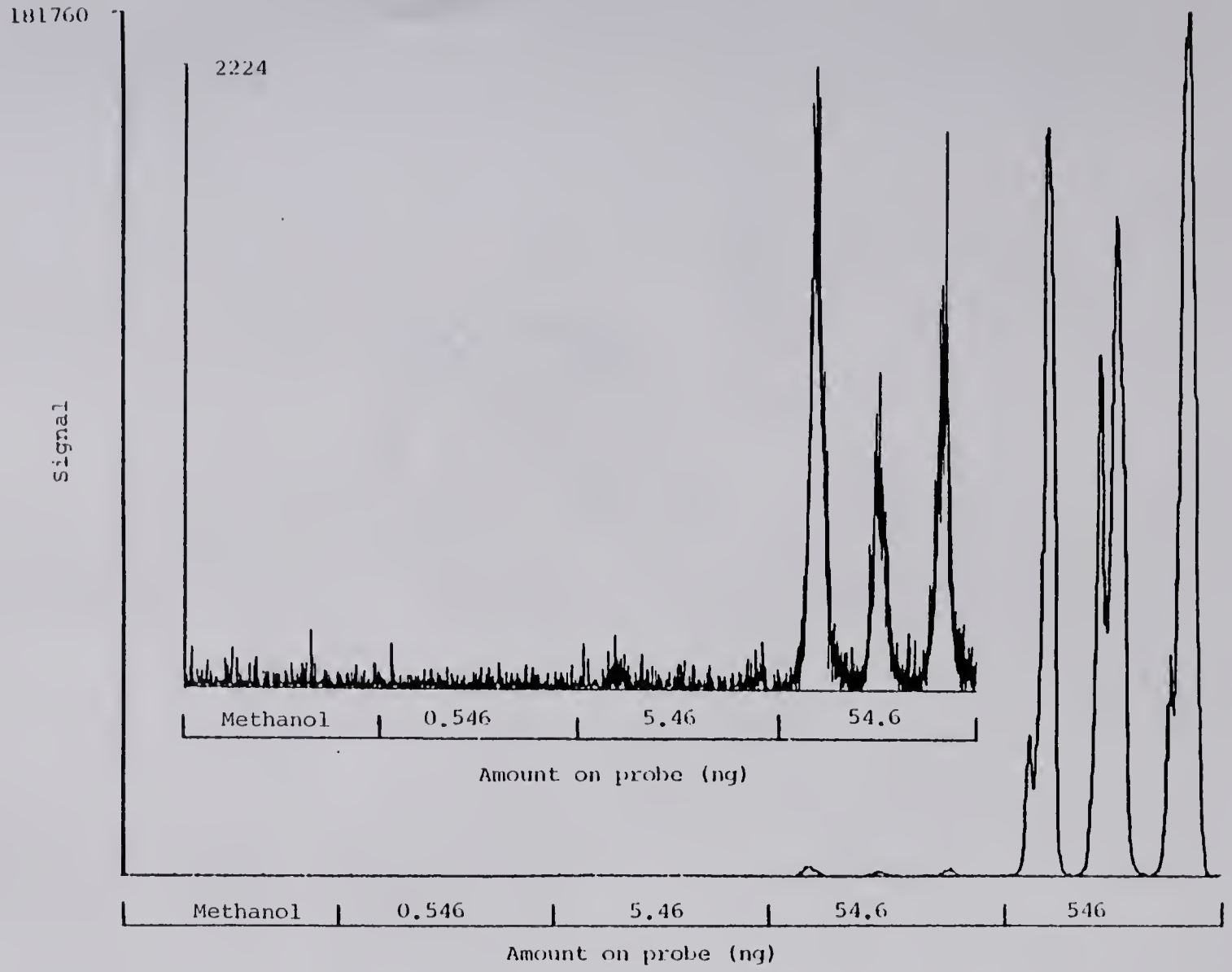

Figure 3-5. Solids probe PCI-SRM (187 → 144) quantitation of MTLN-HCl.

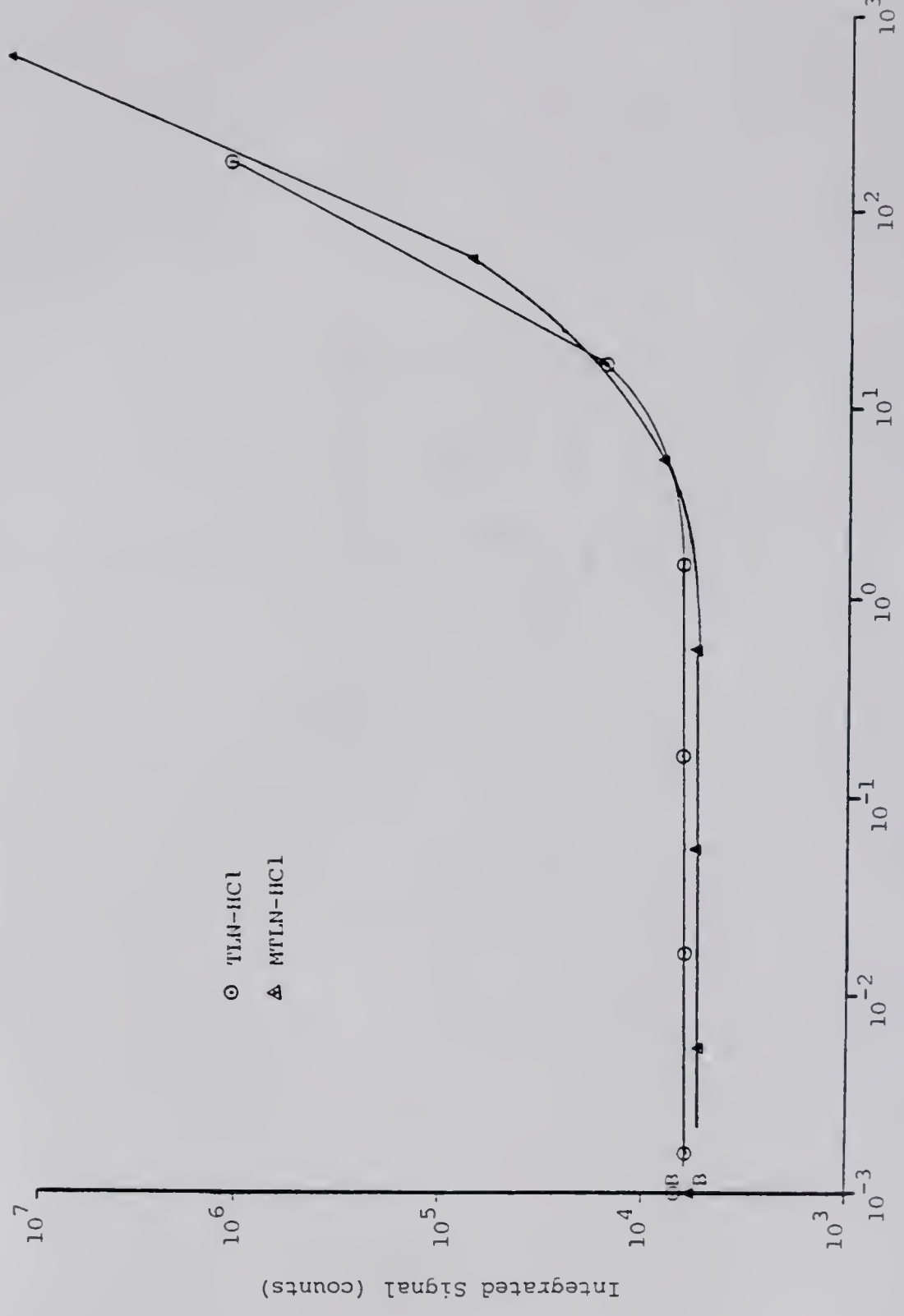

Figure 3-6. Calibration curves for the solids probe PCI-SRM quantitation of TLN-HCl and MTLN-HCl. B denotes the response of the methanol blank.

Table 3-10. PCI-SRM (173^+ --> 144^+) solids probe quantitation of TLN-HCl.

Amount on probe	I^a (144^+)			Mean I^a (144^+)	± %RSD[b]	S/N[c]
Blank	7.8	6.1	6.8	6.9	±12	-
1.62 fg	5.8	6.5	6.6	6.3	±7	0.9
16.2 fg	5.9	6.2	6.7	6.3	±6	0.9
162 fg	6.8	6.0	6.0	6.3	±7	0.9
1.62 pg	6.2	5.9	5.9	6.0	±3	0.9
16.2 pg	5.9	6.2	-	6.1	±4	0.9
162 pg	5.9	6.6	6.8	6.4	±7	0.9
1.62 ng	6.4	6.6	6.4	6.5	±2	1.0
16.2 ng	10.3	20.5	16.6	15.8	±32	2.3
162 ng	1105.9	1099.8	336.4	847.4	±52	124

[a] I is the integrated ion current (10^3 counts) for the m/z 144 daughter ion.

[b] %RSD is % relative standard deviation.

[c] S/N is the signal-to-noise ratio with the mean of the 3 blanks representing the noise level.

Table 3-11. PCI-SRM (187^+ --> 144^+) solids probe quantitation of MTLN-HCl.

Amount on probe	I^a (144^+)			Mean I^a (144^+)	%RSD[b]	S/N[c]
Blank	5.9	5.9	5.5	5.8	±4	-
5.46 pg	4.9	5.2	5.6	5.2	±7	0.9
54.6 pg	5.1	6.0	5.6	5.5	±8	1.0
546 pg	5.0	5.5	5.6	5.3	±6	0.9
5.46 ng	9.8	7.1	7.6	8.2	±18	1.4
54.6 ng	88.8	54.8	69.0	70.9	±24	12.3
546 ng	10338	14516	15499	13451	±20	2326

[a] I is the integrated ion current (10^3 counts) for the m/z 144 daughter ion.

[b] %RSD is the % relative standard deviation.

[c] S/N is the signal-to-noise ratio with the mean of the 3 blanks representing the noise level.

the glass wall. The sample not adhering intimately to the wall may be vaporized first, with hotter temperatures being necessary to vaporize the layer of sample which is interacting with the "active sites" of the glass wall.

From the definition of the limit of detection above, the limits of detection were calculated to be approximately 17 ng for tryptoline-HCl and 13 ng for methtryptoline-HCl on the probe. Tryptoline has been reported to be present in whole rat brain at levels ranging from 400 pg/g to 40 ng/g of tissue (51,53,56,59), while methtryptoline has not, as of yet, been reported to be present in brain tissue. As a typical rat brain weighs ca. 2 g, these LOD's are too high to provide reliable identification and quantitation of the tryptolines which may be present in individual rat brains. It should be possible, however, to determine the tryptolines in the brain homogenates pooled from several rats. However, much of the biological significance as to individual variation would be missing in this case.

Conclusion

In conclusion, it has been shown that the LOD's of PCI-SRM with solids probe sample introduction are not low enough for the determination of underivatized tryptolines in individual rat brain extracts. It should be possible, however, to use this technique with brain homogenates pooled from several rats. With pooled brain homogenates, this technique would eliminate to a large degree the extensive sample clean-up procedures which have been necessary for other methods of analysis and thus, reduce the possibility of artefactual tryptoline formation. In addition, the structural characterization possible with EI-CAD, PCI-

CAD, and NCI-CAD would allow much easier mass spectral structure elucidation of any unknown tryptolines, once isolated.

CHAPTER 4
TANDEM MASS SPECTROMETRY FOR THE IDENTIFICATION AND QUANTITATION OF TRYPTOLINE-HEPTAFLUOROBUTYRYL DERIVATIVES

Tryptoline-HFB Derivatives

Tryptoline has been reported to be present at the ng/g and pg/g of tissue level in brain extracts (51,53,54,56,59), while the presence of the other tryptolines studied in Chapter 3 has not, as yet, been reported in rat brain. Thus, in order to be able to investigate the tryptoline levels in individual rat brains, it is necessary to have a very sensitive and selective detection method. In the previous chapter it was determined that the limits of detection of solids probe PCI-SRM of the underivatized tryptolines were not low enough to accomplish this goal. Derivatization of the tryptolines is an efficient and straightforward method to enhance their chemical ionization sensitivity. Heptafluorobutyryl (HFB) derivatization of the tryptolines has been shown to give greatly enhanced sensitivity and lower limits of detection than reported for the underivatized tryptolines in Chapter 3 (33,53-56,59,101). In addition to increasing the sensitivity, HFB-derivatization improves the chromatographic properties of the tryptolines. Thus, with chromatographic introduction, an increase in the rate of sample introduction into the ion source per unit time might be realized, leading to a narrower, taller peak, a greater S/N ratio, and a still lower LOD. In addition, the speed of analysis may be substantially increased through the use of very short packed columns operated to allow

very short retention times of the analyte with minimal chromatographic separation (85). Rather than use long chromatographic separations, component separation and subsequent quantitation and identification of the tryptolines could be performed by MS/MS.

Thus, in this chapter the HFB-derivatives of the tryptolines (Table 4-1) will be studied by GC/MS and GC/MS/MS. The effects of source temperature and CAD conditions and their optimization will be discussed with regard to the sensitivity of the methods. Quantitative comparisons are made between methane positive and electron-capture negative CI and between selected ion and selected reaction monitoring with a 0.4 m packed column and a 18 m bonded phase fused silica capillary column. A practical application is shown for the determination of tryptoline in a HFB-derivatized crude extract of a rat brain.

Experimental

Materials and Reagents

All chemicals and reagents were of the highest purity available. The standards of the tryptoline-HFB derivatives were kindly supplied by Kym Faull, Ph.D., and Jack Barchas, M.D. (Department of Psychiatry and Behavioral Sciences, Stanford Medical Center, Stanford, CA). Their synthesis is detailed elsewhere (59). The HFB-derivatized crude extracts of rat brains were also supplied by Kym Faull and Jack Barchas and their preparation is described below. Aqueous solutions were prepared in doubly distilled deionized water. Ultrahigh purity methane (Matheson, Morrow, GA), helium, and zero grade nitrogen (Airco Industrial Gases, Research Triangle Park, NC) were used as a CI reagent, GC carrier, and collision gas, respectively.

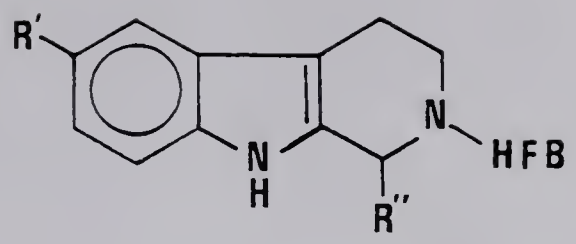

Table 4-1. Characteristics of the HFB-derivatives of the tryptolines of interest.[a]

			Molecular weight	
Compound	R'	R"	Parent	HFB-deriv.
TLN-HFB	H	H	172	368
MTLN-HFB	H	CH_3	186	382
CH_3O-TLN-HFB	CH_3O	H	202	398
HTLN-HFB	HO	H	188	384
HMTLN-HFB	HO	CH_3	202	398
HTLN-$(HFB)_2$	HFB-O	H	188	580
HMTLN-$(HFB)_2$	HFB-O	CH_3	202	594

[a]Tryptoline (TLN), methtryptoline (MTLN), CH_3O-TLN (5-methoxytryptoline), HTLN (5-hydroxytryptoline), HMTLN (5-hydroxymethtryptoline), and HFB (heptafluorobutyryl or C_3F_7CO).

Preparation of Extracts

Male rats (Sprague-Dawley, Simonson Labs, CA) were stunned with a blow to the head and quickly decapitated. The brains were rapidly removed, weighed, and homogenized in ice-cold perchloric acid (0.4 M, 5 mL/g of tissue). After centrifugation (15000 g, 20 min) the supernatant was adjusted to pH 3 with 1 N NaOH and passed through a C-18 reverse phase Sep-PAK® cartridge (Waters Associates, Milford, MA) which had been previously washed with acetonitrile (2 x 5 mL) and water (2 x 5 mL). The cartridge was then washed with water (2 x 500 µL) and eluted with acetonitrile (3 x 500 µL). The solvent was removed from the eluate in a stream of nitrogen and the residue was washed to the bottom of the collection tubes by the addition of acetonitrile (100 µL) which was also removed in a stream of nitrogen. The samples were then ready for chemical derivatization. The Sep-PAK cleanup procedure gives recoveries of added tryptolines of between 65 and 97% (59).

Chemical Derivatization (53)

The authentic compounds and dried extracts were treated with heptafluorobutyrylimidazole (Regis Chemical Co., Morton Grove, IL; 100 µL, 80 °C, 60 min) after which methylene chloride was added (2 mL). The solution was then extracted with water (four times with 2 mL each time) using centrifugation to separate the phases. The aqueous layers were discarded and the methylene chloride was evaporated in a stream of nitrogen. The dried residue (equivalent to ca. 500 mg of tissue for the brain extracts) was redissolved in ethyl acetate or methanol prior to injection onto the GC column.

Instrumentation

All data were collected with a Finnigan MAT (San Jose, CA) triple stage quadrupole GC/MS/MS equipped with a 4500 series ion source, pulsed positive and negative chemical ionization, and INCOS data system. The Finnigan 9610 gas chromatograph was equipped with packed and Grob-type capillary column injectors.

Samples were introduced into the ion source by either an 18-m DB-5 bonded-phase fused silica capillary column (compliments of J & W Scientific, Rancho Cordova, CA) inserted directly into the ion source or a short (38 cm x 0.75 mm i.d.) packed glass column, described more fully in Chapter 3. The capillary column was operated with a Grob-type splitless injector using a carrier gas split of 40 mL/min and a septum sweep of 9 mL/min; both were closed for 1 min following injection. The GC oven was held at 100 °C for 1 min following injection and, thereafter, increased linearly at a rate of 15 °C/min to a maximum of 275 °C. These conditions resulted in retention times for the tryptoline-HFB derivatives in the 9-13 min range. The short glass column was used for rapid sample introduction and provided minimal chromatographic resolution (retention time for TLN-HFB of ca. 55 s). The glass column was silanized with a 10 % solution of dimethylchlorosilane in toluene prior to manual packing with 3% OV-101 on 80/100 mesh Chromosorb 750. The GC/MS interface consisted of a glass-lined stainless steel tube direct inlet fitted with a microneedle valve. The interface and injection ports were maintained at 250 °C and 275 °C for packed and capillary column work, respectively. In the EI mode helium was used as the carrier gas. In the CI mode methane was used as a combined carrier/reagent gas. With the packed column CI analyses, the carrier gas flow was set to 10 mL/min

CH_4. The capillary column CI analyses were conducted with an average linear velocity of ca. 50 cm/s CH_4 (at 275 °C). Additional methane was added in both cases as makeup gas to give the required ion source pressure.

Procedures

Mass spectra of standards. Standards were introduced on the capillary column and the CI (100 eV electron energy, 1.0 torr CH_4 source pressure) and EI (70 eV electron energy) mass spectra were obtained with an ion source temperature of 100 °C in the Q3 normal MS mode. The effect of the ion source temperature on the fragmentation pattern of the heptafluorobutyryl derivatives of the tryptolines was studied with temperatures between 80 and 190 °C. Daughter spectra of M^- and $(M-HF)^-$ and $(M+H)^+$ ions were obtained at collision gas pressures of 1.0 and 2.8 mtorr N_2 and collision energies of 20 and 26 eV (Q2 offset) for negative and positive CI, respectively. The mass spectra acquired during the elution of each GC peak were averaged and background subtracted to yield a representative mass spectrum of each standard.

Collision energy and collison gas pressure studies. For each combination of collision energy and collision gas pressure, duplicate 1.0 µL injections of a standard solution of TLN-HFB were made onto the packed GC column (200 °C isothermal, source temperature at 190 °C). The GC peak areas resulting from the PCI-SRM of 369^+ to 156^+ and the NCI-SRM of 348^- to 179^- were determined with the data system. The collision energy studies were conducted at collision gas pressures of 1.5 and 1.7 mtorr N_2 for positive and negative CI-SRM, respectively. The collision gas pressure studies were conducted at collision energies of 25 and 18 eV for positive and negative CI-SRM, respectively.

Selected ion and selected reaction monitoring. All SIM experiments were conducted in the Q3 normal MS mode. The SRM experiments were conducted in the daughter scan mode with collision gas pressures of 1.0 and 2.8 mtorr N_2 and collision energies of 20 and 26 eV for negative and positive CI, respectively. The SRM daughter and the SIM ions were scanned over a 1 u wide window at 10 Hz. The ions and reactions monitored are listed in Table 4-2.

Quantitative studies. Serial dilutions were made of TLN-HFB with methanol to give solutions with concentrations ranging from 2.0 pptr to 200 ppm. In two separate studies, triplicate or single 1.0-μL injections were made of each standard onto the packed GC column (175 °C isothermal, giving a retention time of ca. 55 s for TLN-HFB). Quantitation was performed under the CI-SIM and CI-SRM conditions above with a source temperature of 100 °C, and an electron multiplier voltage of 1800 V with a preamp sensitivity of 10^{-8} A/V. The areas of the TLN-HFB GC peaks were determined by use of the current data system software and are reported in units of data system counts. Similar analyses were also done for quantitation of the crude brain extracts containing added amounts of TLN-HFB. With the capillary column, a single 1.0-μL splitless injection of each sample was made and quantitation was accomplished as for the packed column. The reproducibility of the capillary column was studied by measuring the peak areas of 6 replicate 1.0 μL injections of 2 different TLN-HFB standards with an electron multiplier voltage of 1300 V and a preamp sensitivity of 10^{-8} A/V.

Table 4-2. The ions and reactions monitored for the techniques used in the determination of the tryptoline-HFB derivatives in crude rat brain extract.

	Ions for CI-SIM		Reactions for CI-SRM	
Compound	$(M+H)^+$	$(M-HF)^-$	$(M+H)^+ \rightarrow (M+H-213)^+$	$(M-HF)^- \rightarrow 179^-$
TLN-HFB	369	348	369 --> 156	348 --> 179 (159[b])
MTLN-HFB	383	362	383 --> 170	362 --> 179 (159)
CH_3O-TLN-HFB	399	378	399 --> 186	378 --> 179 (159)
HTLN-HFB	385	384	385 --> 172	364 --> 179 (184,159)
HMTLN-HFB	399	378	399 --> 186	378 --> 179 (198,159)
HTLN-$(HFB)_2$	581	560	-[a]	560 --> 179 (381,379)
HMTLN-$(HFB)_2$	595	574	-[a]	574 --> 179 (395,393)

[a]Were not determined.

[b]Alternate daughter ions for multiple reaction monitoring.

Results and Discussion

Structure of the Tryptoline-HFB Derivatives

The derivatization of the tryptolines by heptafluorbutyryl imidazole under the experimental conditions used here resulted in the formation of a single mono-HFB derivative of each of the nonhydroxytryptolines and a single di-HFB derivative and a single mono-HFB derivative of each of the 5-hydroxytryptolines as determined by capillary GC/MS (Tables 4-1, 4-3, 4-4, and 4-5). The relative amounts of the di-HFB and mono-HFB derivatives of the hydroxytryptolines varied, presumably depending upon the experimental conditions. Based upon the mass spectral evidence below and that of others (33,53,55,59,101), the mono-HFB derivatives of the tryptolines have the HFB group replacing the hydrogen on the piperidine nitrogen. For the 5-hydroxytryptolines di-HFB derivatives, the HFB groups have replaced the hydrogens on the piperidine nitrogen and the phenolic oxygen. No evidence was observed for the replacement of the indolic nitrogen's hydrogen.

Mass Spectral Characteristics

EI normal mass spectra. The EI mass spectra of the tryptoline-HFB derivatives show prominent molecular ions and relatively abundant $(M-225)^+$ fragment ions (Table 4-3). These fragment ions presumably arise by loss of a $CH_2NCOC_3F_7$ group from the piperidine ring. In addition, the 9-methyl-tryptoline-HFB derivatives show an abundant fragment ion $(M-15)^+$, presumably due to the loss of the methyl side chain group. The mass spectra of the di-HFB derivatives of HTLN and HMTLN, although having prominent molecular ions, are dominated by the uncharacteristic

fragment ion at m/z 69, presumably $(CF_3)^+$. As in the underivatized tryptolines, there is again extensive fragmentation of the molecular ions. As it was desired to analyze samples with minimal, if any chromatograpic separation, it was necessary to use the softer chemical ionization to reduce the fragmentation of all components of the extracts. Thus, there would be less chemical noise at the m/z of the ions of interest.

PCI normal mass spectra. The methane PCI mass spectra of all the HFB derivatives are dominated by the protonated molecules $(M+H)^+$, and the methane adduct ions, $(M+29)^+$ and $(M+41)^+$ (Table 4-4). The only significant fragment ions seen in the spectra of the mono-HFB derivatives correspond to $(M+H-HF)^+$. The di-HFB derivatives of HTLN and HMTLN undergo much more fragmentation than do the mono-HFB derivatives. The fragment ions at $(M+H-198)^+$ are most likely due to the protonation of the phenolic-HFB group and subsequent loss of C_3F_7CHO from the $(M+H)^+$. The other fragment ions are characteristic of the HFB groups, and therefore not specific for the tryptolines: Ions at m/z 215, m/z 199, m/z 179, m/z 161, and m/z 141 presumably correspond to $(C_3F_7C(OH)_2)^+$, $(C_3F_7CHOH)^+$, $(C_3F_6COH)^+$, $(C_3F_5CHOH)^+$, and $(C_3F_4CHO)^+$, respectively.

NCI normal mass spectra. In contrast to PCI, the methane electron-capture NCI mass spectra (at a source temperature of 100 °C) of the derivatives yield molecular ions in relatively low abundance and show extensive fragmentation (Table 4-5). The most abundant ion in the NCI mass spectrum of each mono-HFB derivative and HTLN-$(HFB)_2$ is due to the loss of HF from the molecular ion, with less abundant ions being due to successive losses of F and HF. Although the $(M-HF)^-$ ion is abundant in the NCI mass spectrum of HMTLN-$(HFB)_2$, the most abundant ion corresponds

to $(M-198)^-$, which is also a major fragment ion of HTLN-$(HFB)_2$. This loss of 198 u is most probably due to a hydrogen rearrangement and subsequent loss of C_3F_7CHO from the phenolic portion of the molecular ion. In addition, all of the tryptoline-HFB derivatives yield relatively abundant ions at m/z 179, $(C_3F_6HCO)^-$, and m/z 178, $(C_3F_6CO)^-$, attributable to the heptafluorobutyryl portion of the molecule. For the NCI-SIM experiments, the most abundant and characteristic ion in the CI mass spectrum of each of the tryptoline derivatives is selected by Q3 for monitoring. Although the $(M-198)^-$ ion is the most abundant ion in the NCI of HMTLN-$(HFB)_2$, the more characteristic $(M-HF)^-$ ion was chosen for SIM. This would allow direct comparison to the SRM experiments below.

PCI-CAD daughter mass spectra. The PCI-CAD daughter spectra of HTLN-$(HFB)_2$ and HMTLN-$(HFB)_2$ were inadvertently not acquired. The PCI-CAD daughter mass spectrum of the $(M+H)^+$ ion of each of the derivatives is dominated by the daughter ion resulting from the loss of 213 u (either $NH_2COC_3F_7$ or $HN{=}COHC_3F_7$) from the protonated molecule; as such, this ion is characteristic of the parent tryptoline structure (Table 4-6). This characteristic loss from $(M+H)^+$ could be utilized in the MS/MS neutral loss mode to screen for other possible tryptolines and compounds with a similar derivatized amine structure. In addition, other, less abundant daughter ions were present and were useful structurally. Thus, a loss of the entire HFB group from the $(M+H)^+$ ions of the mono-HFB derivatives resulted in daughter ions of low abundance corresponding to the parent tryptoline structures at $(P-197)^+$. Daughter ions reflecting the R' and R" substituents also resulted with HTLN-HFB and HMTLN-HFB losing H_2O from their $(M+H)^+$ ions, while the mono-HFB derivatives of

Table 4-3. EI mass spectral characteristics of the tryptoline-HFB derivatives.

	M^+	$(M-15)^+$	$(M-169)^+$	$(M-197)^+$	$(M-199)^+$	$(M-212)^+$	$(M-213)^+$	$(M-214)^+$	$(M-225)^+$		
TLN-HFB	368(89)	-	199(17)	171(18)	169(16)	156(13)	155(23)	154(25)	143(100)	129(9)	115(22)
MTLN-HFB	382(62)	367(100)	213(11)	185(8)	183(6)	170(22)	169(34)	168(20)	157(16)	156(20)	154(33)
CH_3O-TLN-HFB	398(100)	-	229(17)	201(10)	199(10)	186(33)	185(34)	184(21)	173(92)	170(18)	158(62)
HTLN-HFB	384(69)	-	215(15)	187(11)	185(11)	172(25)	171(30)	170(23)	159(100)	158(19)	130(13)
HMTLN-HFB	398(62)	383(100)	229(12)	201(9)	199(13)	186(24)	185(34)	184(21)	173(23)	172(25)	170(32)
HTLN-$(HFB)_2$	580(58)	-	411(19)	383(25)	381(6)	368(24)	367(27)	366(11)	355(51)	158(84)	69(100)
HMTLN-$(HFB)_2$	594(25)	574(28)	425(5)	397(6)	395(2)	382(6)	381(7)	380(3)	369(4)	169(61)	69(100)

Table 4-4. PCI normal mass spectral characteristics of the tryptoline-HFB derivatives.

	$(M+41)^+$	$(M+29)^+$	$(M+H)^+$	$(M+H-HF)^+$	$(M+H-198)^+$	$(M+H-199)^+$	161^{+c}	141^{+d}
TLN-HFB	409(3)	397(12)	369(100)	349(8)	171(0.6)	170(0.6)	(0.4)	(0.9)
MTLN-HFB	423(2)	411(8)	383(100)	363(7)	185(2)	184(2)	(4)	(5)
CH_3O-HFB	439(1)	427(8)	399(100)	379(10)	201(0.6)	200(2)	(2)	(3)
HTLN-HFB	425(2)	413(12)	385(100)	365(9)	187(0.6)	186(0.2)	(2)	(3)
HMTLN-HFB	439(3)	427(10)	399(100)	379(8)	201(1)	200(1)	(5)	(4)

	$(M+41)^+$	$(M+29)^+$	$(M+H)^+$	$(M+H-HF)^+$	$(M+H-198)^+$	227^+	215^+	199^+	179^+	161^+	141^+
HTLN-$(HFB)_2$	621(2)	609(9)	581(100)	561(19)	383(34)	(10)	(41)	(62)	(85)	(38)	(36)
HMTLN-$(HFB)_2$	635(2)	623(11)	595(100)	575(13)	397(450	(13)	(32)	(77)	(92)	(36)	(38)

Table 4-5. NCI normal mass spectral characteristics of the tryptoline-HFB derivatives.

	M^-	$(M-HF)^-$	$(M-2HF)^-$	$(M-3HF)^-$	225^-	$(M-200)^-$	179^-	178^-	160^-
TLN-HFB	368(3)	348(100)	328(14)	308(13)	(0.3)	168(0.2)	(4)	(2)	(1)
MTLN-HFB	382(14)	362(100)	342(13)	322(6)	(2)	182(0.7)	(24)	(6)	(5)
CH_3OTLN-HFB	398(2)	378(100)	358(12)	338(14)	(0.2)	198(0.3)	(6)	(1)	(1)
HTLN-HFB	384(1)	364(100)	344(14)	324(14)	(0.1)	184(5)	(2)	(1)	(2)
HMTLN-HFB	398(3)	378(100)	358(14)	338(5)	(0.4)	198(14)	(5)	(1)	(3)

	M^-	$(M-HF)^-$	$(M-2HF)^-$	$(M-3HF)^-$	$(M-178)^-$	$(M-198)^-$	$(M-217)^-$	$(M-237)^-$	197^-	178^-	160^-
HTLN-$(HFB)_2$	580(2)	560(100)	540(7)	520(0.6)	402(0.3)	382(85)	363(2)	343(1)	(2)	(11)	(3)
HMTLN-$(HFB)_2$	594(0.4)	574(24)	554(0.3)	534(<.1)	416(4)	396(100)	377(2)	357(1)	(2)	(14)	(3)

MTLN, CH_3O-TLN, and HMTLN all show loss of CH_3 from their $(M+H)^+$ ions and their $[(M+H)-213]^+$ ions. The $(M+H)^+$ ions of the nonhydroxy- and 5-hydroxytryptoline derivatives fragment by loss of of $R"CH=NCOC_3F_7$ to yield daughter ions at m/z 144 and m/z 160, respectively. The daughter ion at m/z 173 in the CH_3O-TLN-HFB spectrum may also correspond to such a loss.

NCI-CAD daughter mass spectra. The NCI-CAD daughter spectrum of each M^- ion is dominated by the daughter ion at m/z 225, $(CH_2NCOC_3F_7)^-$ (Table 4-7). This ion corresponds to the prominent neutral fragment loss from the molecular ions in the EI mass spectra to yield the ions at $(M-225)^+$ (Table 4-3). This NCI-CAD daughter ion could be used in the MS/MS parent scan mode to screen for other compounds in the brain extract having a derivatized CH_2-NH substructure. The mono-HFB derivatives of HTLN and HMTLN yield, in addition to the m/z 225 ion, prominent $(P-200)^-$ daughter ions which could result from the combined loss of HF and $(C_3F_6H_2CO)$ from the M^- parent ion. This is supported by the abundant $(P-180)^-$ daughter ions in the NCI-CAD of their $(M-HF)^-$ fragment ions (Table 4-8). The NCI-CAD daughter ion mass spectra of the $(M-HF)^-$ ions of the non-hydroxytryptoline-HFB derivatives are dominated by the ion at m/z 179 corresponding to the $(C_3F_6OH)^-$ fragment of the derivatizing group (Table 4-8). Even though this ion is of low mass and low diagnostic value per se, selectivity is maintained in the MS/MS-SRM experiments due to the genetic relationship to the $(M-HF)^-$ ions. Although the $(M-HF)^-$ ions of HTLN-HFB and HMTLN-HFB yield abundant 179^- daughter ions, the most abundant daughter ions, $(P-180)^-$, are presumably due to the loss of $(C_3F_6H_2CO)$. The $(M-HF)^-$ ions of HTLN-$(HFB)_2$ and HMTLN-$(HFB)_2$ yield, in addition to the abundant 179^- ion, two prominent

Table 4-6. PCI-CAD daughter mass spectral characteristics of the $(M+H)^+$ ions of the HFB derivatives of the tryptolines.[a]

	P^+	$(P-15)^+$	$(P-18)^+$	$(P-197)^+$	$(P-213)^+$	b			
TLN-HFB	369(32[c])		-	-	172(0.9)	156(100)		144(2)	129(7)
MTLN-HFB	383(40)	368(1)	-	186(0.6)	170(100)	144(9)	155(4)		
CH_3O-TLN-HFB	399(46)	384(6)	-	202(0.4)	186(100)	173(3)	171(2)	158(2)	155(3)
HTLN-HFB	385(64)	-	367(15)	188(0.9)	172(100)	160(1)	145(2)	154(1)	
HMTLN-HFB	399(59)	384(1)	381(12)	202(0.3)	186(100)	160(7)	171(2)	366(3)	

[a] P is the parent ion, $(M+H)^+$.

[b] $(P-[HR"C{=}NCOC_3F_7])^+$

[c] Percent abundance relative to the most abundant ion.

Table 4-7. NCI-CAD daughter mass spectral characteristics of the M^- ions of the HFB-derivatives of the tryptolines.

	P^-	$(P-HF)^-$	$(P-200)^-$	225^-	179^-	178^-	159^-
TLN-HFB	368(42[a])	348(33)	-	(100)	(38)	(9)	(6)
MTLN-HFB	382(22)	362(1)	-	(100)	(2)	(4)	-
CH_3O-TLN-HFB	398(23)	378(9)	-	(100)	(12)	(2)	(3)
HTLN-HFB	384(100)	364(16)	184(6)	(25)	(14)	(4)	(3)
HMTLN-HFB	398(100)	378(18)	198(12)	(38)	(11)	(5)	-

	P^-	$(P-HF)^-$	$(P-H)^-$	$(P-H_2F)^-$	$(P-197)^-$	$(P-198)^-$	225^-	179^-
HTLN-$(HFB)_2$	580(61)	560(100)	579(22)	559(30)	383(2)	382(2)	(11)	(3)
HMTLN-$(HFB)_2$	594(100)	574(76)	593(77)	573(57)	397(8)	396(12)	(14)	(8)

[a]Percent abundance relative to the most abundant ion.

Table 4-8. NCI-CAD daughter mass spectral characteristics of the $(M-HF)^-$ ions of the HFB derivatives of the tryptolines.

	P^- [a]	$(P-HF)^-$	$(P-2HF)^-$	$(P-179)^-$	$(P-180)^-$	$(P-181)^-$	179^-	159^-
TLN-HFB	348(21[b])	328(1)	308(2)	169(5)	168(5)	167(4)	(100)	(29)
MTLN-HFB	362(16)	342(7)	322(0.3)	183(6)	182(1)	181(0.4)	(100)	(15)
CH_3O-TLN-HFB	378(19)	358(0.3)	338(0.5)	199(3)	198(7)	197(2)	(100)	(23)
HTLN-HFB	364(41)	344(1)	324(1)	185(3)	184(100)	183(1)	(84)	(25)
HMTLN-HFB	378(27)	358(15)	338(1)	199(7)	198(100)	-	(91)	(17)
HTLN-$(HFB)_2$	560(100)	540(1)	520(0.4)	381(23)	-	372(22)	(51)	(2)
HMTLN-$(HFB)_2$	574(99)	554(11)	553(3)[c]	395(71)	-	393(27)	(100)	(2)

[a]Parent ion (P)

[b]Percent abundance relative to the most abundant ion.

[c]$(P-HF-F)^-$.

daughter ions, $(P-179)^-$ and $(P-181)^-$, presumably due to the loss of C_3F_6HCO and C_3F_6HCHOH, respectively. The HFB-derivatives of HTLN and HMTLN are apparently more stable than the nonhydroxytryptolines as evidenced by the lower yield of daughter ions under the same CAD conditions. This can be attributed to the ability of the phenolic oxygen to stabilize the negative charge. This stabilizing effect also explains the large abundance of the $(P-180)^-$ daughter and the $(P-179)^-$ and $(P-181)^-$ daughter ions of their mono- and di-HFB derivatives, respectively.

For the determination of tryptolines in biological extracts by selected reaction monitoring, maximum sensitivity is obtained by monitoring the most abundant daughter ion from the most abundant and characteristic CI parent ion (Table 4-2). Although the 179^- ions are not the most abundant daughter ions for all of the HFB derivatives of the hydroxytryptolines, it was chosen for convenience purposes. This would allow the possibility of using the parent scan of 179^-, instead of several different selected reactions, for screening purposes. The yield of several daughter ions of high abundances can be exploited by multiple reaction monitoring (MRM). MRM would improve the selectivity, and thus, the reliability, of determining the tryptolines without much loss in sensitivity. In the NCI of HMTLN-$(HFB)_2$, the abundance of the $(M-HF)^-$ ion is only about one-fourth that of the most abundant $(M-198)^-$ ion. However, under NCI-CAD, the most abundant daughter ion of the $(M-198)^-$ ion represents only ca. 2 percent of the parent ion's abundance, while the 179^- daughter ion represents ca. 30 percent of the parent $(M-HF)^-$ ion. Thus, for increased sensitivity, the more characteristic, and more selective $(M-HF)^-$ ion fragmenting to the 179^- ion was chosen for SRM of HMTLN-$(HFB)_2$. Because the derivatives behave in a similar fashion under

CI-CAD conditions, and because of our particular interest in the natural occurrence of tryptoline in mammalian tissues, efforts were concentrated on this compound.

Optimization of Experimental Parameters

Source temperature. The relative intensities of the NCI molecular and fragment ions of TLN-HFB were greatly influenced by the ion source temperature (Figure 4-1). At a source temperature of 80 °C, the NCI spectrum was dominated by an intense $(M-HF)^-$ ion with relatively small contribution from the other ions. As the source temperature was increased, the amount of fragmentation in the NCI mass spectrum increased dramatically. In particular, the $(M-HF)^-$ ion decreased from approximately 67 percent of the reconstructed ion current at 80 °C to only 9 percent at 190 °C. This would represent a significant loss in sensitivity in the SIM and SRM techniques (selecting $(M-HF)^-$). This susceptibility of the fragmentation of these types of derivatives to experimental conditions in the ion source has been noted previously (102). In contrast, the PCI mass spectra showed little variability with source temperature (Figure 4-1). Because it was difficult to reproducibly maintain the ion source temperature below 100 °C and because contamination of the ion source occurs more rapidly at such low temperatures, subsequent analyses were run with an ion source temperature of 100 °C.

CAD conditions. In the collisionally activated dissociation process, the yield of the daughter ions is very much dependent upon the collision energy and the pressure of the collision gas, as was demonstrated in Chapter 3. With NCI-SRM (at a collision gas pressure of 1.7

mtorr N_2) the GC peak area from injections of TLN-HFB showed a maximum at a collision energy of ca. 20 eV (Figure 4-2a). At a collision energy of 18 eV, a maximum GC peak area was observed at a collision gas pressure of ca. 1.0 mtorr N_2 (Figure 4-2b). The decrease in signal after the maxima is due largely to an increase in the yield of other daughter ions. With PCI-SRM, the GC peak area showed a general increase in intensity with higher collision energy (Figure 4-2a) and with increased collision gas pressure (Figure 4-2b). These results, in conjunction with those of the ion source temperature study and the characteristics of the CI spectra, suggest that the PCI ions are much more stable than are the NCI ions. From Figure 4-2, collision energies of 20 eV and 26 eV and collision gas pressures of 1.0 mtorr and 2.8 mtorr N_2 were chosen as optimum for the negative and positive CI-SRM techniques, respectively.

Quantitative Studies

Standard calibration curves. To compare the sensitivities and limits of detection of the different techniques, calibration curves were obtained from analysis of standard TLN-HFB solutions (Figure 4-3). The calibration curves for all the techniques are summarized in Table 4-9. The limits of detection were calculated from the calibration data and corresponded to the amounts of TLN-HFB which would give GC peak areas three times greater than those obtained with solvent blank. The blank gave a visible response, presumably due to adsorption on the column and septum and subsequent desorption by the next injection (59). By frequent replacement of the septum and several injections of solvent between concentration series, this problem was reduced to a manageable

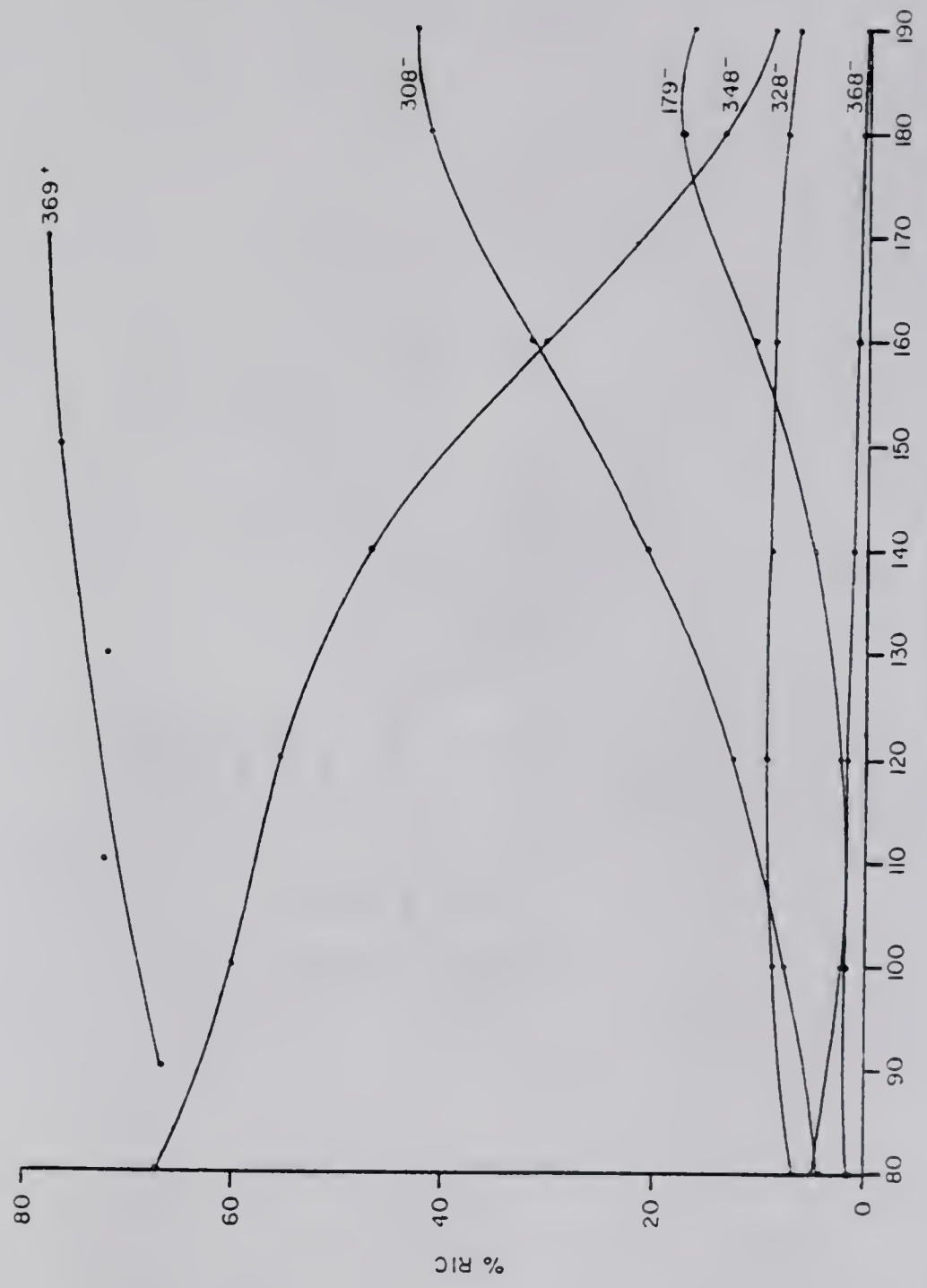

Figure 4-1. Effect of source temperature upon the fragmentation of tryptoline-HFB under CI conditions.

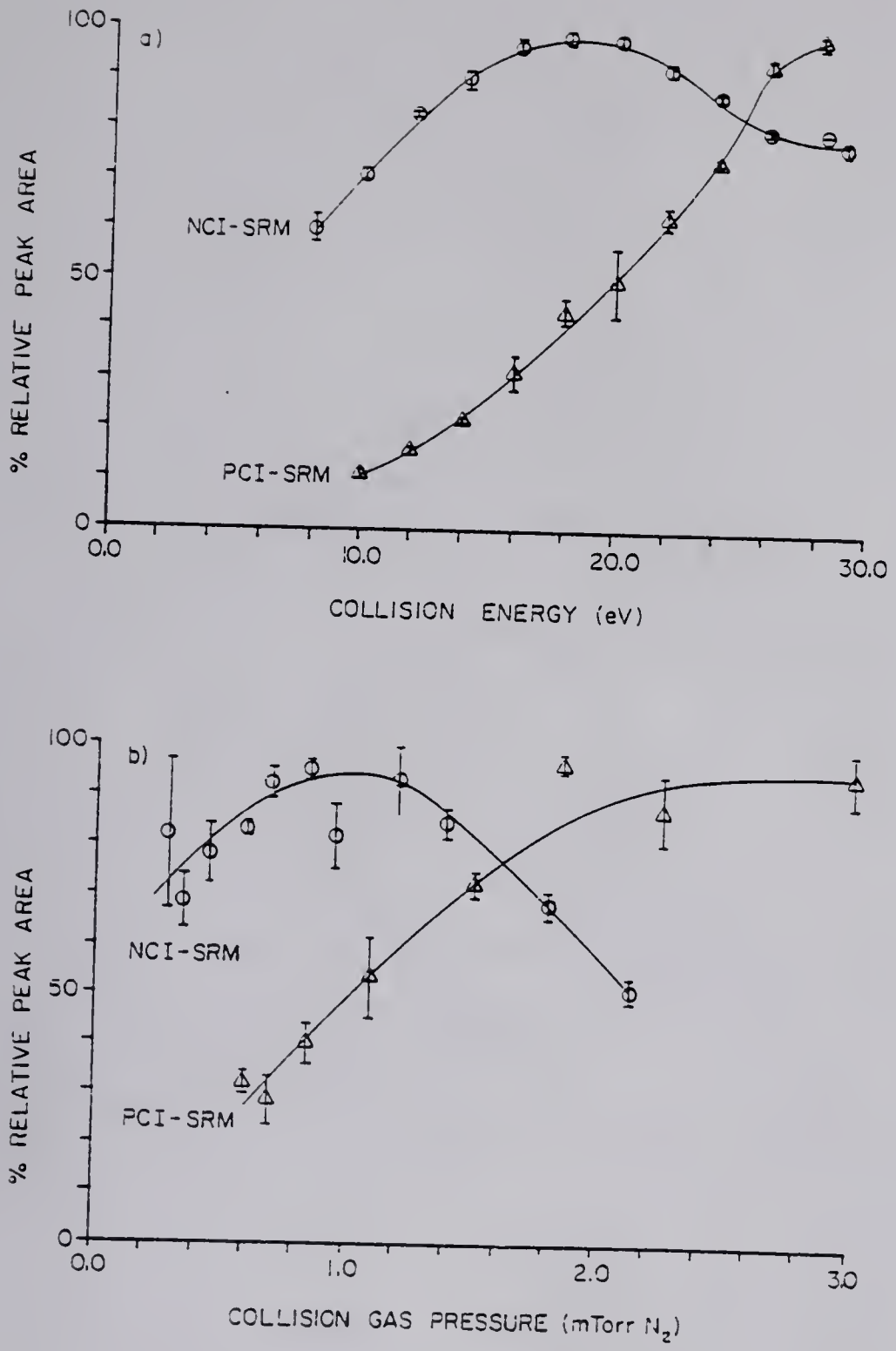

Figure 4-2. Effect of collision energy (a) and collision gas pressure (b) upon the tryptoline-HFB GC peak areas.

degree. The limits of detection thus defined are in the linear portion of the calibration curves (Figure 4-3). Figure 4-4 illustrates the method utilized with the short, packed GC column for determination of the noise and signal levels for the assay of the TLN-HFB standards. After monitoring the background for approximately 50 s, the filament was turned off and, simultaneously, 1.0 μL of a standard was injected. Approximately 10 s later, following elution of most of the solvent, the filament was turned on again, and monitoring continued. The signal or GC peak area of the TLN-HFB was determined by integrating the ion current above an estimated baseline threshold for a given number of scans, as shown in Figure 4-4. The noise was determined by a similar integration over the same number of scans (or a number of scans multiplied by an appropriate factor to equal the same number of scans) in the background-monitoring region of the chromatogram prior to injection of TLN-HFB (Figure 4-4). With the capillary column, the electron multiplier and filament remained off until approximately 90 s prior to elution of TLN-HFB. The signal or GC peak area of TLN-HFB and the noise level were determined as above in the regions of the chromatograms indicated in Figure 4-5. The signal-to-noise ratio (S/N) of all the limits of detection ranged from 2 to 6 with the exception of the packed column PCI-SRM limit of detection which had a S/N of 11 due to a high solvent blank response. All the calibration curves showed good linearity above their respective limits of detection for the range of concentrations studied. The linear portion of the log-log calibration curves of all the techniques had a mean slope of 1.0 ± 5%.

NCI is observed to give significantly better sensitivity and limits of detection than does PCI for these heptafluorobutyryl derivatives

(Table 4-9). This is readily explained by the highly electrophilic nature of the perfluorinated portion of the derivative and the underlying process of electron-capture NCI (94,95). The limits of detection obtainable with the NCI-SIM and NCI-SRM techniques are similar, despite the significantly greater sensitivity of the SIM technique. The lower sensitivity of the SRM technique is expected because of the inefficiencies of the CAD conversion of the parent ion to the daughter ion of interest and the daughter ion's subsequent mass analysis. However, the selectivity gained by this parent-daughter reaction reduces the chemical noise to a greater extent than the analytical signal and compensates to some extent for the lost sensitivity. This reduction in chemical noise is apparent in the relative heights of the chromatogram baselines in the NCI-SIM and NCI-SRM capillary column chromatograms (Figure 4-5). With the packed GC column, the reduction in chemical noise with PCI-SRM resulted in it having a limit of detection 13 times lower than that of the corresponding PCI-SIM (Figure 4-4). The difference in the limits of detection between the packed column GC techniques and those of the capillary column techniques may be due to ion optics tuning, conditions of the injection port and GC columns, and cleanliness of the ion source, lenses, and quadrupole rods. It was found that the LOD's of the techniques could vary by as much as a factor of 10 when obtained on different days. The above should represent what can be expected after cleaning the instrument and optimal tuning.

The reproducibility of the GC peak areas obtained with the packed column NCI-SRM for triplicate injections varied from $\pm$31 % relative standard deviation (RSD) near the limit of detection to $\pm$4.5 % RSD at levels well above the LOD. In a limited study with capillary column

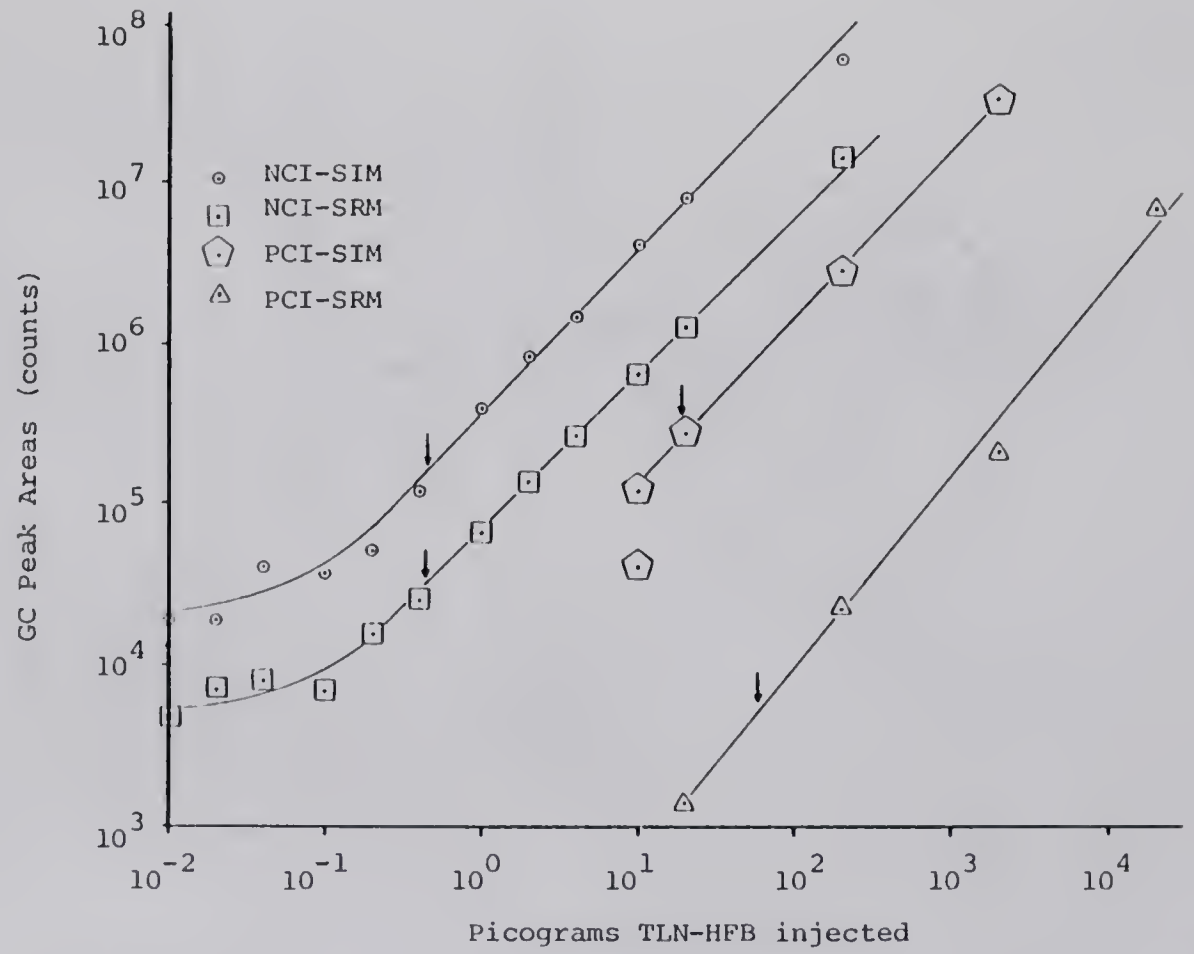

Figure 4-3. Calibration curves for the capillary GC techniques for the determination of TLN-HFB standards. The GC peak areas have been noise corrected. The signal obtained with the solvent blank is indicated by B. The arrows indicate the calculated limit of detection for each technique.

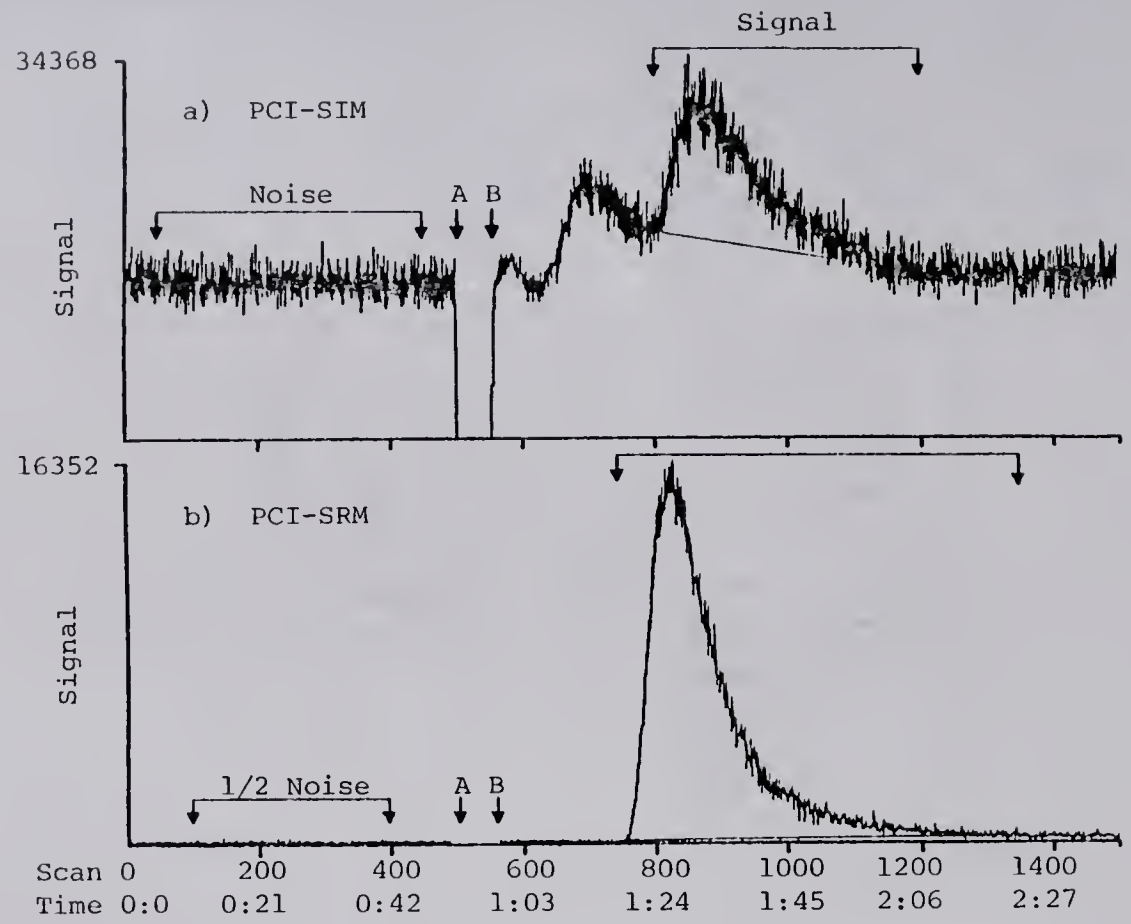

Figure 4-4. Comparison of packed column (a) GC/PCI-SIM (369) and (b) GC/PCI-SRM (369 → 156) of 20.3 ng TLN-HFB. The filament was turned off and the sample simultaneously injected at A. After elution of most of the solvent, the filament was turned on at B.

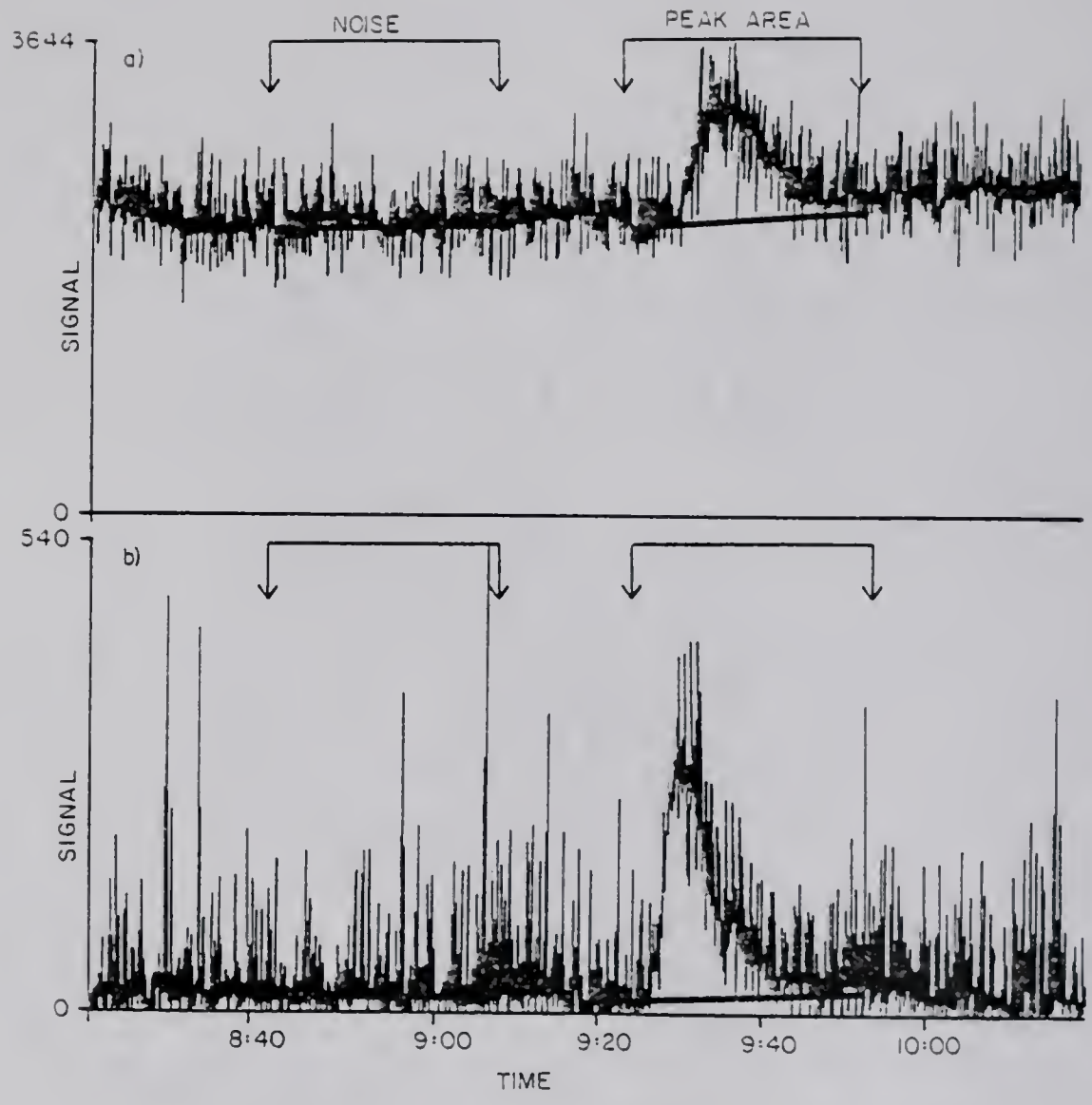

Figure 4-5. Chromatograms showing the method of determining the TLN-HFB peak areas and noise levels. Injections of TLN-HFB (0.2 pg above) were made onto an 18 m bonded-phase fused silica capillary column under NCI conditions. The signals (GC peak areas) were determined by integrating the ion current above the indicated thresholds over the scans indicated by the arrows. The noise levels were evaluated similarly for the same number of scans, as indicated, just prior to the sample peak. (a) GC/NCI-SIM. (b) GC/NCI-SRM.

Table 4-9. Characteristics of the calibration curves of standard concentrations of tryptoline-HFB.

	Packed Column[a]		Capillary column[b]	
Technique	LOD[c] (picograms)	Sensitivity[d] (counts/pg)	LOD[c] (picograms)	Sensitivity[d] (counts/pg)
NCI-SIM	0.07	2×10^6	0.50	3×10^5
NCI-SRM	0.11	1×10^5	0.45	7×10^4
PCI-SIM	5.7×10^3	9×10^1	19	2×10^4
PCI-SRM	4.3×10^2	1×10^2	60	4×10^2

[a]Single 1.0 µL injections of standard TLN-HFB solutions onto a short packed 3% OV-101 glass GC column at 175 °C isothermal.

[b]Single 1.0 µL injections of standard TLN-HFB solutions onto a 18 meter fused silica capillary GC column. See the text for detail of program rate and CI conditions.

[c]Limit of detection (LOD) calculated as the amount of tryptoline-HFB which would give a peak area approximately three times greater than the peak area of the methanol blank.

[d]Calculated as the slope of the calibration line in the range of linearity.

NCI-SRM, the precision of the GC peak areas for 6 replicate injections was slightly better, with ±10.2 % RSD near the limit of detection and ±8 % RSD at a level ca. 10 times higher than the LOD. The use of internal standards should substantially improve the precision of quantitation.

With regard to speed of analysis, the packed column techniques offer a definite advantage: with isothermal operation, TLN-HFB has a retention time of ca. 45 s. With background monitoring prior to injection, it is possible to make injections every 2 min. However, with the capillary column GC techniques, not only does TLN-HFB have a much longer retention time (ca. 9 min 30 s) but the column must be cooled in order to start the temperature programming necessary for the splitless injection technique. Thus, the cycle time between injections is on the order of 20 min.

Analyses of derivatized crude brain extracts. The use of a short packed GC column coupled with selected reaction monitoring was evaluated for rapid analyses of crude brain extract for trace quantities of the tryptoline-HFB derivatives. Injections of derivatized brain extracts (1.0 μL, corresponding to 10 mg of tissue), with and without TLN-HFB, were made successively after the return to baseline of the signal due to TLN-HFB (Table 4-10). The NCI-SRM signal from the extract with 2.5 ng TLN-HFB is approximately six times less than that for a 2.5 ng standard. There are undoubtedly a large number of derivatized components in the brain extract in relatively large quantities. In the CI source there is a limited pool of thermal electrons which are available for electron capture (95). Because there is little separation with the short GC column, the co-elution of electrophilic substances creates a competition for and a depletion of these thermal electrons by the

constituents having a greater electrophilicity and/or are present in larger quantities. Thus, the signal due to the relatively small amounts of TLN-HFB is quenched in the NCI techniques, making this approach unsuitable for analyses with the short GC column.

In contrast, PCI-SRM shows an enhancement of the signal from the crude brain extract with 2.5 ng of TLN-HFB by a factor of 23 in comparison to the signal due to 2.5 ng of the standard (Table 4-10). This can be rationalized by the equilibrium which exists in the ion source between the TLN-HFB molecules, the $(M+H)^+$ ions (from reaction with CH_5^+), and the M^- ions (from the capture of thermal electrons). As the formation of the negative ions is decreased due to the quenching effect, there are presumably more of the neutral TLN-HFB molecules available for the formation of positive ions. This enhancement effect may offer a method of improving the limits of detection of PCI techniques in general, especially with the enhanced selectivity of PCI-SRM. By continuously introducing into the ion source a perfluorinated reagent gas, the negative sample ions can be quenched and the positive sample ions enhanced. A preliminary study with the mass calibration compound perfluoro-tri-N-butylamine has shown a reduction in the packed column GC/PCI-SRM limit of detection for TLN-HFB standards by a factor of 10. This is, however, still above the limits of detection necessary for the determination of TLN-HFB at the sub-ppb level in crude brain extract.

Further analyses were performed with a 18 meter fused silica capillary GC column using a 15 minute temperature program. In the positive and negative CI-SIM analyses of brain extract containing TLN-HFB numerous GC peaks were detected (Figures 4-6a and 4-7a, respectively). With SRM the number of GC peaks detected has been reduced essentially to that

due to TLN-HFB (Figures 4-6b and 4-7b, respectively). These figures show that the improved chromatographic separation was not necessary for increased chemical selectivity, in that essentially the only responses in the SRM chromatograms were due to TLN-HFB. Rather, the chromatographic separation was necessary in order to reduce the number of electrophilic substances in the ion source during the elution of TLN-HFB, and thus, to prevent the quenching of the TLN-HFB NCI-SRM signal as was seen to occur in the packed column work above. The advantage of GC/MS/MS is more dramatically demonstrated in the NCI determinations of MTLN-HFB added to derivatized crude brain extract (Figure 4-8). In the NCI-SIM chromatogram the MTLN-HFB peak is a small shoulder on a much larger peak (Figure 4-8a). Identification and subsequent quantitation of MTLN-HFB would be difficult at best. However, with the increased chemical selectivity of NCI-SRM, identification and quantitation of MTLN-HFB would be straightforward (Figure 4-8b).

With the reduction of the chemical interferences in the PCI analyses provided by the chromatographic separation of the capillary column (Figure 4-7a) and the greater sensitivity of SIM over SRM (Table 4-9), the former would be preferable for the determination of tryptolines in heptafluorobutyryl derivatized crude brain extracts with methane PCI. However, even with its decreased limit of detection with the capillary column (Table 4-9), PCI-SIM does not have the sensitivity to detect the low picogram amounts of tryptolines which have been found in crude brain extracts.

Analyses of a derivatized crude brain extract on the capillary column by NCI-SIM and NCI-SRM showed there to be a GC peak corresponding to TLN-HFB with peak areas significantly above those of the solvent

Table 4-10. Matrix effects of the derivatized crude brain extract upon the positive and negative CI-SRM signals with the short packed column.[a]

Technique	Tryptoline-HFB Sample	Mean peak area (Counts ± %RSD[b])	(2.5 ng + extract)/2.5 ng
	2.5 ng	$1.3 \times 10^8 \pm 5$ %	
NCI-SRM	extract	$2.2 \times 10^4 \pm 20$ %	0.16
	2.5 ng + extract	$2.1 \times 10^7 \pm 5$ %	
	2.5 ng	$2.0 \times 10^5 \pm 2$ %	
PCI-SRM	extract	$8.3 \times 10^3 \pm 11$ %	23
	2.5 ng + extract	$4.5 \times 10^6 \pm 9$ %	

[a]Triplicate 1.0 µL injections on a short packed GC column at 175 °C.

[b]Percent relative standard deviation.

blank (sample to solvent peak area ratio of 6 and 19 for NCI-SIM and NCI-SRM, respectively) (Figure 4-9 and Table 4-11). Due to the greater complexity of the NCI-SIM chromatogram and the high background levels of the m/z 348^- signal during its elution (as noted in Figure 4-9a), it was more difficult to discern and quantitate the TLN-HFB peak. The NCI-SRM analysis, on the other hand, had a relatively low background level for the 348^- to 179^- signal (see Figure 4-9b) and the TLN-HFB peak was easily discerned and quantitated. Thus, NCI-SRM gives a more reliable determination of trace amounts of TLN-HFB in crude brain extracts. By comparing the TLN-HFB peak area of the crude brain extract with the peak area of another crude brain extract with 1.4 pg of TLN-HFB and taking into account the response of the solvent blank (Table 4-11), it was estimated that the amount of TLN-HFB detected in the former sample is approximately 0.4 picogram. This amount would correspond to approximately 40 pg of TLN per gram of rat brain tissue. In order to obtain a more reliable determination of the tryptolines present in brain tissue, further work with internal standards was necessary and is presented in Chapter 5.

This is a preliminary determination and serves to demonstrate the capability of GC/MS/MS to determine femtogram levels of heptafluorobutyryl derivatives of the tryptolines in derivatized crude brain extracts. The controversy over the possibility of artefactual formation mentioned in the introduction has not been addressed in this study and must be borne in mind. The work (Chapter 5) with isotopically-labelled tryptoline precursors will shed more light on this aspect of the tryptoline controversy.

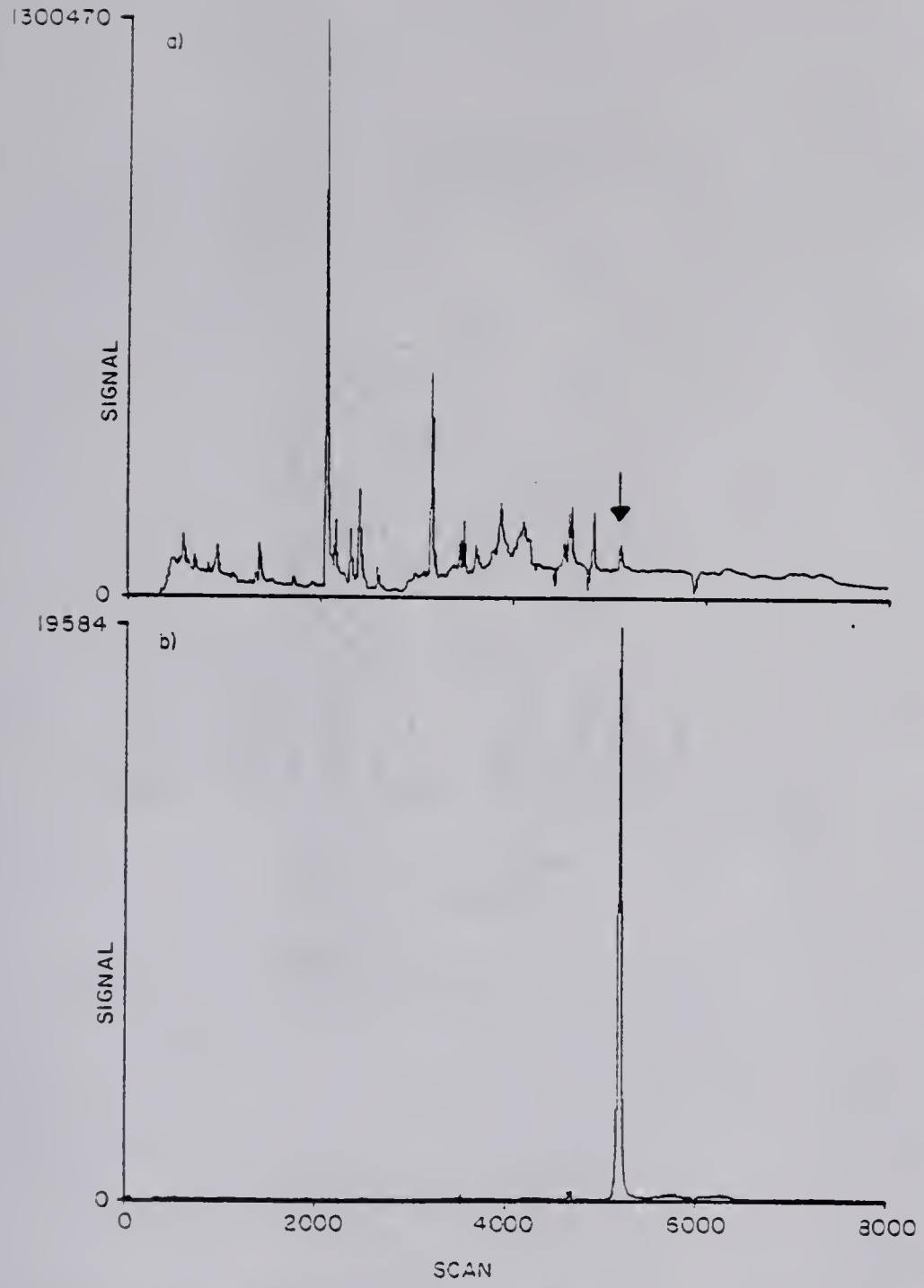

Figure 4-6. Comparison of (a) GC/NCI-SIM (348) and (b) GC/NCI-SRM (348 → 179) of derivatized crude rat brain extract with 1.4 pg of TLN-HFB (indicated by the arrow at a retention time of 9 min 28 s).

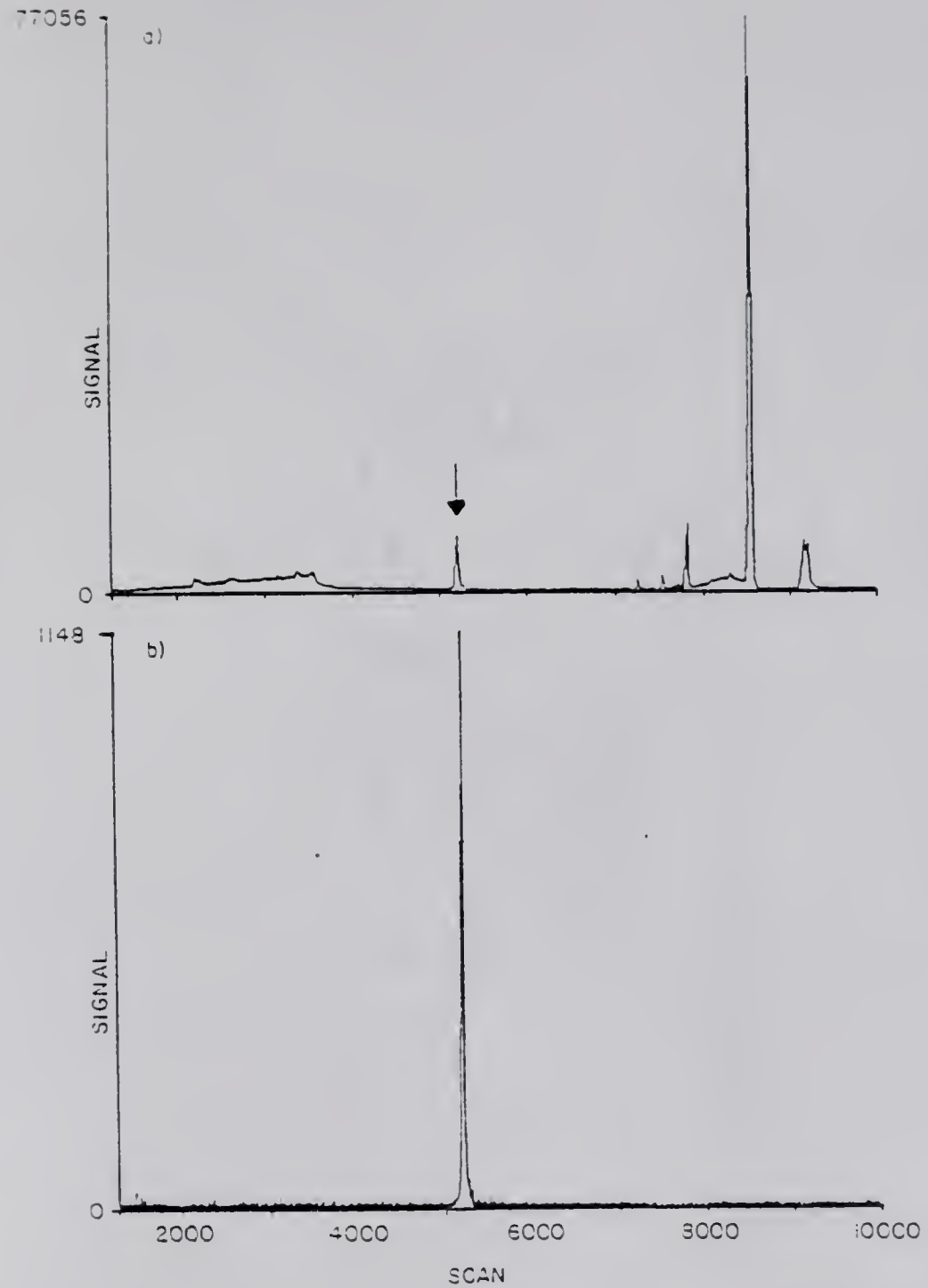

Figure 4-7. Comparison of (a) GC/PCI-SIM (369) and (b) GC/PCI-SRM (369 → 156) of derivatized crude rat brain extract with 2.5 ng of TLN-HFB (indicated by the arrow at a retention time of 9 min 28 s).

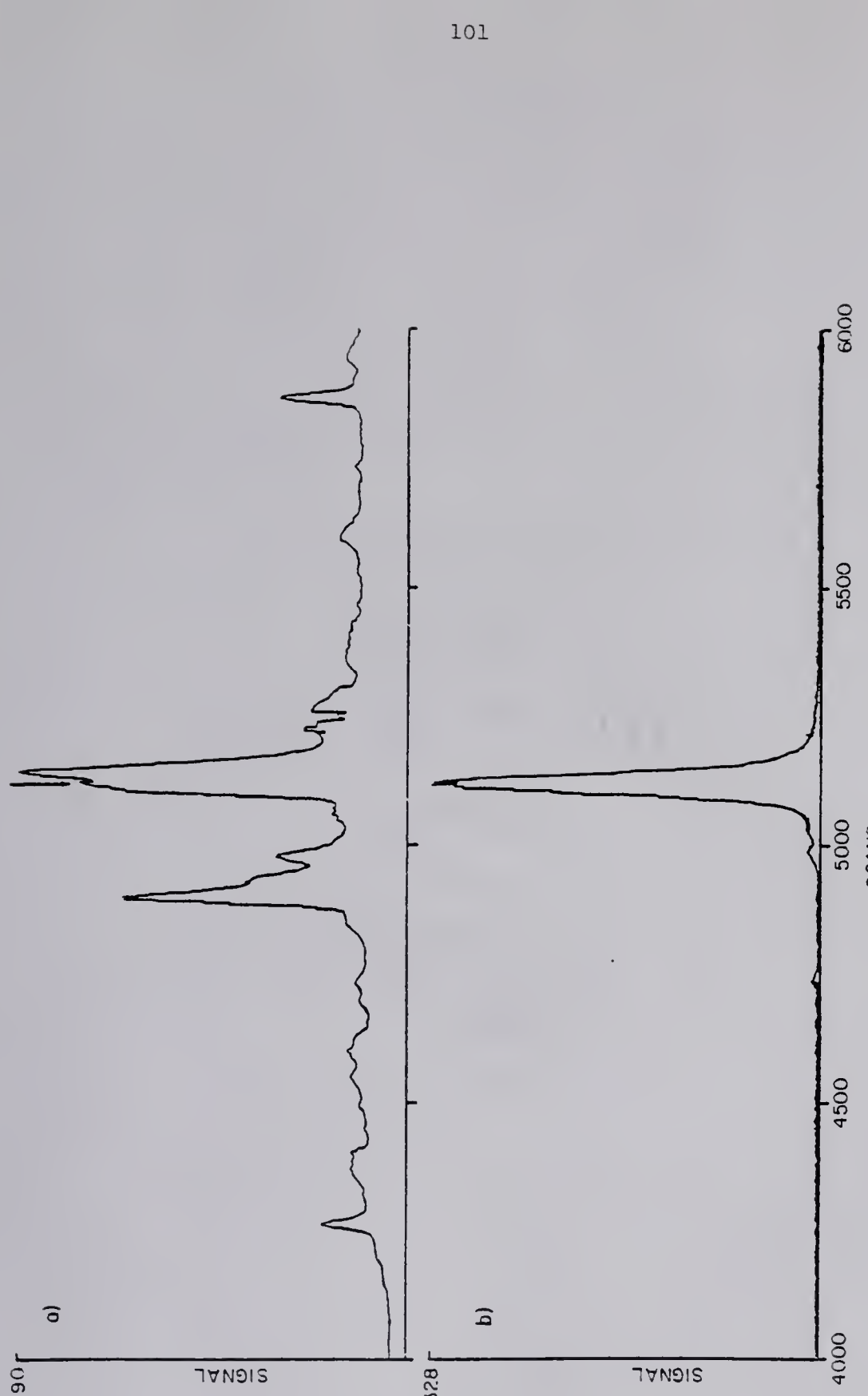

Figure 4-8. Comparison of (a) GC/NCI-SIM (362) and (b) GC/NCI-SRM (362 → 179) of derivatized crude rat brain extract with 36.5 pg of MTLN-HFB (indicated by the arrow at a retention time of 9 min 18 s).

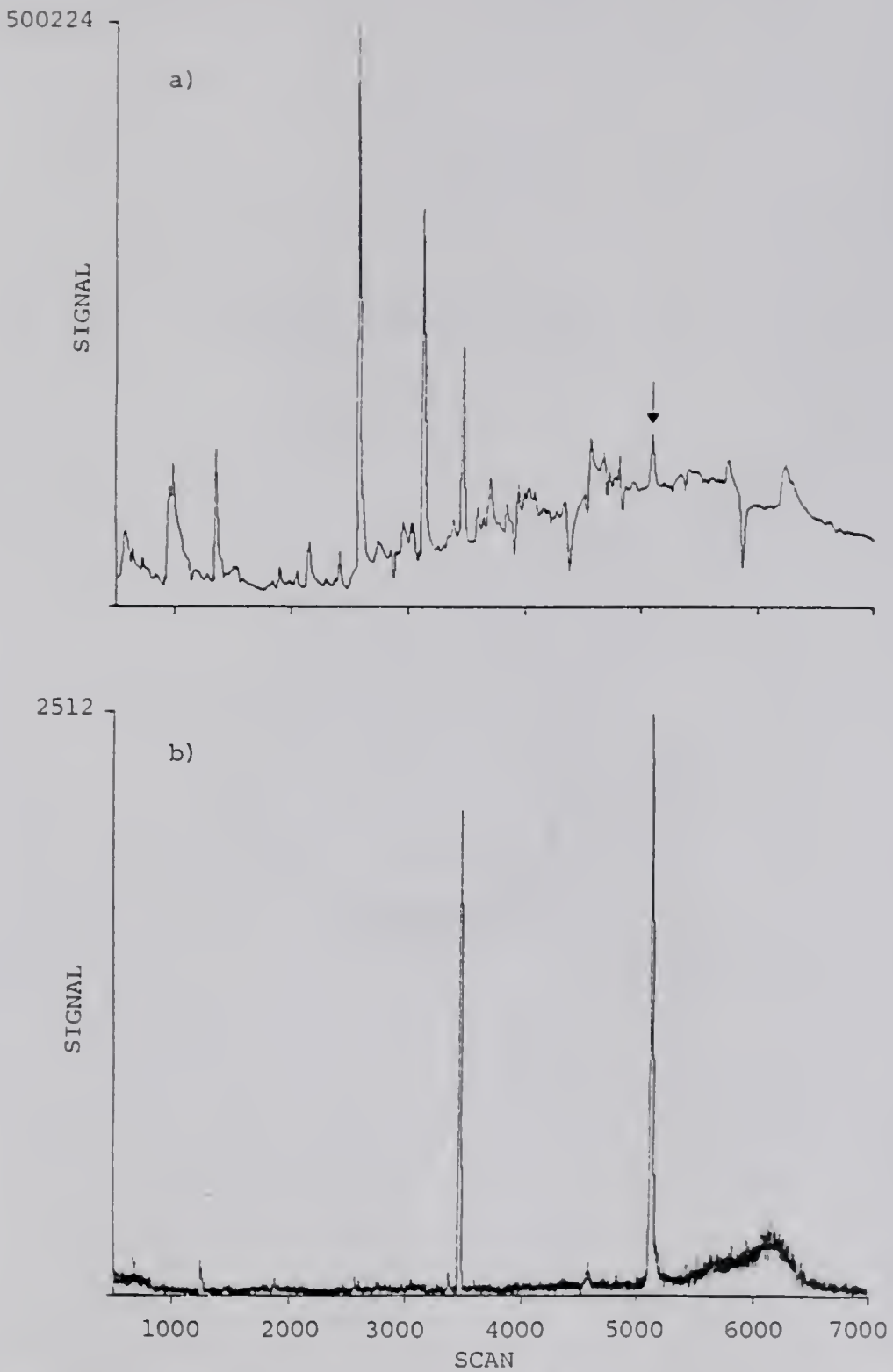

Figure 4-9. Comparison of (a) GC/NCI-SIM (348) and (b) GC/NCI-SRM (348 → 179) for the determination of TLN in HFB-derivatized crude rat brain extract.

Table 4-11. NCI Analyses of derivatized crude brain extract for the determination of tryptoline-HFB[a].

	Tryptoline-HFB GC Peak Area (counts)[b]		
Technique	Solvent blank	Extract	1.4 pg + extract
NCI-SIM	3.9×10^5	2.3×10^6	7.1×10^6
NCI-SRM	4.3×10^3	8.3×10^4	3.1×10^5

[a] 1.0 µL injections (equivalent to ca. 10 mg brain tissue) were made of each sample on a DB-5 fused silica capillary column.

[b] The peak areas of the SIM analyses are for single injections of each sample and those of the SRM analyses are the mean of duplicate injections. The SRM and SIM analyses were conducted on separate days with different electron multipliers and therefore the peak areas are not comparable.

Conclusion

The NCI-SRM technique, with capillary column chromatographic separation to prevent the quenching of the NCI signal, appears to be the method of choice for determining trace levels of tryptolines in heptafluorobutyryl-derivatized crude extracts of rat brain. With this technique, a preliminary determination of tryptoline in crude extract of a rat brain at a level of ca. 40 pg tryptoline per gram of brain tissue is reported. Although the PCI-SRM technique would allow rapid analysis with minimal chromatographic separation (on a short packed column), it lacks the sensitivity necessary to detect trace levels of the tryptolines.

CHAPTER 5
THE USE OF TANDEM MASS SPECTROMETRY FOR THE IDENTIFICATION AND QUANTITATION OF TRYPTOLINES IN RAT BRAIN EXTRACTS

In Chapter 4, a GC/MS/MS technique was developed which enabled the determination of HFB-derivatives of tryptoline standards at the sub-parts-per-billion level (femtograms injected). With this technique a very crude estimation was made of the amount of endogenous TLN in rat brains. In this chapter, with the use of deuterium-labelled TLN as an internal standard, TLN is more accurately quantitated in several individual rat brains. With the addition of deuterium-labelled tryptamine (d_4-TA), the presumed precursor of TLN, to two brain samples, an assessment is made of the possibility of artefactual formation of tryptoline during the sample clean-up procedure. In addition, the capillary column GC/NCI-SRM technique is extended to GC/NCI-multiple reaction monitoring (MRM). In this technique, instead of monitoring a single reaction, Q1 and Q3 are "jumped" between the parent ion and daughter ion, respectively, of the selected reactions characteristic of the analytes. Thus, the simultaneous screening and semi-quantitation of six compounds (four tryptolines and their presumed precursor indoleamines, Figure 5-1 and Table 5-1) are demonstrated in the derivatized extracts of individual rat brains. This permitted the relative amounts of these compounds to be studied.

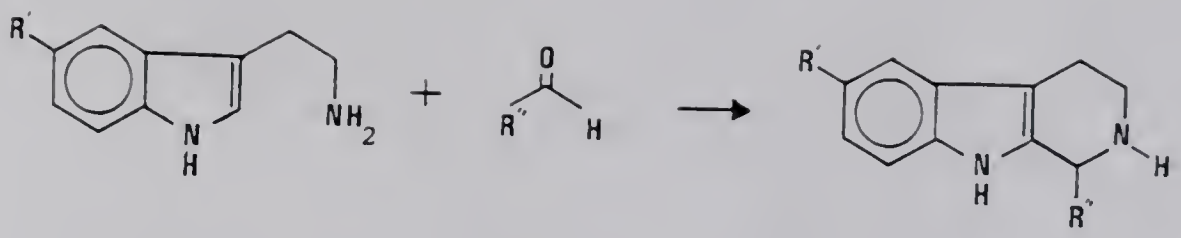

Figure 5-1. The Pictet-Spengler condensation reaction of an indoleamine and aldehyde to yield the corresponding tryptoline. See Table 5-1 for assignments of R' and R".

Table 5-1. Characteristics of the indoleamines and tryptolines.

Compound(Abbr.)	R'	R"	Molecular Weight Parent	Molecular Weight HFB-der.
Tryptamine(TA)	H	-	160	552[a]
5-Hydroxytryptamine(5HT)	HO	-	176	764[b]
Tryptoline(TLN)	H	H	172	368[c]
Methtryptoline(MTLN)	H	CH_3	186	382[c]
5-Methoxytryptoline(CH_3O-TLN)	CH_3O	H	202	398[c]
5-Hydroxytryptoline(HTLN)	HO	H	188	580[d]
5-Hydroxymethtryptoline(HMTLN)	HO	CH_3	202	594[d]

[a]Di-HFB, C_3F_7CO groups on both nitrogens.

[b]Tri-HFB, C_3F_7CO groups on phenolic oxygen and both nitrogens.

[c]Mono-HFB, C_3F_7CO group on piperidine nitrogen.

[d]Di-HFB, C_3F_7CO groups on phenolic oxygen and piperidine nitrogen.

Experimental

Materials and Methods

Chemicals and reagents. All chemicals and reagents were of the highest purity available. Aqueous solutions were prepared in doubly-distilled, deionized water. Tryptamine (TA) and 5-hydroxytryptamine (5-HT) were purchased commercially (Sigma Chemical Co., St. Louis, MO, and Regis Chemical Co, Morton Grove, IL, respectively). Deuterated 5-hydroxytryptamine was kindly supplied by colleagues at the NIH (to Dr. Faull) (103). Deuterated tryptamine was purchased commercially (Merck, Sharp, and Dohme, Canada). The standards of the tryptoline- and indoleamine-HFB derivatives were synthesized and kindly supplied by Olof Beck, Ph.D., Kym F. Faull, Ph.D., and Jack D. Barchas, M.D. (Department of Psychiatry and Behavioral Sciences, Stanford Medical Center, Stanford, CA) and their synthesis is detailed elsewhere (59). The preparation of the extracts of rat brains was also carried out at Stanford. Ultra-high purity methane (Matheson, Morrow, GA) and zero grade nitrogen (Airco Industrial Gases, Research Triangle Park, NC) were used as CI reagent/GC carrier and collision gases, respectively.

Synthesis of standards. Tetradeuterated analogues of tryptoline, methtryptoline, 5-hydroxytryptoline, and 5-hydroxymethtryptoline were prepared from the corresponding ($\alpha,\alpha,\beta,\beta$-$^2H_4$)-indoleamines (59). Synthesis of the deuterated tryptolines was carried out on a small scale (ca. 100 mg starting material), which precluded recrystallization of the final products. Identity of the deuterated tryptolines was confirmed by GC/MS of their PFP and HFB derivatives.

Preparation of brain extracts. Male rats (Sprague-Dawley, Simonson Labs, CA) were sacrificed by decapitation. The brains were rapidly removed, weighed, and homogenized in ice-cold perchloric acid (0.4 M, 5 mL/g tissue) containing either 1.94 ng of ($\alpha,\alpha,\beta,\beta$-$^2H_4$)-tryptamine ($d_4$-TA), 229 pg of (2,2,3,3-$^2H_4$)-TLN (d_4-TLN), or 1140 pg of d_4-TLN (Table 5-2). For two rat brains, either 1.94 ng d_4-TA or 1140 pg d_4-TLN were added separately after the Sep-Pak separation (Samples 8 and 9, Table 5-2). After centrifugation (15000 g, 20 min) the supernatant was adjusted to pH 3 with 1 N NaOH and passed through a C-18 reverse phase Sep-Pak® cartridge (Waters Associates, Milford, MA) which had been previously washed with acetonitrile (2 x 5 mL) and water (2 x 5 mL). The cartridge was then washed with water (2 x 500 µL) and eluted with acetonitrile (3 x 500 µL). The solvent was removed from the eluate in a stream of nitrogen and the residue was washed to the bottom of the collection tubes by the addition of acetonitrile (100 µL) which was also removed in a stream of nitrogen. The samples were then ready for chemical derivatization. The Sep-Pak clean-up procedure gives recoveries of added tryptolines of between 65 and 97 percent (59).

Chemical derivatization. The authentic compounds (HCl salts) and dried extracts were treated with heptafluorobutyryl imidazole in benzene (Regis Chemical Co., Morton Grove, IL; 50 percent solution in benzene, 100 µL, 85 °C, 60 min) after which methylene chloride was added (3 mL). The solutions were then extracted with water (4 x 2 mL) using centrifugation to separate the phases. The aqueous layers were discarded and the methylene chloride was evaporated in a stream of nitrogen. The dried residues were redissolved in ethyl acetate just prior to analysis.

Table 5-2. Treatment of the individual rat brains.

Rat	Brain wet weight (g)	Compound added during sample clean-up
1	1.77	229 pg d_4-TLN, during homogenization
2	1.77	229 pg d_4-TLN, during homogenization
3	1.56	229 pg d_4-TLN, during homogenization
4	1.81	1140 pg d_4-TLN, during homogenization
5	1.83	1140 pg d_4-TLN, during homogenization
6	1.87	1140 pg d_4-TLN, during homogenization
7	1.89	1140 pg d_4-TLN, after Sep-Pak®
8	1.85	1.94 ng d_4-TA, during homogenization
9	1.81	1.94 ng d_4-TA, after Sep-Pak®

Gas Chromatography/Tandem Mass Spectrometry (GC/MS/MS)

Data were collected with a Finnigan MAT (San Jose, CA) triple stage quadrupole GC/MS/MS equipped with a 4500 series ion source, pulsed positive and negative chemical ionization, INCOS data system, and a Finnigan 9610 gas chromatograph equipped with a Grob-type splitless capillary column injector.

Gas chromatographic separations were achieved using an 11 m DB-5 bonded-phase fused silica capillary column (compliments of J & W Scientific, Rancho Cordova, CA) inserted directly into the ion source, with methane as a carrier gas at an average linear velocity of 63 cm/s, measured at 275 °C. Injections of 1.0 μL samples were made with a carrier gas split of 28 mL/min and a septum sweep of 5 mL/min, with both closed for 1 minute following injection. For the quantitation of TLN in the extracts, the GC oven was held at 100 °C for 1 minute following injection, then increased linearly at a rate of 20 °C/min to a maximum of 275 °C. Following the reproducibility studies, the assay of the brain extracts for other tryptolines was conducted with an initial GC oven temperature of 60 °C. The injection port and interface were maintained at 275 °C. These latter conditions resulted in the retention times shown in Table 5-3.

All mass spectral data were acquired under methane electron-capture NCI conditions: source temperature of 100 °C, electron energy of 100 eV, emission current of 0.3 mA, and reagent gas of ca. 1.0 torr CH_4. The NCI mass spectra of the standards were acquired in the Q3 normal MS mode. Daughter spectra of the $(M-HF)^-$ ions of each of the standards were obtained at the previously optimized CAD conditions (Chapter 4): collision gas pressure of ca. 1.0 mtorr N_2 and collision energy of 20 eV

Table 5-3. Retention times and selected reactions monitored for the HFB-derivatives of the indoleamines and tryptolines in rat brain extract assays.

Compound	Retention time (min:s)	Selected Reactions Monitored[a]
d_0-TA-$(HFB)_2$	7:21	$532^- \rightarrow 307^-$
d_4-TA-$(HFB)_2$	7:21	$536^- \rightarrow 309^-$
d_0-5-HT-$(HFB)_3$	7:19	$744^- \rightarrow 519^-$
d_0-TLN-HFB	9:06	$348^- \rightarrow 179^-$
d_4-TLN-HFB	9:06	$352^- \rightarrow 179^-$
d_0-MTLN-HFB	8:49	$362^- \rightarrow 179^-$
d_4-MTLN-HFB	8:49	$366^- \rightarrow 179^-$
d_0-5-CH_3O-TLN-HFB	10:30	$378^- \rightarrow 179^-$
d_0-5-HTLN-$(HFB)_2$	10:18	$560^- \rightarrow 179^-$
d_4-5-HTLN-$(HFB)_2$	10:18	$564^- \rightarrow 179^-$
d_0-5-HMTLN-$(HFB)_2$	10:00	$574^- \rightarrow 179^-$
d_4-5-HMTLN-$(HFB)_2$	10:00	$578^- \rightarrow 179^-$

[a]NCI-SRM of $(M-HF)^-$ to the most abundant daughter ion.

(Q2 offset). The ion optics were tuned to maximize the 169^- daughter ion from the NCI-CAD of 452^- of perfluoro-tri-N-butylamine (PFTBA). The mass spectra acquired during the elution of each GC peak were averaged and background subtracted to yield a representative mass spectrum of each standard. For the quantitative assays, the resolution of Q1 and Q3 was adjusted to give approximately a 50% valley of the m/z 220 peak of the 219/220 pair in the EI-MS of PFTBA. All SIM experiments were conducted with Q3 and monitored the $(M-HF)^-$ ions. The SRM experiments were conducted in the daughter scan mode and monitored the selected reactions listed in Table 5-3. The SIM ions and the SRM daughter ions were scanned over a 1 u wide window at ca. 18 Hz. In the assays of brain extracts, the GC peak areas of the tryptolines' HFB-derivatives were determined using the data system and are reported in units of data system counts (1 count is ca. 1 ion detected, 1800 V on the electron multiplier with a preamp sensitivity of 10^{-8} A/V).

Results and Discussion

Mass Spectral Characteristics

Indoleamines. Derivatization of tryptamine and 5-hydroxytryptamine by heptafluorobutyryl imidazole yielded the di- and tri-HFB derivatives, respectively (Table 5-1 and Figure 5-1). The electron-capture NCI mass spectra of these compounds are dominated by the $(M-HF)^-$ ions and ions at m/z 225 and m/z 178, presumably due to $(CH_2{=}NCOC_3F_7)^-$ and $(C_3F_6CO)^-$, respectively, with only very weak molecular ions (Table 5-4). The characteristic $(M-HF)^-$ ions fragment under CAD conditions to yield several prominent daughter ions (Table 5-5). The most abundant daughter

ion of each compound is due to the characteristic loss of 225 u, presumably $CH_2=NCOC_3F_7$, from the parent ion to yield the ions at m/z 307 and m/z 519 for tryptamine-$(HFB)_2$ and 5-hydroxytryptamine-$(HFB)_3$, respectively. In order to achieve the maximum sensitivity and selectivity in the SRM assays of derivatized rat brain extracts, the fragmentation of the $(M-HF)^-$ ion to the most abundant daughter ion, $(M-HF-225)^-$, of each indoleamine derivative was monitored (Table 5-3).

Tryptolines. Heptafluorobutyryl imidazole was employed to convert the non-hydroxytryptolines to mono-HFB derivatives (with the HFB group replacing the hydrogen on the piperidine nitrogen) and the hydroxytryptolines to di-HFB derivatives (with the HFB groups replacing the hydrogens on the phenolic oxygen and the piperidine nitrogen) (Table 5-1 and Figure 5-1). The NCI mass spectra of the non-hydroxytryptoline HFB-derivatives are dominated by the $(M-HF)^-$ ions, with the molecular ions being present but of low relative abundance (Table 5-4). Although the $(M-HF)^-$ ions are prominent in the NCI mass spectra of the di-HFB derivatives of the hydroxytryptolines, the most abundant ions correspond to the $(M-198)^-$ ions, presumably due to the loss of C_3F_7COH from the phenolic portion of the molecular ions.

The NCI-CAD daughter spectra of the $(M-HF)^-$ ions of all the tryptolines are dominated by the daughter ion at m/z 179, presumably $(C_3F_6HCO)^-$ (Table 5-5). The $(M-HF)^-$ ions of the hydroxytryptolines also yield prominent daughter ions due to loss of 179 and 181 (presumably C_3F_6HCO and C_3F_6HCHOH, respectively) from the parent ion. In the assay of the brain extracts the selected reactions $(M-HF)^- \rightarrow 179^-$ were monitored (Table 5-3). Although the $(M-198)^-$ ions are the most abundant ions in the NCI mass spectra of the hydroxytryptolines' di-HFB

Table 5-4. NCI mass spectral characteristics of the HFB-derivatives of the indoleamines and tryptolines.

Compound	M^-	$(M-HF)^-$	$(M-198)^{-a}$	b	c
d_0-TA-$(HFB)_2$	552(<0.01)[d]	532(100)	354(4)	225(17)	178(22)
d_4-TA-$(HFB)_2$	556(<0.01)	536(100)	358(4)	227(22)	178(25)
5-HT-$(HFB)_3$	764(<0.01)	744(77)	566(15)	225(39)	178(100)
d_0-TLN-HFB	368(3)	348(100)	-	225(0.3)	179(4)
d_4-TLN-HFB	372(2)	352(100)	-	227(0.6)	179(20)
d_0-MTLN-HFB	382(14)	362(100)	-	225(1.5)	179(24)
d_4-MTLN-HFB	386(4)	366(97)	-	227(4)	179(100)
5-CH_3O-TLN-HFB	398(2)	378(100)	-	225(0.2)	179(6)
d_0-5-HTLN-$(HFB)_2$	580(<0.05)	560(31)	382(100)	225(0.7)	178(92)
d_4-5-HTLN-$(HFB)_2$	584(<0.05)	564(39)	386(100)	227(0.4)	178(22)
d_0-5-HMTLN-$(HFB)_2$	594(0.4)	574(24)	396(100)	225(0.1)	178(14)
d_4-5-HMTLN-$(HFB)_2$	598(0.2)	578(34)	400(100)	227(0.3)	178(14)

[a] $(M-C_3F_7COH)^-$. [b] $(CH_2NCOC_3F_7)^-$. [c] m/z 179, $(C_3F_6HCO)^-$; m/z 178, $(C_3F_6CO)^-$. [d] Percent abundance relative to the most abundant ion.

Table 5-5. NCI-CAD daughter mass spectral characteristics of the $(M-HF)^-$ ions of the HFB-derivatives of the indoleamines and tryptolines.

	Parent (P) -->		Daughter ions						
Compound	$(M-HF)^-$	-->	$(P-HF)^-$	$(P-179)^-$ [a]	$(P-180)^-$ [b]	$(P-181)^-$ [c]	$(P-225)^-$ [d]	$(P-257)^-$ [e]	[f]
d_0-TA-$(HFB)_2$	532(62)[g]	-->	512(56)	353(6)	352(7)	351(10)	307(100)	275(32)	178(47)
d_4-TA-$(HFB)_2$	536(67)	-->	515(38)	356(4)	354(2)	352(4)	309(100)	277(16)	178(43)
5-HT-$(HFB)_3$	744(51)	-->	724(40)	565(61)	564(40)	563(32)	519(100)	487(37)	178(5)
d_0-TLN-HFB	348(21)	-->	328(1)	169(5)	168(5)	167(4)	-	-	179(100)
d_4-TLN-HFB	352(26)	-->	332(1)	173(3)	172(0.2)	171(2)	-	-	179(100)
d_0-MTLN-HFB	362(16)	-->	342(7)	183(6)	182(1)	181(<1)	-	-	179(100)
d_4-MTLN-HFB	366(21)	-->	346(12)	187(5)	185(0.04)	183(0.03)	-	-	179(100)
5-CH_3O-TLN-HFB	378(19)	-->	358(0.3)	199(3)	198(7)	197(2)	-	-	179(100)
d_0-5-HTLN-$(HFB)_2$	560(196)	-->	540(2)	381(45)	-	379(43)	-	-	179(100)
d_4-5-HTLN-$(HFB)_2$	564(177)	-->	544(4)	385(27)	383(24)	381(2)	-	-	179(100)
d_0-5-HMTLN-$(HFB)_2$	574(99)	-->	554(11)	395(71)	-	393(27)	-	-	179(100)
d_4-5-HMTLN-$(HFB)_2$	578(101)	-->	558(10)	399(52)	397(16)	395(2)	-	-	179(100)

[a] $(P-C_3F_6HCO)^-$. [b] $(P-C_3F_6HCHO)^-$. [c] $(P-C_3F_6HCHOH)^-$. [d] $(P-CH_2NCOC_3F_7)^-$. [e] $(P-CH_2NCOC_3F_7-CHF)^-$.

[f] m/z 179, $(C_3F_6HCO)^-$; m/z 178, $(C_3F_6CO)^-$. [g] Percent abundance relative to most abundant daughter ion.

derivatives, they did not have a good yield of daughter ions under the NCI-CAD conditions used here. As the more characteristic $(M-HF)^-$ ions of these derivatives did give good yields of the 179^- daughter ion, these selected reactions were more sensitive and also more selective due to their higher m/z parent ions.

It is noteworthy that the characteristic fragmentation of the $(M-HF)^-$ ions of the tryptoline-HFB derivatives to the 179^- daughter ion could be advantageously used to screen HFB-derivatized tissue extracts in the parent scan mode for the presence of unreported tryptolines in the manner of Perchalski, Yost, and Wilder (104). In the parent scan MS/MS mode, Q1 is scanned over a specific mass range, allowing parent ions of varying m/z to undergo CAD in Q2 while Q3 transmits only a specific daughter ion of interest, i.e. 179^-. Thus, only parent ions yielding a 179^- daughter ion would give a response at the detector. Identification of these parent ions could then be made from a complete daughter mass spectrum of each parent ion. Such experiments are currently underway in this laboratory.

Assay of Derivatized Rat Brain Extracts

With chromatographic separation of the heptafluorobutyryl derivatives of the tryptolines on a fused silica capillary column, it was possible to obtain limits of detection for TLN-HFB of 500 and 450 femtograms injected for NCI-SIM and NCI-SRM, respectively (Chapter 4). Although both of these techniques have the sensitivity necessary to detect the trace levels of tryptolines, the added selectivity of MS/MS increases the reliability of identification and quantitation of these trace compounds in brain extracts. Although there is a GC peak at the

retention time of authentic TLN-HFB in the NCI-SIM chromatogram of HFB-derivatized crude extract of a rat brain (Figure 5-2a), interference from other unresolved components would lead to difficulty in obtaining reliable identification and quantitation. However, NCI-SRM was transparent to the interfering components and the well-defined GC peak due to TLN-HFB resulted in reliable identification and quantitation (Figure 5-2b). In addition, because of the complexity of the chromatograms which are obtained in conventional GC/MS, even with SIM, the analyte peak may be completely obscured by other, coeluting substances. This is dramatically demonstrated by the lack of a discernible GC peak for MTLN-HFB with NCI-SIM (Figure 5-3a). This lack of selectivity in GC/MS may be one reason why MTLN has not been reported in brain extracts by other researchers. With NCI-SRM, however, the selectivity was greatly enhanced and produced a clean chromatogram with an intense GC peak at the retention time of authentic MTLN-HFB (Figure 5-3b).

Artefactual tryptoline formation. In order to determine if artefactual formation of TLN is occurring during the sample clean-up procedure, 1.94 ng of d_4-TA was added to two brain extracts either during the brain homogenization step or after the Sep-Pak extraction (Samples 8 and 9, Table 5-2). With NCI-SRM, the HFB-derivatized extracts of the 2 rat brains were analyzed for the presence of the d_0- and d_4-isomers of TA-$(HFB)_2$ and TLN-HFB. In the d_4-TLN-HFB NCI-SRM chromatograms, there were very small peaks at the retention time of authentic d_4-TLN-HFB (Figure 5-4c and Table 5-6). The presence of d_4-TLN-HFB indicates the possibility of artefactual formation of tryptoline from the condensation of tryptamine with formaldehyde during the sample clean-up procedure. However, even though the level of added d_4-TA was up to 6 times greater

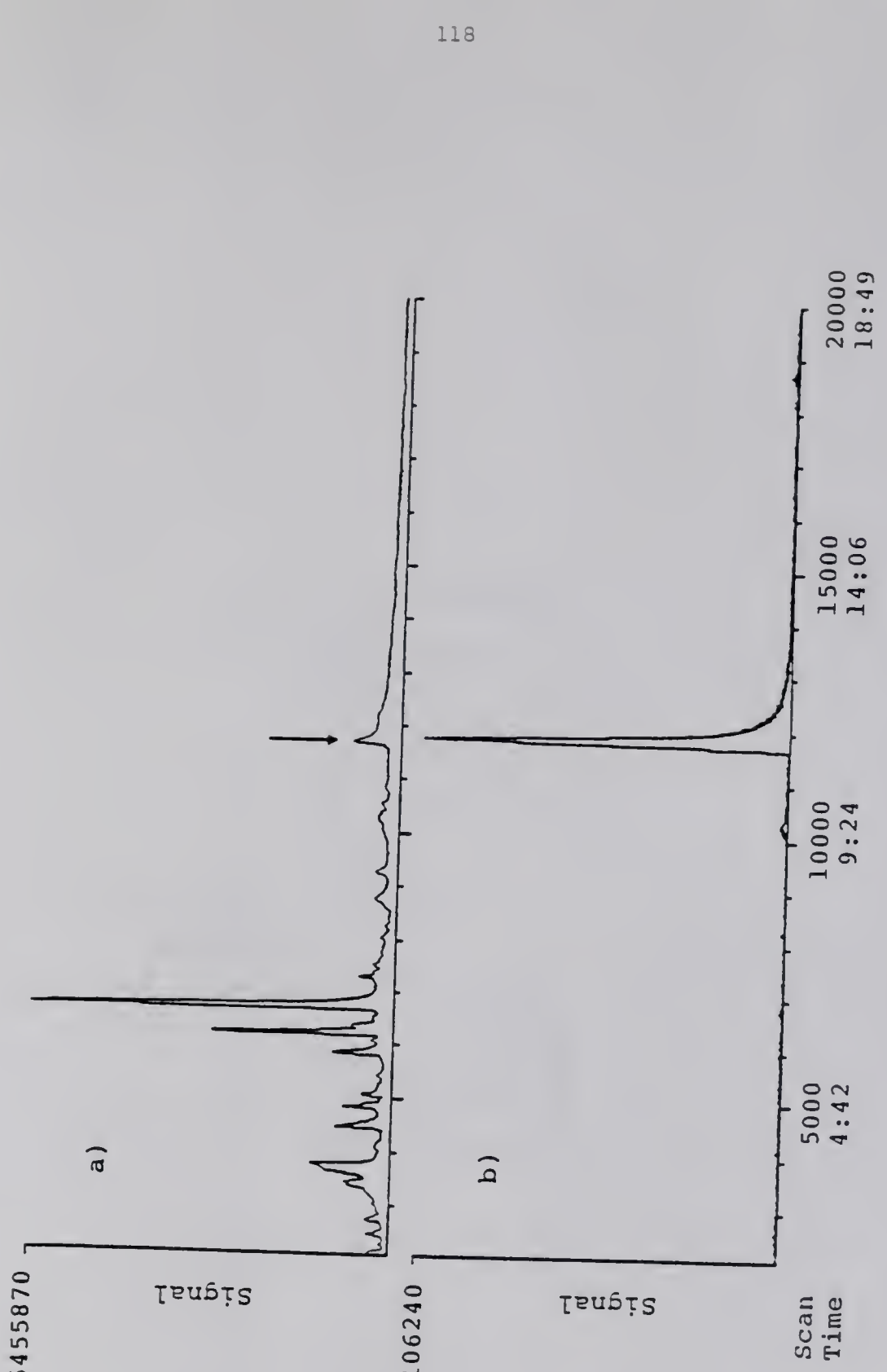

Figure 5-2. Determination of TLN (indicated by the arrow) in HFB-derivatized rat brain extract by (a) NCI-SIM (348) and by (b) NCI-SRM (348 -- 179).

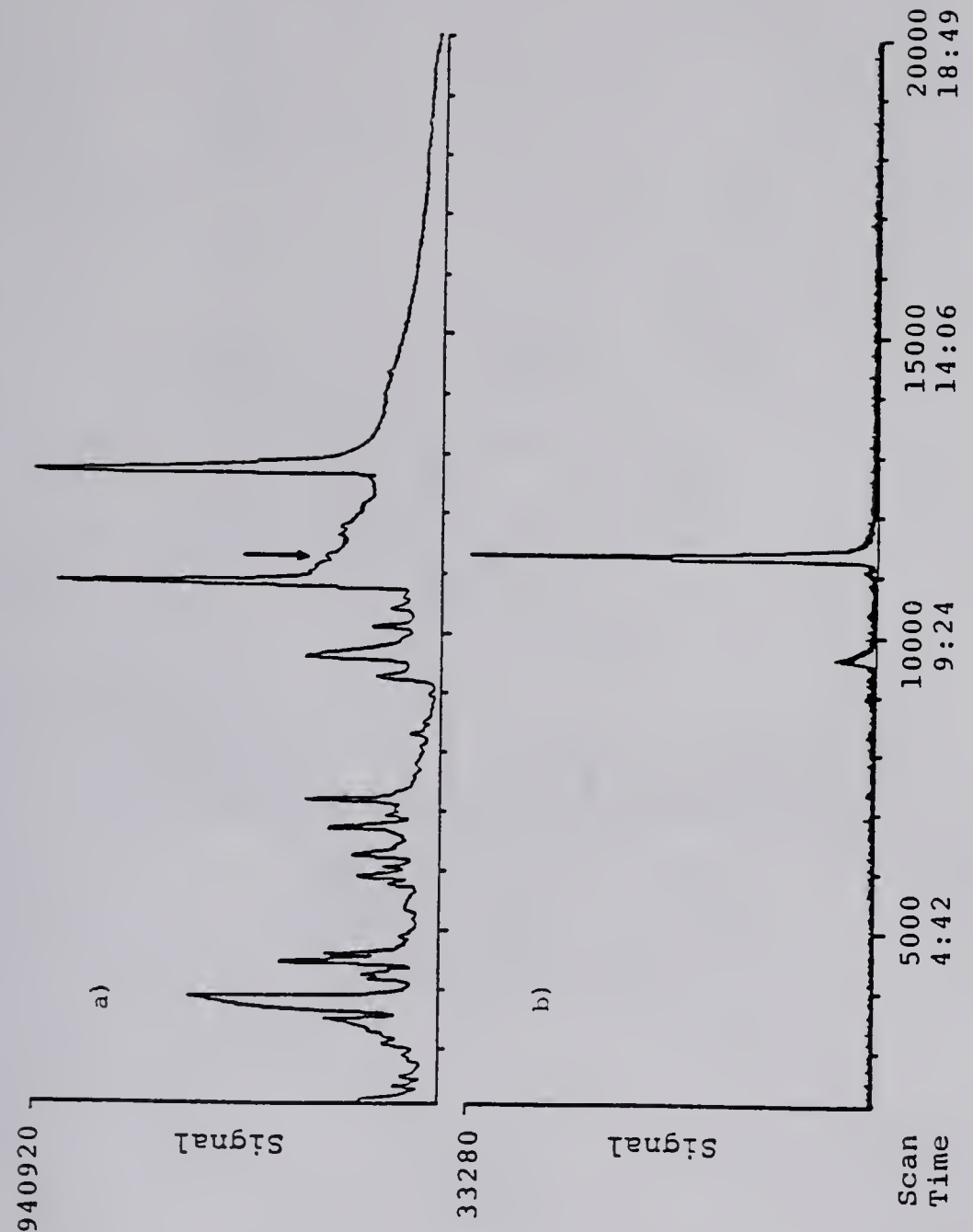

Figure 5-3. Determination of MTLN (indicated by the arrow) in HFB-derivatized rat brain extract by (a) NCI-SIM (362) and by (b) NCI-SRM (362 -- 179).

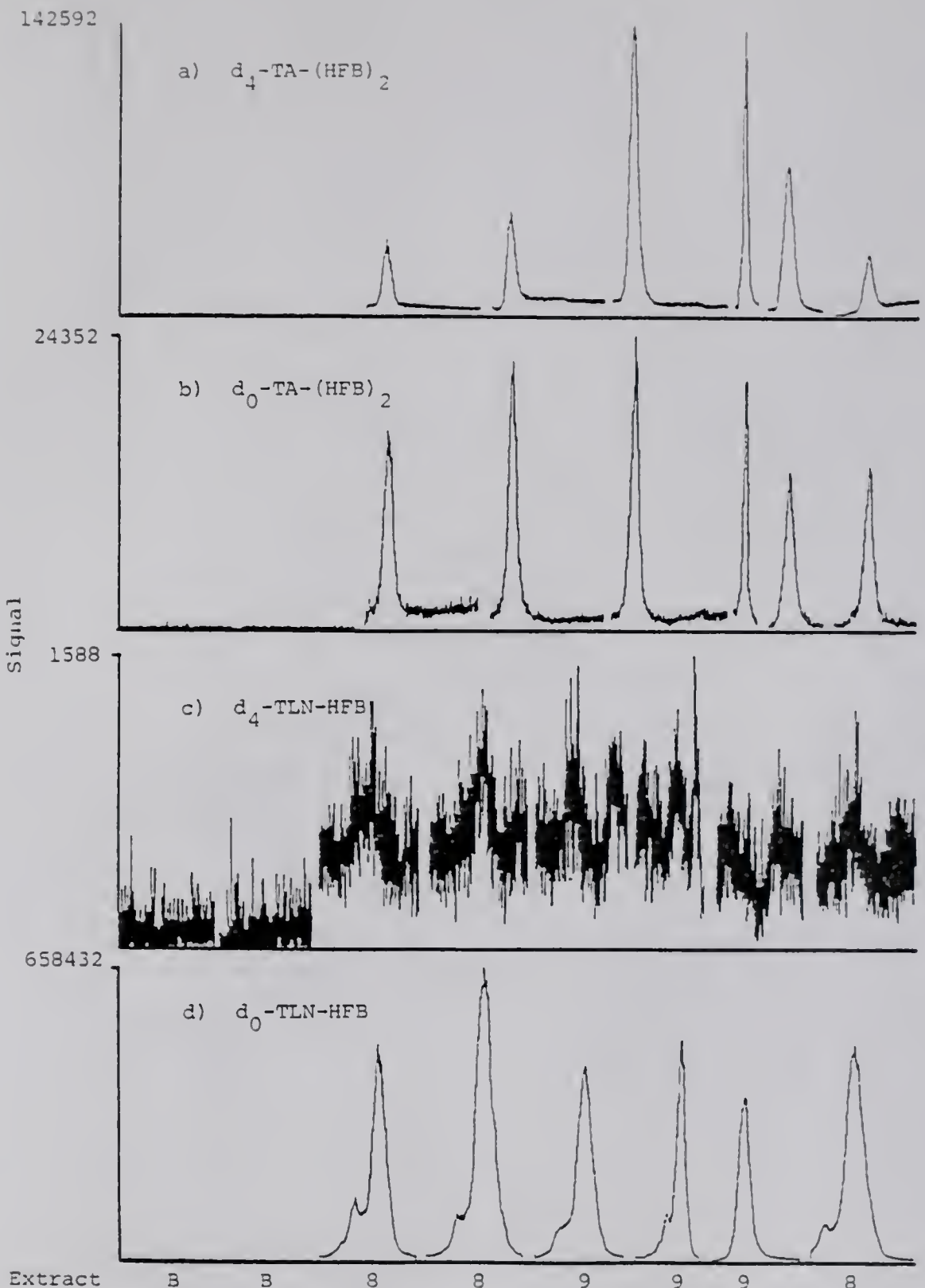

Figure 5-4. GC peaks from GC/NCI-MRM of the HFB-derivatized brain extract of rats 8 and 9. 1.94 ng of d_4-TA was added to extract 8 during the homogenization step and to extract 9 after the Sep-Pak extraction. B denotes injection of a solvent blank. See the text for more details.

Table 5-6. Assay of HFB-derivatized brain extracts 8 and 9 for artefactual formation of TLN-HFB (see Figure 5-4).

	GC Peak Areas ($/10^5$ counts)				$\frac{d_0\text{-TLN}}{d_4\text{-TLN}}$	$\frac{d_4\text{-TA}}{d_0\text{-TA}}$
Sample[a]	d_0-TA-$(HFB)_2$	d_4-TA-$(HFB)_2$	d_0-TLN-HFB	d_4-TLN-HFB		
Solvent	[b]	0.27	[b]	[b]	-	-
Solvent	[b]	0.12	[b]	[b]	-	-
Rat 8	5.112	8.98	322.9	0.412	784	1.8
Rat 8	6.648	12.84	560.2	0.380	1474	1.9
Rat 9	6.239	38.22	346.3	0.327	1059	6.1
Rat 9	3.172	19.16	208.3	[c]	-	6.0
Rat 9	4.567	23.96	226.2	[c]	-	5.2
Rat 8	4.363	8.23	432.9	[c]	-	1.9

[a]Samples are listed in the order in which they were analyzed. For rats 8 and 9, 1.94 ng of d_4-TA were added during the homogenization step and after the Sep-Pak extraction, respectively. The first five analyses were done with a multiexperiment, whereby only two selected reactions characteristic of the d_0- and d_4-analyte were monitored during its elution. The sixth analysis, rat 9, was carried out monitoring four selected reactions for all the analytes simultaneously. These analyses were carried out at 50% valley resolution. The last two analyses were carried out with the original multiexperiment, but with "normal", <10% valley, resolution.

[b]No rise was seen in baseline.

[c]A rise was seen in the baseline, but it was not quantitated.

than the endogeneous d_0-TA levels (Figures 5-4a and 5-4b and Table 5-6), the d_4-TLN detected was much less than the d_0-TLN levels. In analyzing the commercial d_4-TA standards, relatively small amounts of d_4-TLN were also observed and may be the source of the d_4-TLN detected above. Extract 9 (Table 5-2) was also analyzed for the presence of the d_4-labeled MTLN-HFB, HTLN-$(HFB)_2$, and HMTLN-$(HFB)_2$. No evidence was found for any artefactual formation of these tryptolines from the added d_4-TA. Based on the above evidence, it appears that the sample clean-up procedure used in these studies results in little, if any, artefactual tryptoline formation. However, this does not preclude artefactual tryptoline formation occurring during the interval following the death of the rat but prior to the clean-up procedure. Research is ongoing to determine if this may be a possible source of the tryptolines identified in these studies.

Quantitation of endogenous TLN. With NCI-multiple reaction monitoring (MRM) analysis of each of the derivatized extracts from 6 rat brains, d_0-TA-$(HFB)_2$, d_4-TLN-HFB, and d_0-TLN-HFB were identified and their GC peak areas determined (Figure 5-5). From similar analyses of standard solutions containing d_0- and d_4-TLN, calibration curves were obtained which allowed the endogenous levels of TLN to be calculated in individual rat brain extracts (Figure 5-6 and Table 5-7). The levels of endogenous TLN were higher than expected, and, as a result, the area ratios d_0-TLN to d_4-TLN (A_0/A_4) of the brain extracts are not within the range used to obtain the calibration curve. It was assumed that the calibration curve extended linearly to these area ratios. Although this may lead to inaccurate calculations of the endogenous TLN levels, the results should be more reliable than those obtained in Chapter 4, where

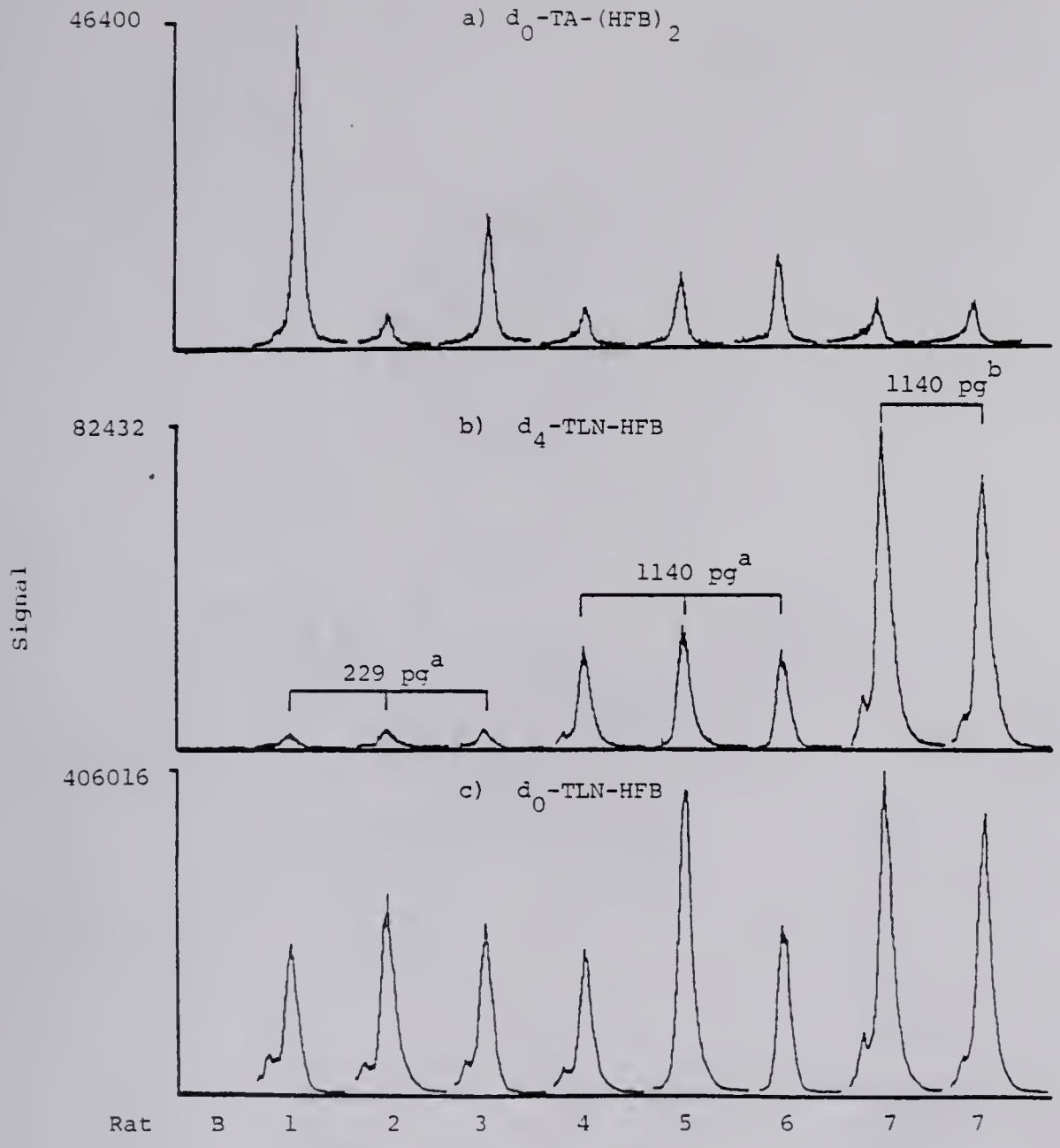

Figure 5-5. Determination of endogenous TLN in HFB-derivatized extracts of individual rat brains. [a]Added during the homogenization step. [b]Added after the Sep-Pak extraction. B denotes a solvent blank.

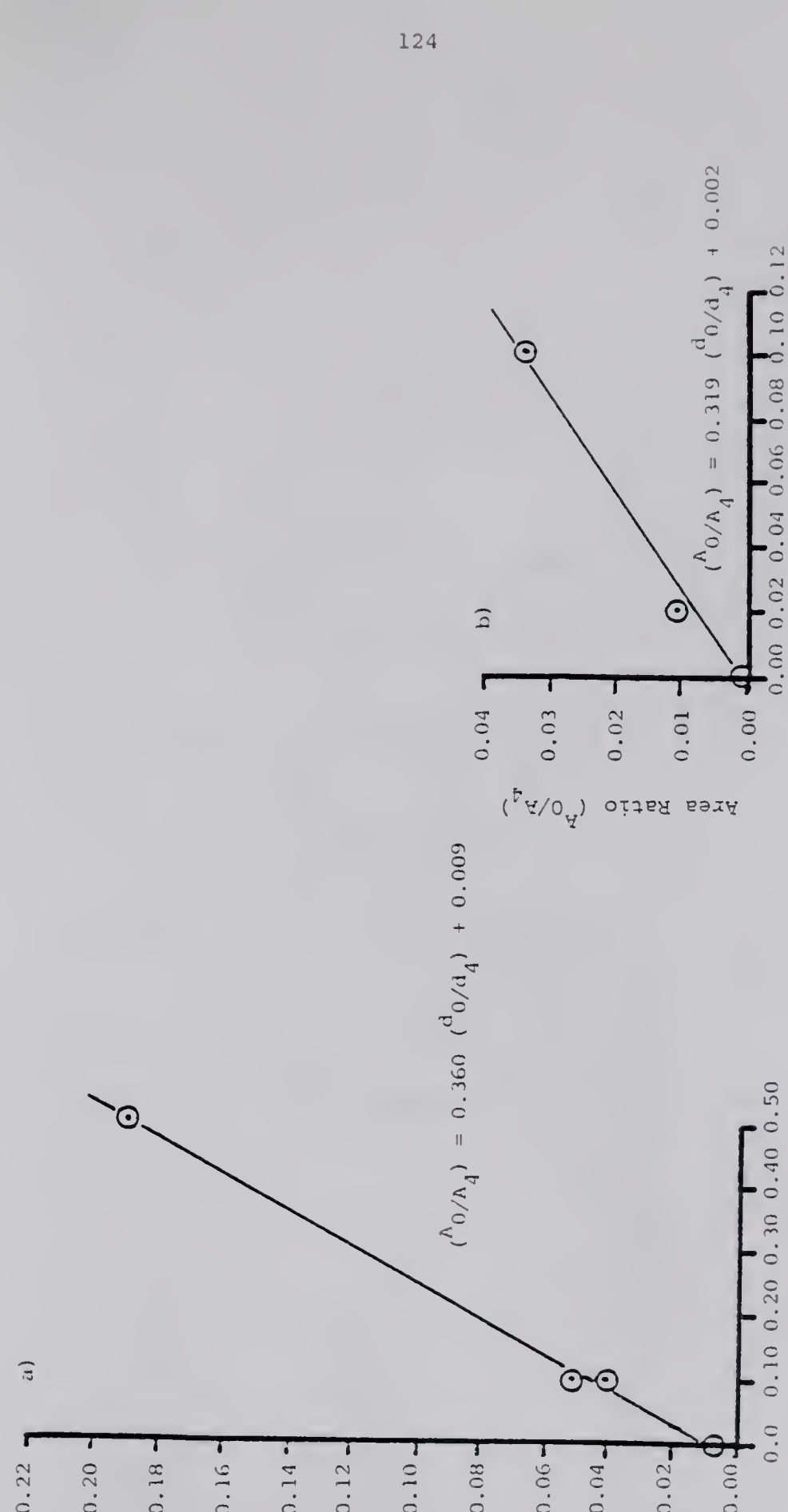

Figure 5-6. Calibration curves obtained from the GC/NCI-SRM analysis of standard mixtures of d_0-TLN and either (a) 229 pg d_4-TLN or (b) 1140 pg d_4-TLN. These mixtures were subsequently derivatized to form the HFB derivatives. The lines and equations are the least squares linear regression of the data.

Table 5-7. Determination of endogenous TLN levels in individual rat brains (see Figure 5-5).

Rat	Brain wet weight (g)	d_4-TLN added[a] (pmoles)	Area Ratios[b] A_0/A_4	Endogenous TLN[c] (ng/g wet tissue)
1	1.77	1.301	56.45	19.8
2	1.77	1.301	57.56	20.2
3	1.56	1.301	47.58	19.0
4	1.81	6.477	7.425	14.3
5	1.83	6.477	13.13	25.0
6	1.87	6.477	9.235	17.2
7	1.89	6.477	4.956	9.14
7	1.89	6.477	4.939	9.11

[a]The d_4-TLN was added in the homogenization step for rats 1-6 and after the Sep-Pak extraction for rat 7.

[b]The GC peak areas were corrected for the solvent blank before calculating their ratios.

[c]Levels of TLN in rat brains 1-3 and 4-7 were calculated using the least squares equations of the calibration lines in Figures 5-6a and 5-6b, respectively.

comparisons were made between two unrelated brain extracts in order to estimate the endogenous level of TLN. With this assumption in mind and with extrapolation of the least squares equations of the calibration curves to the d_0-TLN to d_4-TLN area ratios of extracts 1-6, the mean level of endogenous TLN in whole rat brain was calculated to be 19.2 ± 3.6 ng/g wet brain tissue. The analysis of extract 7 was not used in determining the mean, as the d_4-TLN was added after the Sep-Pak extraction and consistently gave the lowest d_0-TLN levels. Also, the contribution of d_0-TLN from the d_4-TLN internal standard was negligible as the analyses of the standard solutions of d_4-TLN revealed A_0/A_4 ratios less than 0.007, which are much less than the A_0/A_4 ratios found in the extracts. Although these TLN levels are in the same range as those reported by other researchers (Table 5-8), previous work by others suggests these are abnormally high. Although Barker's group has reported similar levels of TLN (17.5 ±4.86 ng/g tissue) in whole rat brain (54), they feel the levels of TLN have been elevated by conditions of animal housing and other stressors (56). They suggest that a more normal TLN level would be below the 2 ng/g tissue levels. Similarly, in discussions with Drs. Kym Faull and Olof Beck, and in light of their previous findings (59) and the finding of Chapter 4, we feel that the levels we report here are possibly elevated, also. Due to an unexpected delay (ca. 30 min) in the preparation of the brains following decapitation, there may have been artefactual formation of tryptolines during the enzymatic breakdown of tissues. Experiments are currently underway to investigate this possibility.

Reproducibility of the TLN-HFB quantitation. Eight replicate analyses of the brain extract #6 were performed in order to determine

Table 5-8. Endogenous levels of tryptolines in rat brain as reported by other researchers.

Tryptoline	TLN Level (ng/g wet tissue)	Method of Quantitation	Reference
CH_3O-TLN	a	laser fluorometry	50
CH_3O-TLN	35.6 ± 16.6	HFB[b]-deriv., GC/EI-SIM	54
CH_3O-TLN	not detected (nd)	(^3H)-deriv., TLC, scintillation	49
CH_3O-TLN, HMTLN, HTLN, MTLN	nd (<0.1)	HFB-deriv., GC/NCI-SIM	59
HMTLN	nd (<0.05)	PFP[c]-deriv., GC/EI-SIM	106
HTLN	a, d	(^3H)-deriv., TLC, scintillation	52
TLN	47.3 ± 13.4[d]	(^3H)-deriv., TLC, scintillation	49
TLN	17.5 ± 4.86	HFB-deriv., GC/EI-SIM	54
TLN	2.0 ± 1.2	HFB-deriv., GC/EI-SIM	53
TLN	0.37 ± 0.03	HFB-deriv., GC/NCI-SIM	59

[a]Detected but not quantitated.

[b]HFB-heptafluorobutyryl.

[c]PFP-pentafluoropropionyl.

[d]In rat forebrain.

the reproducibility of the peak area measurements and peak area ratios (Figure 5-7 and Table 5-9). From Figure 5-7, it can be seen that the peak shapes varied considerably: injections 2, 3, 7, and 8 show a shoulder on the TLN-HFB peak which is lacking in the other injections. This had been noted in the brain extract assays above, especially in the repetitive injections of the extracts used in determing the possiblity of artefactual formation (Figure 5-4). This effect was not seen to occur to any great extent with the TA-$(HFB)_2$ peaks (Figures 5-4a and 5-4b) or with the analysis of TLN-HFB standards (Figure 5-8). The shoulder was initially attributed to an interfering compound, possibly a positional isomer, in the brain extract. However, as the peak shape of the d_4-TLN-HFB mimicked that of the d_0-TLN-HFB, and as the peak shaped varied with the injection technique, the shoulder was attributed to TLN-HFB and was probably the result of the injection technique. By decreasing the speed of the injection from < 1 s (injections 1-3) to 3-5 s (injections 4-7), a general improvement in peak shape was obtained. Apparently, the volatilization of sample in the splitless mode is a much more complex phenomenon when introducing a complex mixture into the injection port, than when introducing the relatively simple TLN-HFB standard solutions. The latter consistently yielded "normal" peak shapes lacking any evidence of shoulders (Figure 5-8). The TLN-HFB GC peak of injection 8 resulted from a relatively "slow" injection at an initial GC oven temperature of 60 °C instead of the 100 °C used previously. Although there is a small shoulder, it is reduced in size compared to injections 2, 3, and 7, and the overall TLN-HFB peak area has been increased. This was attributed to the better thermal focusing which occurs at the lower GC oven temperature. Therefore, the assays

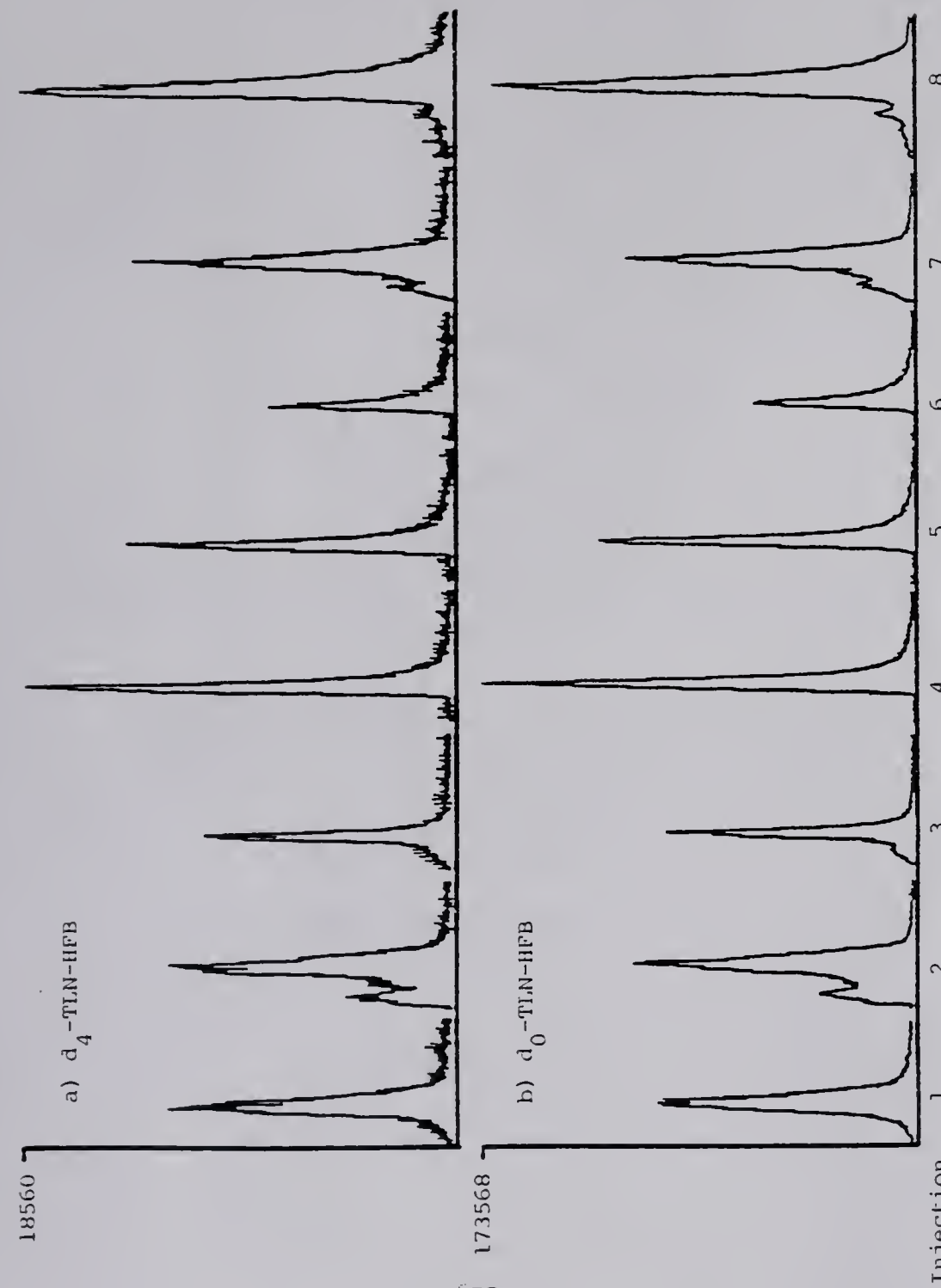

Figure 5-7. Replicate analyses of extract 6 by GC/NCI-MRM (see Table 5-9).

Table 5-9. Reproducibility of GC peak areas and area ratios of the HFB-derivatives of d_0-TA, d_0-TLN, and d_4-TLN from the repetitive analyses of extract 6 (See Figure 5-7).

	GC Peak Areas ($/10^5$ counts)			$\frac{d_0\text{-TLN}}{d_4\text{-TLN}}$	$\frac{d_0\text{-TLN}}{d_0\text{-TA}}$
Injection[a]	d_0-TA-$(HFB)_2$	d_0-TLN-HFB	d_4-TLN-HFB		
1	2.630	78.25	9.090	8.61	29.8
2	2.196	74.90	8.501	8.81	34.1
3	2.479	40.06	4.666	8.59	16.2
4	3.083	79.41	8.271	9.60	25.8
5	3.182	62.61	6.496	9.64	19.7
6	2.027	32.60	3.556	9.17	16.1
7	2.150	74.24	8.440	8.80	34.5
8	-	116.2	12.78	9.09	-
Mean[b]	2.535	63.15	7.003	9.03	25.2
%RSD	±18%	±30%	±31%	±4.9%	±32%

[a]See text for details of the injection methods.

[b]Mean obtained only with injections 1-7.

below were conducted with an initial GC oven temperature of 60 °C, with the other conditions remaining the same. This oven temperature consistently gave improved peak shape with little or no shoulder formation (Figure 5-9).

The variability in the GC peak shapes is reflected in the low precision, ±30% relative standard deviation (RSD), of the GC peak areas of TLN-HFB for injections 1-7 (the shoulders were not included in the peak area measurements) (Table 5-9). If TA-$(HFB)_2$ is used as an internal standard, the precision of quantitation of TLN with the use of the area ratios TLN/TA (±32 % RSD) was not improved. However, with the isotopically-labelled internal standard, the precision of quantitation of TLN-HFB with the area ratios (d_0-TLN)/(d_4-TLN) was increased to ±5% RSD. This dramatically increased precision can be directly attributed to the chemical similarity and to the elution at approximately the same time of the analyte and the isotopically-labelled form of the analyte used as the internal standard. Therefore, they are volatilized, chromatographically separated, ionized and detected under the same experimental conditions. As demonstrated above, the use of other compounds as internal standards may not adequately compensate for the variation in the experimental techniques and parameters. In addition, isotopically-labeled standards become even more important in trace analysis, as they can compensate for the varying recoveries and may act as "carriers".

Assay for other tryptolines. In the assay of nine rat brain extracts (Table 5-2) by NCI-MRM, the following compounds were simultaneously identified and their peak areas determined: tryptamine, 5-hydroxytryptamine, tryptoline, methtryptoline, 5-hydroxytryptoline, and 5-hydroxymethtryptoline (Table 5-10 and Figure 5-9). Methtryptoline and

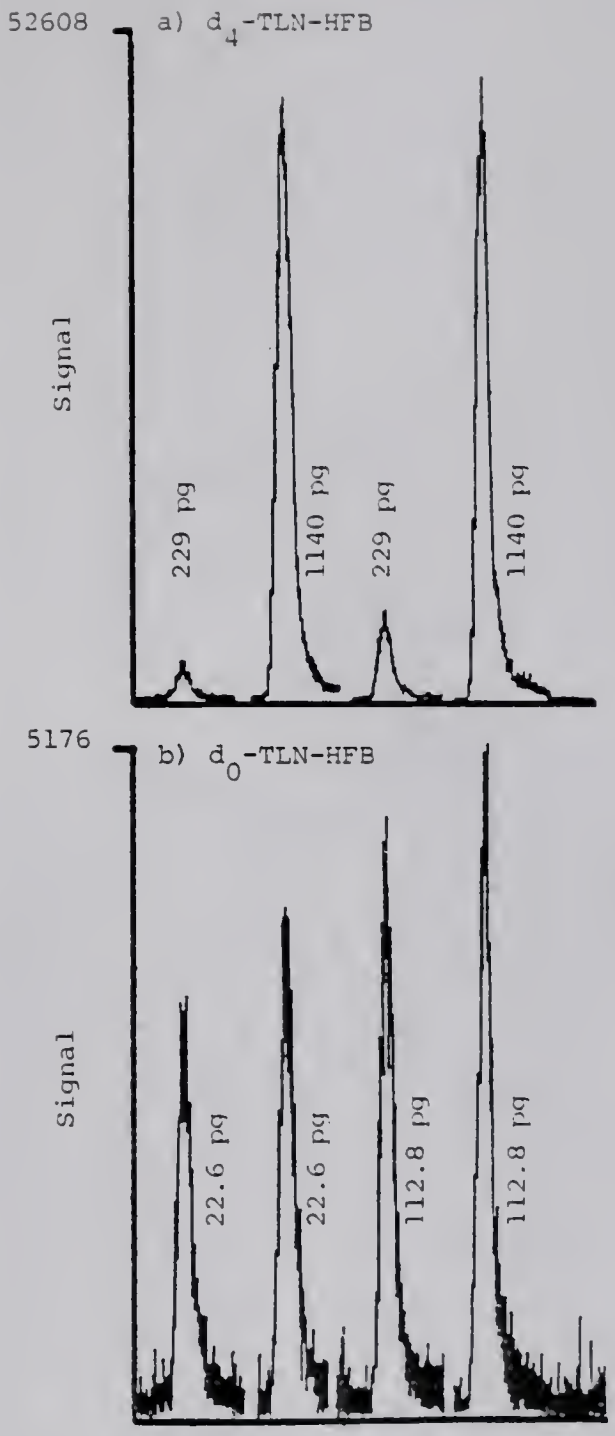

Figure 5-8. GC/NCI-MRM analyses of standard mixtures containing (a) d_4-TLN-HFB and (b) d_0-TLN-HFB.

5-hydroxymethtryptoline have not been previously reported in rat brain, while HMTLN has only been detected but not quantitated (52). Although 5-methoxytryptoline has been reported by others (50,54), no evidence for the presence of 5-methoxytryptoline was obtained in these assays. This agrees with the findings of others (49,59).

No accurate quantitation of these compounds was possible due to the absence of internal standards in the experiments described here. However, the normalized GC peak areas permitted estimation of relative amounts of each of the tryptolines and indoleamines detected (Table 5-10). There was a large degree of variability in the normalized peak areas of each of the components. From the results of 7 replicative analyses of the same extract, the peak areas of tryptoline-HFB had a relative standard deviation of ±30% (Table 5-9). This was largely attributed to the variability of the splitless injection technique, and accounts for much of the variability of the brain extract assays. The remainder of the variability in the rat brain assays is probably due to the variability between animals. The sensitivities for tryptoline and methtryptoline can be assumed to be comparable due to the similarity of their mass spectral features, as can those for 5-hydroxytryptoline and 5-hydroxymethtryptoline. On this basis, tryptoline appears to have been present at levels greater than those of methtryptoline, while the levels of the two hydroxytryptolines were nearly the same. Comparison of the levels of the non-hydroxy- and hydroxy-compounds must be made more cautiously due to the dissimilarity in their mass spectra. However, it does seem that the non-hydroxytryptolines are present at levels much greater than those of the hydroxytryptolines, while 5-hydroxytryptamine levels are greater than those of tryptamine. The latter trend agrees

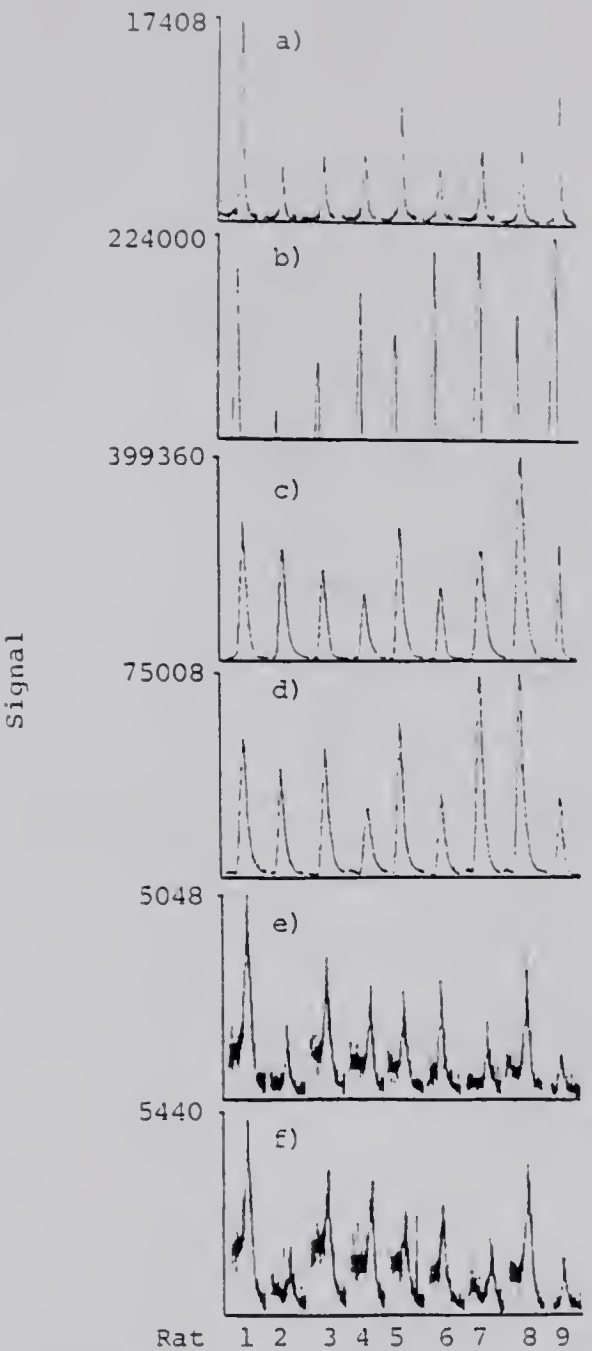

Figure 5-9. GC peaks from the GC/NCI-MRM analyses of HFB-derivatized extracts from individual rat brains. (a) TA-$(HFB)_2$. (b) 5-HT-$(HFB)_3$. (c) TLN-HFB. (d) MTLN-HFB. (e) 5-HTLN-$(HFB)_2$. (f) 5-HMTLN-$(HFB)_2$.

Table 5-10. Normalized GC peak areas of the HFB derivatives of the indoleamines and tryptolines detected in the assay of rat brain extracts (see Figure 5-9)[a].

	NORMALIZED GC PEAK AREAS[b]					
Rat	TA	5HT	TLN	MTLN	5HTLN	5HMTLN
1	226	2552	15681	2037	130	170
2	66	89	14370	1212	28	30
3	85	705	11693	1851	76	73
4	91	1516	7822	946	50	69
5	122	917	14724	1829	45	42
6	61	1733	7452	908	55	42
7	93	2975	15603	2259	33	43
8	84	1079	26175	2317	74	86
9	136	3415	7357	835	22	25
Mean	107	1665	13431	1577	57	65
%RSD	±47%	±67%	±44%	±38%	±58%	±69%

[a]The NCI selected reactions of Table 5-2 were monitored for each component.

[b]Normalization was accomplished by dividing the GC peak areas (expressed as 10^3 data system counts) by the wet weight of the respective brain tissue.

well with the finding that 5-hydroxytryptamine may be present in the brain at levels up to 1000 times those of tryptamine (13). In addition, other researchers have shown that 5-hydroxytryptamine has *in vitro* reactivities with formaldehyde and acetaldehyde similar to or slightly greater than tryptamine (7,105). If the tryptolines are formed by simple, non-enzymatic condensation reactions between indoleamines and aldehydes, it would be expected that the relative levels of the non-hydroxy- and hydroxy-condensation products would reflect the relative levels and reactivities of their precursor indoleamines. However, just the opposite is found to occur. This difference in the relative levels of indoleamines and the relative levels of their condensation products may point to the presence of a specific enzymatic process which is selective for tryptamine, for which some evidence has previously been shown (56). Other explanations for this discrepancy could include the possible existence of mechanisms which protect 5-hydroxytryptamine from condensation with aldehydes and the possibility that the hydroxytryptolines, once formed, are more readily metabolized than are the non-hydroxytryptolines.

Conclusion

In conclusion, the increased selectivity of GC/MS/MS over GC/MS has been shown to increase the reliability of identification and quantitation of the HFB-derivatives of the tryptolines in crude brain extracts. The following tryptolines have been tentatively identified in the assay of rat brain extracts using electron-capture NCI-SRM: tryptoline, methtryptoline, 5-hydroxytryptoline, and 5-hydroxymethtryptoline. Results suggest that the first two compounds are present in much

greater abundance, with tryptoline being present at an average level of 19.2 ng/g wet brain tissue. Future work will involve careful quantitation of these compounds, using a deuterated internal standard for each compound, and experiments to assess the possibility of artefactual tryptoline formation during the interval following the death of the rat but prior to the sample workup.

CHAPTER 6
CONCLUSIONS AND SUGGESTIONS FOR FUTURE WORK

Tandem mass spectrometry has been shown to offer several advantages over the more conventional methods for determination of trace quantities of tryptolines. In Chapter 3, it was shown that MS/MS with solids probe sample introduction could detect underivatized methtryptoline and tryptoline standards in the 10-20 ng range. This would enable the analysis of brain homogenate pooled from several rats. Research into the use of other CI reagent gases (e.g. ammonia) may lower these limits of detection, such that analysis of indiviual rat brain extracts would be feasible. The use of solids probe PCI-SRM would minimize the sample clean-up and preparation procedures, and thus the possibility of artefactual tryptoline formation. Actual evaluation of this method with crude brain extracts is necessary in order to determine if these limits of detection apply in "real" samples.

It has also been demonstrated throughout the dissertation, that MS/MS provides an added dimension to structure elucidation of compounds. Specifically, in Chapter 3, it was demonstrated that a "genetic tree" can be generated by systematically obtaining the daughter spectrum of each of the fragment ions resulting from the EI ionization of a compound. The completeness of the structural information contained in such a "genetic tree" should be well suited to computerized structure elucidation of an unknown compound. Reserch is proceeding along these lines in this and other laboratories.

In Chapter 4, the limit of detection of short, packed column GC/NCI-SRM for TLN-HFB standards was in the low femtogram range. However, quenching of TLN-HFB's signal by other components in the derivatized brain extract prevented the use of this method. Research with real negative chemical ionization, as opposed to electron-capture NCI, might overcome this quenching problem and allow use of this rapid sample introduction method. Research is also continuing in order to determine the exact nature of the enhancing effect of perfluoro-tri-N-butylamine on the PCI signal of the tryptoline-HFB derivatives. A better understanding of this effect may lead to its exploitation as a general method to increase the PCI sensitivity for these and other compounds.

In order to prevent the quenching problem observed in the short, packed column GC/NCI techniques, separation of the components of the brain extracts was accomplished with capillary column GC. The limits of detection for GC/NCI-SRM were still in the femtogram region. In Chapter 5, with capillary column GC/NCI-MRM, tryptoline, methtryptoline, 5-hydroxytrptoline, and 5-hydroxymethtryptoline were tentatively identified in 9 individual rat brain extracts. The *in vivo* presence of the methtryptoline and 5-hydroxymethtryptoline had previously been unreported. Comparison of the GC/NCI-SRM analysis to the GC/NCI-SIM analysis of the same extracts revealed that the most likely explanation was the lack of selectivity with the more conventional GC/MS technique. Results so far suggest that tryptoline and methtryptoline are present in much greater abundance that the hydroxytryptolines, with tryptoline being present at an average level of 19.2 ng/g wet brain tissue. Future work will involve accurate quantitation of these tryptolines with the use of deuterated internal standards and experiments to

assess the possibility of artefactual tryptoline formation during the interval following the death of the rat but prior to the sample workup.

BIBLIOGRAPHY

1. McIsaac, W. M. Biochim. Biophys. Acta. 1961, 52,607-609.

2. Johnson, J. V.; Yost, R. A.; Faull, K. F. Anal. Chem. 1984,56,1655-1661.

3. Johnson, J. V.; Yost, R. A.; Beck, O.; Faull, K. F.; In "Aldehyde Adducts in Alcoholism"; Alan R. Liss, Inc.: New York. In press.

4. Whaley, W. M.; Govindachari, T. R. Org. React. 1951, 6, 151-190.

5. Hahn, G.; Ludewig, H. Chem. Gesell B 1934, 67, 2031-2035.

6. Björklund, A.; Falck, G.; Lindvall, O. In "Methods in Brain Research"; John Wiley & Sons: New York, 1975; pp 249-294.

7. Wyatt, R. J.; Erdelyi, E.; Domaral, J. R.; Elliott, G. R.; Renson, J; Barchas, J. D. Science 1975, 187, 853-855.

8. Lauwers, W.; Leysen, J.; Verhoeven, H.; Laduron, P.; Claeys, M. Biomed. Mass Spectrom. 1975, 2, 15-22.

9. Mandel, L. R.; Rosegay, A.; Walker, R. W.; VandenHeuvel, W. J. A.; Rokach, J. Science 1974, 186, 741-743.

10. Meller, E.; Rosengarten, H.; Friedhoff, A. J.; Stebbins, R. D.; Silber, R. Science 1975, 187, 171-173.

11. Pearson, A. G. M.; Turner, A. J. Nature (London) 1975, 258, 173-174.

12. Stebbins, R. D.; Meller, E.; Rosengarten, H.; Friedhoff, A.; Silber, R. Arch. Biochem. Biophys. 1976, 173, 673-679.

13. Artigas, F.; Gelpi, E. Anal. Biochem. 1979, 92, 233-242.

14. Cattabeni, F.; Koslow, S.H.; Costa, E. Science 1972, 178, 166-168.

15. Markey, S. P.; Colburn, R. W.; Johannessen, J. N. Biomed. Mass Spectrom. 1981, 8, 301-304.

16. Beck, O.; Jonsson, G.; Lundman, A. Naunyn-Schmiedeberg's Arch. Pharmacol. 1981, 318, 49-55.

17. Heck, H. d'A.; White, E. L.; Casanova-Schmitz, M. Biomed. Mass Spectrom. 1982, 9, 347-353.

18. McIsaac, W. M.; Estevez, V. Biochem. Pharmacol. 1966, 15, 1625-1627.

19. Glover, V.; Liebowitz, J.; Armando, I.; Sandler, M. J. Neural. Transm. 1982, 54, 209-218.

20. Buckholtz, N. S. Naunyn-Schmiedeberg's Arch. Pharmacol. 1980, 314, 215-221.

21. Holman, R. B. In "Beta-Carbolines and Tetrahydroisoquinolines"; Alan R. Liss, Inc.: New York, 1982; pp 167-181.

22. Rommelspacher, H.; Strauss, S.; Cohnitz, C.H. Naunyn-Schmiedeberg's Arch. Pharmacol. 1978, 303, 229-233.

23. Tuomisto, L.; Tuomisto, J. Naunyn-Schmiedeberg's Arch. Pharmacol. 1973, 279, 371-380.

24. Komulainen, H.; Tuomisto, J.; Airaksinen, M. M.; Kari, I; Peura, P.; Pollari, L. Acta. Pharmacol. Toxicol. 1980, 46, 299-307.

25. Friedman, E.; Meller, E.; Hallock, M. J. Neurochem. 1981, 36, 931-937.

26. Krassner, M. B. Chem. Eng. News 1983 (Aug. 29), 22-33.

27. McIsaac, W. M. Postgrad. Med. 1961, 30, 111-118.

28. Elliott, G. R.; Holman, R. B. In "Neuroregulators and Psychiatric Disorders"; Usdin, E.; Hamburg, D. A.; Barchas, J. D., Eds.; Oxford University Press: New York, 1977; p 220.

29. Buckholtz, N. S. Life Science 1980, 27, 893-903.

30. Holman, R. B.; Elliott, G.R.; Faull, K. F.; Barchas, J. D. In "Psychopharmacology of Alcohol"; Sandler, M., Ed.; Raven Press: New York, 1980; p 155.

31. Westcott, J. Y.; Weiner, H.; Schultz, J.; Myers, R. D. Biochem. Pharmacol. 1980, 29, 411-417.

32. Tabakoff, B.; Anderson, R. A.; Ritzmann, R. F. Biochem. Pharmacol. 1976, 25, 1305-1309.

33. Peura, P.; Kari, I.; Airaksinen, M. M. Biomed. Mass Spectrom. 1980, 7, 553-555.

34. Rommelspacher, H.; Strauss, S.; Lindemann, J. FEBS Lett. 1980, 109, 209.

35. Beck, O.; Bosin, T. R.; Lundman, A.; Borg, S. Biochem. Pharmacol. 1982, 31, 2517.

36. Beck, O.; Bosin, T. R.; Holmstedt, B.; Lundman, A. In "Beta-Carbolines and Tetrahydroisoquinolines"; Alan R. Liss, Inc.: New York, 1982; pp 29-40.

37. Myers, R. D.; Oblinger, M. M. Drug Alcohol Depend. 1977, 2, 469-483.

38. Deitrich, R.; Erwin, V. Ann. Rev. Pharmacol. Toxicol. 1980, 20, 55-80.

39. Squires, R. F.; Braestrup, C. Nature (London) 1977, 266, 733-734.

40. Braestrup, C.; Albrechsten, R.; Squires, R. F. Nature (London) 1977, 269, 702-704.

41. Hamon, M.; Soubrie, P. Neurochem. Internat. 1983, 5, 663-672.

42. Marangos, P. J.; Paul, S. M.; Goodwin, F. K. Life Sci. 1979, 25, 1093-1102.

43. Braestrup, C.; Nielsen, M.; Olsen, C. E. Proc. Natl. Acad. Sci. USA 1980, 77, 2288-2292.

44. Rommelspacher, H.; Nanz, C.; Borbe, H. O.; Fehske, K. J.; Müller, W. E.; Wollert, U. Naunyn-Schmiedeberg's Arch. Pharmacol. 1980, 314, 97-100.

45. White, F. J.; Nielsen, E. B.; Appel, J. B. Adv. Biochem. Psychopharmacol. 1982, 34 (Serotonin Biol. Psychiatry), 322-323.

46. Nielsen, E. B.; White, F. J.; Holohean, A. M.; Callahan, P. M.; Appel, J. B. Life Sci. 1982, 31, 2433-2439.

47. Airaksinen, M. M.; Mikkonen, E. Naunyn-Schmiedeberg's Arch. Pharmacol. 1980, 313, R34.

48. Panchenko, L. F.; Brusov, O. S.; Balashov, A. M.; Grinevich, V. P.; Ostrovskii, Yu. M. Vopr. Med. Khim. 1982, 28, 88-92.

49. Honecker, H.; Rommelspacher, H. Naunyn-Schmiedeberg's Arch. Pharmacol. 1978, 305, 125-141.

50. Shoemaker, D. W.; Cummins, J. T.; Bidden, T. G. Neuroscience 1978, 3, 233-239.

51. Rommelspacher, H.; Barbey, M.; Strauss, S.; Greiner, B.; Fähndrich, E. In "Beta-Carbolines and Tetrahydroisoquinolines"; Alan R. Liss, Inc.: New York, 1982; pp 41-55.

52. Rommelspacher, H; Honecker, H.; Barbey, M.; Meinke, B. Naunyn-Schmiedeberg's Arch. Pharmacol. 1979, 310, 35-41.

53. Barker, S. A.; Harrison, R. E.; Brown, G. B.; Christian, S. T. Biochem. Biophys. Res. Commun. 1979, 87, 146-154.

54. Barker, S. A.; Harrison, R. E. W.; Monti, J. A.; Brown, G. B.; Christian, T. Biochem. Pharm. 1981, 30, 9-17.

55. Kari, I.; Peura, P.; Airaksinen, M. M. Biomed. Mass Spectrom. 1980, 7, 549-552.

56. Barker, S. A. In "Beta-Carbolines and Tetrahydroisoquinolines"; Alan R. Liss, Inc.: New York, 1982; pp 113-124.

57. Allen, J. R. F.; Beck, O.; Borg, S.; Skröder, R. Eur. J. Mass Spectrom. Biochem. Med. Environm. Res. 1980, 1, 171-177.

58. Bosin, T. R.; Holmstedt, B.; Lundman, A.; Beck, O. In "Beta-Carbolines and Tetrahydroisoquinolines"; Alan R. Liss, Inc.: New York, 1982; pp 15-27.

59. Faull, K. F.; Holman, R. B.; Elliott, G. R.; Barchas, J. D. In "Beta-Carbolines and Tetrahydroisoquinolines"; Alan R. Liss, Inc.: New York, 1982; pp 135-154.

60. Holmes, J. C.; Morrell, F. A. Appl. Spectrosc. 1957, 11, 86-87.

61. McFadden, W. H. "Techniques of Combined Gas Chromatography/Mass Spectrometry: Applications in Organic Analysis"; J. Wiley & Sons, Inc.: New York, 1973.

62. Arpino, P. J.; Guiochon, G. Anal. Chem. 1979, 51, 682A-701A.

63. Franklin, J. L.; Ed. "Ion Molecule Reactions"; Plenum: New York, 1972.

64. Vestal, M. L.; Futrell, J. H. Chem. Phys. Lett. 1974, 28, 559-561.

65. McGilvery, D. C.; Morrison, J. D. Int. J. Mass Spectrom. Ion Phys. 1978, 28, 81-92.

66. Beynon, J. H.; Caprioli, R. M.; Ast, T. Org. Mass Spectrom. 1971, 5, 229.

67. Beynon, J. H.; Cooks, R. G.; Amy, J. W.; Baitinger, W. E.; Ridley, T. Y. Anal. Chem. 1973, 45, 1023A-1031A.

68. Cooks, R. G.; Beynon, J. H.; Caprioli, R. M.; Lester, G. R. "Metastable Ions"; Elsevier: Amsterdam, 1973.

69. Kruger, T. L.; Litton, J. F.; Kondrat, R. W.; Cooks, R. G. Anal. Chem. 1976, 48, 2113-2119.

70. Kondrat, R. W.; Cooks, R. G. Anal. Chem. 1978, 50, 81A-92A.

71. McLafferty, F. W.; Bockhoff, F. M. Anal. Chem. 1978, 50, 69-76.

72. Yost, R. A.; Enke, C. G. Anal. Chem. 1979, 51, 1251A-1264A.

73. Yost, R. A.; Fetterolf, D. D. Mass Spectrom. Rev. 1983, 2, 1-45.

74. Henion, J. D.; Thomson, B. A.; Dawson, P. H. Anal. Chem. 1982, 54, 451-456.

75. Endele, R.; Senn, M. Int. J. Mass Spectrom. Ion Phys. 1983, 48, 81-84.

76. Cheng, M. T.; Kruppa, G. H.; McLafferty, F. W. Anal. Chem. 1982, 54, 2204-2207.

77. Glish, G. L.; Shaddock, V. M.; Harmon, K.; Cooks, R. G. Anal. Chem. 1980, 52, 165-167.

78. Brotherton, H. O.; Yost, R. A. Anal. Chem. 1983, 55, 549-553.

79. McLafferty, F. W., Ed. "Tandem Mass Spectrometry"; John Wiley & Sons, Inc.: New York, 1983.

80. Cooks, R. G.; Glish, G. L. Chem. Eng. News 1981 (Nov. 30), 40-52.

81. McLafferty, F. W. Science 1981, 214, 280-287.

82. McLafferty, F. W. Biomed. Mass Spectrom. 1981, 8, 446-448.

83. Cooks, R. G.; Busch, K. L. J. Chem. Educ. 1982, 59, 926-933.

84. Penzer, G. R. In "An Introduction to Spectroscopy for Biochemists"; Brown, S. B., Ed.; Academic Press: New York, 1980; pp 70-114.

85. Yost, R. A.; Fetterolf, D. D.; Hass, J. R.; Harvan, D. J.; Weston, A. F.; Skotnicki, P. A.; Simon, N. M. Anal. Chem. 1984, 56, 2223-2228.

86. Kondrat, R. W.; McClusky, G. A.; Cooks, R. G. Anal. Chem. 1978, 50, 2017-2021.

87. Levsen, K.; Schwartz, H. Mass Spectrom. Rev. 1983, 2, 77-148.

88. Levsen, K. In "Tandem Mass Spectrometry"; McLafferty, F. W., Ed.; John Wiley & Sons, Inc.: New York, 1983; pp 41-66.

89. McLafferty, F. W. "Interpretation of Mass Spectra," 3rd Ed.; University Science Books: Mill Valley, CA, 1980.

90. Budzikiewicz, H.; Djerassi, C.; Williams, D. H. "Mass Spectra of Organic Compounds"; Holden-Day: San Francisco, 1967.

91. Slayback, J. R. B.; Story, M. S. Ind. Res. Dev. 1981 (Feb.), 128-133.

92. Coutts, R. T.; Locock, R. A.; Slywka, G. W. Org. Mass Spectrom. 1970, 3, 879-889.

93. Johnson, J. V.; Yost, R. A. Presented at the 6th International Conference on Computers in Chemical Research and Education, Washington, DC, July 11-16, 1982. Abstract No. 25. In "Computer Applications in Chemistry"; Heller, S. R.; Potenzone, Jr., R., Eds.; Elsevier: Amsterdam, 1983; pp 326-327.

94. Dougherty, R. C. Anal. Chem. 1981, 53, 625A-636A.

95. Hunt, D. F.; Crow, F. W. Anal. Chem. 1978, 50, 1781-1784.

96. Bush, K. L.; Parker, C. E.; Harvan, D. J.; Bursey, M. M.; Hass, J. R. Appl. Spectrosc. 1981, 35, 85-88.

97. Garnett, J. L.; Gregor, I. K.; Guilhaus, M.; Pakternieks, D. R. Inorganica Chimica. Acta. 1980, 44, L121-L124.

98. Yinon, J.; Harvan, D. J.; Hass, J. R. Org. Mass Spectrom. 1982, 17, 321-326.

99. Garland, W. A.; Miwa, B. J. Biomed. Mass Spectrom. 1983, 10, 126-129.

100. Stöckl, D.; Budzikiewikz, H. Org. Mass Spectrom. 1982, 17, 470-474.

101. Faull, K. F.; Barchas, J. D. In "Methods of Biochemical Analysis," Vol. 29; Glick, D., Ed.; John Wiley & Sons, Inc.: New York, 1982; pp 325-383.

102. Wood, P. L. Biomed. Mass Spectrom. 1982, 9, 302-306.

103. Shaw, G. J.; Wright, G. J.; Milne, G. W. A. Biomed. Mass Spectrom. 1976, 3, 146-148.

104. Perchalski, R. J.; Yost, R. A.; Wilder, B. J. Anal. Chem. 1982, 54, 1466-1471.

105. Davis, V. E.; Cashaw, J. L.; McMurtney, K. D.; Ruchirawat, S; Nimit, Y. In "Beta-Carbolines and Tetrahydroisoquinolines"; Alan R. Liss, Inc.: New York, 1982; pp 99-111.

106. Beck, O.; Lundman, A. Biochem. Pharmacol. 1983, 32, 1507-1510.

BIOGRAPHICAL SKETCH

Jodie Vincent Johnson was born November 16, 1954, at Ft. McClellan, Alabama, as the second of eventually six children. As his father was an Army officer, he attended different schools every 2 to 3 years. He attended Reid Ross Senior High School in Fayetteville, North Carolina, graduating as the class valedictorian in 1972. While in North Carolina, he earned his Eagle Scout award.

While attending Florida State University, he was in the Honors Program, was a member of the FSU Flying High Circus, joined the Phi Kappa Phi and Phi Beta Kappa honorary societies, and received the American Chemical Society Undergraduate Analytical Chemistry Award in 1977. He graduated Magna Cum Laude in June, 1977, with a B.S. in biology and chemistry.

In October, 1977, Jodie was married and moved to the Jacksonville, Florida, area where he obtained employment with SCM Organic Chemicals in July, 1978. Working in their R & D analytical support laboratory, he acquired experience and a "love" for the analytical applications of gas chromatography/mass spectrometry. Although happy with his positicn, in 1980 he decided to further his education and entered the University of Florida, where he studied under the direction of Dr. Richard A. Yost. Upon graduation in 1984, he will remain with Dr. Yost for a period of time to continue MS/MS research as a Postdoctoral Associate.

I certify that I have read this study and that in my opinion it conforms to acceptable standards of scholarly presentation and is fully adequate, in scope and quality, as a dissertation for the degree of Doctor of Philosophy.

Richard A. Yost, Chairman
Associate Professor of Chemistry

I certify that I have read this study and that in my opinion it conforms to acceptable standards of scholarly presentation and is fully adequate, in scope and quality, as a dissertation for the degree of Doctor of Philosophy.

John G. Dorsey
Assistant Professor of Chemistry

I certify that I have read this study and that in my opinion it conforms to acceptable standards of scholarly presentation and is fully adequate, in scope and quality, as a dissertation for the degree of Doctor of Philosophy.

Gerhard M. Schmid
Associate Professor of Chemistry

I certify that I have read this study and that in my opinion it conforms to acceptable standards of scholarly presentation and is fully adequate, in scope and quality, as a dissertation for the degree of Doctor of Philosophy.

Martin T. Vala
Professor of Chemistry

I certify that I have read this study and that in my opinion it conforms to acceptable standards of scholarly presentation and is fully adequate, in scope and quality, as a dissertation for the degree of Doctor of Philosophy.

Clyde M. Williams
Professor of Radiology

This dissertation was submitted to the Graduate Faculty of the Department of Chemistry in the College of Liberal Arts and Sciences and to the Graduate School, and was accepted as partial fulfillment of the requirements for the degree of Doctor of Philosophy.

December, 1984

Dean for Graduate Studies and Research